JOURNAL OF MATHEMATICAL SCIENCES AND MODELLING

ISSN: 2636-8692

VOLUME I
ISSUE III

VOLUME I ISSUE III
ISSN 2636-8692

December 2018
http://dergipark.gov.tr/jmsm

JOURNAL OF MATHEMATICAL SCIENCES AND MODELLING

Editors

Editorial Board of Journal of Mathematical Sciences and Modelling

Contents

Journal of Mathematical Sciences and Modelling, 1 (3) (2018) 138-152
Research Article

Journal of Mathematical Sciences and Modelling

Journal Homepage: www.dergipark.gov.tr/jmsm
ISSN 2636-8692

Semi-Analytical Option Pricing Under Double Heston Jump-Diffusion Hybrid Model

Rehez Ahlip[a*], Laurence A. F. Park[a] and Ante Prodan[a]

[a]*School of Computing, Engineering and Mathematics , Western Sydney University, Australia*
[*]*Corresponding author*

Article Info

Keywords: *Finance, Double Heston Jump Diffusion model, Lévy process, Affine processes, Calibration of stochastic volatility.*
2010 AMS: *53C40, 53C42*
Received: *8 June 2018*
Accepted: *26 September 2018*
Available online: *30 December 2018*

Abstract

We examine European call options in the jump-diffusion version of the Double Heston stochastic volatility model for the underlying price process to provide a more flexible model for the term structure of volatility. We assume, in addition, that the stochastic interest rate is governed by the Cox– Ross – Ingersoll (CIR) dynamics. The instantaneous volatilities are correlated with the dynamics of the stock price process, whereas the short-term rate is assumed to be independent of the dynamics of the price process and its volatility. The main result furnishes a semi-analytical formula for the price of the European call option in the hybrid call option/interest rates model. Numerical results show that the model implied volatilities are comparable for in-sample but outperform out-of-sample implied volatilities compared to the benchmark Heston model [1], and Double Heston volatility model put forward by Christoffersen *et al.* [2] for calls on the S&P 500 index.

1. Introduction

In this paper we derive a semi-analytical pricing formula for European options in a model where the volatility of the stock price process is specified by a jump diffusion version of double Heston volatility model considered by Christoffersen et al.[2], whereas, the interest rate is governed by CIR dynamics postulated in Cox *et al.* [3]. In particular, the model put forward in the present work allows for a non-zero correlation between the stock price process and its instantaneous volatilities. According to the model given by (2.1), the CIR interest rate processes are independent of one another, and they are also independent of the stock price process and its volatility, which in turn is jointly governed by a jump process an extension of Heston's model. It is well established that the Heston model is not always able to fit the implied volatility smile very well, particularly at short maturities Gatheral [4]. Further, these models are particularly restrictive in their modeling of the relationship between the volatility level and the slope of the smirk, crucially the Heston one factor model can generate steep smirks at a given volatility level but cannot generate both for a given parametrization. Christofferson *et al.* [2], considered a two-factor structure for the volatility and demonstrate that the two-factor model gives much more flexibility in controlling the level and slope of the smirk. In their empirical estimates, one of the factors has a high mean reversion and determines the correlation between the short-term returns and variance. The other factor has lower mean reversion and determines the correlation between long-term returns and variance. Recchioni *et al.* [5] consider a two factor model, specifically, the dynamics of the asset price is described through two stochastic factors, one related to the stochastic volatility and the second to the stochastic interest rate.

In papers by Bakshi *et al.* [6], Bates [7] and Duffie *et al.* [8], the authors showed that stochastic volatility models do not offer reliable prices for close to expiration derivatives. This motivated Bates [7] and Bakshi *et al.* [6] to introduce jumps to the dynamics of the underlying. However, as observed by Andersen and Andreasen [9] and Alizadeh *et al.* (2002), the addition of jumps to the dynamics of the underlying is not sufficient to capture the sudden increase in volatility due to market turbulence. Since the overall volatility in financial markets consists of a highly persistent slow moving and a rapid moving components, Eraker *et al.* [10] proposed to introduce jump process to the dynamics of the volatility process in order to enhance the cross-sectional impact on option prices(see also Lewis [11]). A distinct advantage of an affine specification using Lévy processes as building block leads to analytically tractable pricing formulas for volatility derivatives, such as VIX options, as well as efficient numerical methods for pricing European options on the underlying asset, Cont *et al.* [12]. As observed by Gatheral [4] a more significant aspect as to why we consider jumps, though jumps have very little effect on the shape of the volatility surface

Email addresses and ORCID numbers: **r.ahlip@westernsydney.edu.au, 0000-0003-2426-4265 (R. Ahlip),l.park@westernsydney.edu.au, 0000-0003-0201-4409 (L. A. F. Park),a.prodan@westernsydney.edu.au, 0000-0001-9684-7967 (A. Prodan)**

for long-dated options; the impact on the shape of the volatility surface is all at the short-expiration end, and further might explain why the skew is so steep for very short expirations and why the very short-dated term structure of skew is inconsistent with any stochastic volatility model. In this paper we have demonstrated implied volatilities based Double Heston Jump-Diffusion Hybrid Model for the underlying asset and volatility dynamics clearly outperform implied volatilities based on single and Double Heston volatility models when compared with market implied volatilities compatible with observations of Carr *et al.* [13] and Christofferson *et al.* [2] with regard to out-of-sample implied volatilities. Van Haastrecht *et al.* [14] have extended the stochastic volatility model of Schöbel and Zhu [15] to equity/currency derivatives by including stochastic interest rates and assuming all driving model factors to be instantaneously correlated. Since their model is based on the Gaussian processes, it enjoys analytical tractability even in the most general case of a full correlation structure. On the other hand,, when the squared volatility is driven by the CIR process and the interest rate is driven either by the Vasicek [16] or the Cox *et al.* [3] process, a full correlation structure leads to intractability of equity options even under a partial correlation of the driving factors, as have been documented by, among others, Van Haastrecht and Pelsser [17] and Grzelak and Oosterlee [18], [19] who examined, in particular, the Heston/Vasicek and Heston/CIR hybrid models (see also Grzelak *et al.* [20], where the Schöbel–Zhu/Hull–White and Heston/Hull–White models for equity derivatives are studied). Andrei Cozma *et al.* [21] consider the Heston-CIR stochastic-local volatility model in the context of foreign exchange markets under a full correlation structure. They derive a full truncation scheme for simulating the stochastic volatility component and the stochastic domestic and foreign interest rates. More recently Andrei Cozma *et al.* [21] propose a calibration technique for four-factor foreign-exchange hybrid local-stochastic volatility models (LSV) with stochastic short rates. However, their model specification do not include jumps . In this paper we do not follow this line of research here and we focus instead on finding a semi-analytical solution, since this goal can be achieved under Assumptions (A.1)–(A.6).

In this paper we extend the results put forward in Ahlip-Rutkowski [22] by considering the double Heston Volatility model, further we provide a complete pricing formula which speeds numerical calibration substantially (refer to Lemma 4.3) Our goal is to derive a semi-analytical solution for prices of plain-vanilla options in a model in which the volatility components are specified by the extended double Heston model with log-normal and exponential jumps, whereas the short-term interest rate is governed by the independent CIR processes. The model thus incorporates important empirical characteristics of stock price return variability: (a) the correlation between the stock price dynamics and its stochastic volatility, (b) the presence of jumps in the stock price process and in one of the stochastic factors and a second stochastic factor the usual Heston volatility and (c) the random character of interest rate. The practical importance of this feature of newly developed equity models is rather clear in view of the existence of complex equity products that have a short lifetime and are sensitive to smiles or skews in the market.

The paper is organised as follows. In Section 2, we set the option pricing model examined in this work. The options pricing problem is introduced in Section 3. The main result, Theorem 4.1 of Section 4, furnishes the pricing formula for European call options. And in particular the result in Lemma 4.3 is crucial in the derivation of the semi analytical pricing formula Section 4,which in turn significantly speeds up calibration of the model parameters to market and most important the model implied volatility surface . It is worth stressing that the independence of volatility and interest rates appears to be a crucial assumption from the point of view of analytical tractability and thus it cannot be relaxed. Numerical illustrations of our method are provided in Section 5 where the Single Heston, Double Heston and Double Heston jump-diffusion models are compared applied to S&P 500 index data and further our model can fit market implied volatilities across strikes and maturities particularly well for out-of-sample options.

2. The double Heston-Jump diffusion/CIR model

Let $(\Omega,\mathscr{F},\mathbb{P})$ be an underlying probability space. Let the stock price process $S=(S_t)_{t\in[0,T]}$, its instantaneous squared volatility $v=(v_t)_{t\in[0,T]}$, the short-term interest rate $r=(r_t)_{t\in[0,T]}$ be governed by the following system of SDEs:

$$\begin{cases} dS_t = S_t\,(r_t-\lambda_S\mu_S)\,dt + S_t\,\sqrt{v_t}\,dW_t^S + S_t\,\sqrt{\widehat{v}_t}\,d\widehat{W}_t^S + S_t dZ_t^S, \\ dv_t = \big(\theta-\kappa v_t\big)dt + \sigma_v\sqrt{v_t}\,dW_t^v + dZ_t^v, \\ d\widehat{v}_t = \big(\widehat{\theta}-\widehat{\kappa}\widehat{v}_t\big)dt + \sigma_{\widehat{v}}\sqrt{\widehat{v}_t}\,d\widehat{W}_t^v, \\ dr_t = \big(a-br_t\big)dt + \sigma_r\sqrt{r_t}\,dW_t^r. \end{cases} \tag{2.1}$$

We work under the following standing assumptions:

(A.1) Processes $W^S=(W_t^S)_{t\in[0,T]}$, $W^v=(W_t^v)_{t\in[0,T]}$ are correlated Brownian motions with a constant correlation coefficient, so that the quadratic covariation between the processes W^S and W^v satisfies $d[W^S,W^v]_t=\rho\,dt$ for some constant $\rho\in[-1,1]$.
(A.2) Processes $\widehat{W}^S=(\widehat{W}_t^S)_{t\in[0,T]}$, $\widehat{W}^v=(\widehat{W}_t^v)_{t\in[0,T]}$ are correlated Brownian motions with a constant correlation coefficient, so that the quadratic covariation between the processes $\widehat{W}^S$ and $\widehat{W}^v$ satisfies $d[\widehat{W}^S,\widehat{W}^v]_t=\widehat{\rho}\,dt$ for some constant $\widehat{\rho}\in[-1,1]$. Further the processes $W^v=(W_t^v)_{t\in[0,T]}$ and $\widehat{W}^v=(\widehat{W}_t^v)_{t\in[0,T]}$ are independent.
(A.3) Processes $W^r=(W_t^r)_{t\in[0,T]}$ is independent of the Brownian motions W^S, $\widehat{W}^S$ and W^v, $\widehat{W}^v$.
(A.4) The process $Z_t^S=\sum_{k=1}^{N_t^S}J_k^S$ is the compound Poisson process; specifically, the Poisson process N^S has the intensity $\lambda_S>0$ and the random variables $\ln(1+J_k^S)$, $k=1,2,\dots$ have the probability distribution $N(\ln[1+\mu_S]-\frac{1}{2}\sigma_S^2,\sigma_S^2)$; hence the jump sizes $(J_k^S)_{k=1}^{\infty}$ are lognormally distributed on $(-1,\infty)$ with mean $\mu_S>-1$.
(A.5) The process $Z_t^v=\sum_{k=1}^{N_t^v}J_k^v$ is the compound Poisson process; specifically, the Poisson process N^v has the intensity $\lambda_v>0$ and the jump sizes J_k^v are exponentially distributed with mean μ_v.
(A.6) The Poisson process N^v and sequence of random variables $(J_k^v)_{k=1}^{\infty}$ are independent of the Brownian motions $W^S,W^v,\widehat{W}^S,\widehat{W}^v,W^r$.
(A.7) The model's parameters satisfy the stability conditions: $2\theta>\sigma_v^2>0$, $2\widehat{\theta}>\sigma_{\widehat{v}}^2>0$ and $2a>\sigma_r^2>0$ (see, for instance, Wong and Heyde [23]).

Note that we postulate that the instantaneous squared volatility processes v, $\widehat{v}$ the short-term interest rate r are independent stochastic processes. We will argue in what follows that this assumption is indeed crucial for analytical tractability. For brevity, we refer to the model given by SDEs (2.1) under Assumptions (A.1)–(A.6) as the Double Heston/CIR jump-diffusion hybrid model(DHJDH).

3. Call option

We will first establish the general representation for the value European call option with maturity $T > 0$ and a constant strike level $K > 0$. The probability measure $\mathbb{P}$ is interpreted as the spot martingale measure (i.e., the risk-neutral probability). We denote by $\mathbb{F} = (\mathscr{F}_t)_{t\in[0,T]}$ the filtration generated by the Brownian motions $W^S, W^v, \widehat{W}^v, W^r$ and the compound Poisson processes Z^S and Z^v. We write $\mathbb{E}_t^{\mathbb{P}}(\cdot)$ and $\mathbb{P}_t(\cdot)$ to denote the conditional expectation and the conditional probability under $\mathbb{P}$ with respect to the σ-field $\mathscr{F}_t$, respectively. Hence the arbitrage price $C_t(T,K)$ of the call option at time $t \in [0,T]$ is given as the conditional expectation with respect to the σ-field $\mathscr{F}_t$ of the option's payoff at expiration discounted by the money market account, that is,

$$C_t(T,K) = \mathbb{E}_t^{\mathbb{P}}\left\{\exp\left(-\int_t^T r_u\,du\right)C_T(T,K)\right\} = \mathbb{E}_t^{\mathbb{P}}\left\{\exp\left(-\int_t^T r_u\,du\right)(S_T-K)^+\right\}$$

or, equivalently,

$$C_t(T,K) = \mathbb{E}_t^{\mathbb{P}}\left\{\exp\left(-\int_t^T r_u\,du\right)S_T\mathbb{1}_{\{S_T>K\}}\right\} - K\mathbb{E}_t^{\mathbb{P}}\left\{\exp\left(-\int_t^T r_u\,du\right)\mathbb{1}_{\{S_T>K\}}\right\}.$$

Similarly, the arbitrage price of the discount bond maturing at time T equals, for every $t \in [0,T]$,

$$B(t,T) = \mathbb{E}_t^{\mathbb{P}}\left\{\exp\left(-\int_t^T r_u\,du\right)\right\}$$

(see Musiela and Rutkowski ([24], Chapter 14)).

As a preliminary step towards the general valuation result presented in Section 4, we state the following well-known proposition (see, e.g, Cox *et al.* [3] or Chapter 10 in Musiela and Rutkowski [24]).

Proposition 3.1. *The price at date t of the discount bond maturing at time $T > t$ in the CIR model are given by the following expressions*

$$B(t,T) = \exp\big(m(t,T) - n(t,T)r_t\big),$$

$$m(t,T) = \frac{2a}{\sigma_r^2}\log\left[\frac{\widetilde{\gamma}e^{\frac{1}{2}b(T-t)}}{\widetilde{\gamma}\cosh(\widetilde{\gamma}(T-t)) + \frac{1}{2}b\sinh(\widetilde{\gamma}(T-t))}\right],$$

$$n(t,T) = \frac{\sinh(\widetilde{\gamma}(T-t))}{\widetilde{\gamma}\cosh(\widetilde{\gamma}(T-t)) + \frac{1}{2}b\sinh(\widetilde{\gamma}(T-t))}.$$

and

$$\widetilde{\gamma} = \frac{1}{2}\sqrt{b^2+2\sigma_r^2}.$$

The dynamics of the bond price under the spot martingale measure $\mathbb{P}$ is given by

$$dB(t,T) = B(t,T)\big(r_t\,dt - \sigma_r n(t,T)\sqrt{r_t}\,dW_t^r\big),$$

The following result is also well known (see, for instance, Section 11.3.1 in Musiela and Rutkowski [24]).

Lemma 3.2. *The forward rate $F(t,T)$ at time t for settlement date T equals*

$$F(t,T) = \frac{S_t}{B(t,T)}. \tag{3.1}$$

Since manifestly $S_T = F(T,T)$, the option's payoff at expiration can also be expressed as follows

$$C_T(T,K) = F(T,T)\mathbb{1}_{\{F(T,T)>K\}} - K\mathbb{1}_{\{F(T,T)>K\}}.$$

Consequently, the option's value at time $t \in [0,T]$ admits the following representation

$$\begin{aligned} C_t(T,K) \quad &= \mathbb{E}_t^{\mathbb{P}}\left\{\exp\left(-\textstyle\int_t^T r_u\,du\right)F(T,T)\mathbb{1}_{\{F(T,T)>K\}}\right\} \\ &\quad - K\mathbb{E}_t^{\mathbb{P}}\left\{\exp\left(-\textstyle\int_t^T r_u\,du\right)\mathbb{1}_{\{F(T,T)>K\}}\right\}. \end{aligned}$$

In what follows, we will frequently use the notation $x_t = \ln F(t,T)$ where $t \in [0,T]$.

4. Pricing formula for the European call option

In this section we present the main result of the paper, which furnishes a semi-analytical formula for the arbitrage price of the call option of European style under the Double Heston Jump- Diffusion Hybrid model for the stock price process combined with the independent CIR model for short-term rate.

Theorem 4.1. *Let the model be given by SDEs (2.1) under Assumptions (A.1)–(A.6). Then the price of the European call option equals, for every* $t \in [0,T]$,

$$C_t(T,K) = S_t P_1\big(t,S_t,v_t,\widehat{v}_t,r_t,K\big) - KB(t,T)P_2\big(t,S_t,v_t,\widehat{v}_t,r_t,K\big)$$

where the bond price $B(t,T)$ *is given in Proposition 3.1, and the functions* P_1 *and* P_2 *are given by*

$$P_1\big(t,S_t,v_t,\widehat{v}_t,r_t,K\big) = \frac{1}{2} + \frac{1}{\pi}\int_0^\infty \mathrm{Re}\left(f_1(\phi)\,\frac{\exp(-i\phi\ln K)}{i\phi}\right)d\phi. \tag{4.1}$$

and

$$P_2\big(t,S_t,v_t,\widehat{v}_t,r_t,K\big) = \frac{1}{2} + \frac{1}{\pi}\int_0^\infty \mathrm{Re}\left(f_2(\phi)\,\frac{\exp(-i\phi\ln K)}{i\phi}\right)d\phi.$$

where the $\mathscr{F}_t$*-conditional characteristic functions* $f_j(\phi) = f_j(\phi,t,S_t,v_t,\widehat{v}_t,r_t)$, $j = 1,2$ *of the random variable* $x_T = \ln(S_T)$ *under the probability measure* $\widehat{\mathbb{P}}_T$ *(see Definition 4.6) and* $\mathbb{P}_T$ *(see Definition 4.4), respectively, are given by*

$$\begin{aligned} f_1(\phi) &= c_t \exp\left[\lambda_S\tau\left((1+\mu_S)^{i\phi}e^{-\frac{1}{2}(\phi^2+i\phi)\sigma_S^2}-1\right)\right] \\ &\quad\times\exp\left[-\left(i\phi\lambda_S\mu_S\tau+\lambda_v\tau\left(\frac{\rho(1+i\phi)\mu_v}{\sigma_v+\rho(1+i\phi)\mu_v}\right)\right)\right] \\ &\quad\times\exp\left[-\left(\frac{(1+i\phi)\rho}{\sigma_v}(v_t+\theta\tau)+\frac{(1+i\phi)\widehat{\rho}}{\sigma_{\widehat{v}}}(\widehat{v}_t+\widehat{\theta}\tau)\right)\right] \\ &\quad\times\exp\left[-i\phi\left(n(t,T)r_t+a\int_t^T n(u,T)\,du\right)\right] \\ &\quad\times\exp\left[-G_1(\tau,s_1,s_2)v_t-G_2(\tau,s_3,s_4)\widehat{v}_t-G_3(\tau,s_5,s_6)r_t\right] \\ &\quad\times\exp\left[-\theta H_1(\tau,s_1,s_2)-\widehat{\theta}H_2(\tau,s_3,s_4)-aH_3(\tau,s_5,s_6)\right] \end{aligned} \tag{4.2}$$

and

$$\begin{aligned} f_2(\phi) &= c_t \exp\left[\lambda_S\tau\left((1+\mu_S)^{i\phi}e^{-\frac{1}{2}(\phi^2+i\phi)\sigma_S^2}-1\right)\right] \\ &\quad\times\exp\left[-\left(i\phi\lambda_S\mu_S\tau+\lambda_v\tau\left(\frac{i\phi\rho\mu_v}{\sigma_v+i\phi\rho\mu_v}\right)\right)\right] \\ &\quad\times\exp\left[-\left(\frac{(i\phi)\rho}{\sigma_v}(v_t+\theta\tau)+\frac{(i\phi)\widehat{\rho}}{\sigma_{\widehat{v}}}(\widehat{v}_t+\widehat{\theta}\tau)\right)\right] \\ &\quad\times\exp\left[(1-i\phi)\left(n(t,T)r_t+a\int_t^T n_d(u,T)\,du\right)\right] \\ &\quad\times\exp\left[-G_1(\tau,q_1,q_2)v_t-G_2(\tau,q_3,q_4)\widehat{v}_t-G_3(\tau,q_5,q_6)r_t\right] \\ &\quad\times\exp\left[-\theta H_1(\tau,q_1,q_2)-\widehat{\theta}H_2(\tau,q_3,q_4)-aH_3(\tau,q_5,q_6)\right] \end{aligned} \tag{4.3}$$

where the functions G_1,G_2,G_3,H_1,H_2,H_3, *are given in Lemma 4.3 and* c_t *equals*

$$c_t = \exp\big(i\phi x_t\big) = \exp\left(i\phi\ln F(t,T)\right).$$

Moreover, the constants s_1,s_2,s_3,s_4,s_5,s_6 *are given by*

$$\begin{aligned} s_1 &= -\frac{(1+i\phi)\rho}{\sigma_v}, \\ s_2 &= -\frac{(1+i\phi)^2(1-\rho^2)}{2} - \frac{(1+i\phi)\rho\kappa}{\sigma_v} + \frac{1+i\phi}{2}, \\ s_3 &= -\frac{(1+i\phi)\widehat{\rho}}{\sigma_{\widehat{v}}}, \\ s_4 &= -\frac{(1+i\phi)^2(1-\widehat{\rho})^2}{2} - \frac{(1+i\phi)\widehat{\rho}\widehat{\kappa}}{\sigma_{\widehat{v}}} + \frac{1+i\phi}{2}, \\ s_5 &= 0,\ s_6 = -i\phi, \end{aligned} \tag{4.4}$$

and the constants $q_1, q_2, q_3, q_4, q_5, q_6$ equal

$$\begin{aligned}
q_1 &= -\frac{i\phi\rho}{\sigma_v},\\
q_2 &= -\frac{(i\phi)^2(1-\rho^2)}{2} - \frac{i\phi\rho\kappa}{\sigma_v} + \frac{i\phi}{2},\\
q_3 &= -\frac{i\phi\widehat{\rho}}{\sigma_{\widehat{v}}},\\
q_4 &= -\frac{(i\phi)^2(1-\widehat{\rho}^2)}{2} - \frac{i\phi\widehat{\rho}\widehat{\kappa}}{\sigma_{\widehat{v}}} + \frac{i\phi}{2},\\
q_5 &= 0, q_6 = i\phi - 1.
\end{aligned} \tag{4.5}$$

4.1. Auxiliary results

The proof of Theorem 4.1 hinges on a number of lemmas. We start by stating the well known result, which can be easily obtained from Proposition 8.6.3.4 in Jeanblanc et al. [25]. Let us denote $\tau = T - t$ and let us set, for all $0 \le t < T$,

$$J^S(t,T) := \sum_{k=N_t^S+1}^{N_T^S} \ln(1+J_k^S). \tag{4.6}$$

Note that we use here Assumptions (A.3)–(A.5). The property (A.3) (resp. (A.4)) implies that the random variable $J^S(t,T)$ (resp. $Z_T^v - Z_t^v$) is independent of the σ-field $\mathscr{F}_t$. Let ν_1 stand for the Gaussian distribution $N\big(\ln(1+\mu_S) - \frac{1}{2}\sigma_S^2, \sigma_S^2\big)$ and let ν_2 stand for the exponential distribution with the mean μ_v.

Lemma 4.2. *(i) Under Assumptions (A.3) and (A.5), the following equalities are valid*

$$\begin{aligned}
\mathbb{E}_t^{\mathbb{P}}\Big\{\exp\big(i\phi J^S(t,T)\big)\Big\} &= \mathbb{E}_t^{\mathbb{P}}\Big\{\exp\Big(i\phi\textstyle\sum_{k=N_t^S+1}^{N_T^S}\ln\big(1+J_k^S\big)\Big)\Big\}\\
&= \exp\big[\lambda_S\tau\textstyle\int_{-\infty}^{+\infty}\big(e^{i\phi z}-1\big)\,\nu_1(dz)\big]\\
&= \exp\Big[\lambda_Q\tau\Big((1+\mu_S)^{i\phi}e^{-\frac{1}{2}\sigma_S^2(\phi^2+i\phi)}-1\Big)\Big].
\end{aligned}$$

(ii) Under Assumptions (A.4) and (A.5), the following equalities are valid for $c = a + bi$ with $a \le 0$

$$\begin{aligned}
\mathbb{E}_t^{\mathbb{P}}\Big\{\exp\big(c\,(Z_T^v - Z_t^v)\big)\Big\} &= \mathbb{E}_t^{\mathbb{P}}\Big\{\exp\Big(c\textstyle\sum_{k=N_t^v+1}^{N_T^v}J_k^v\Big)\Big\}\\
&= \exp\big[\lambda_v\tau\textstyle\int_0^{+\infty}(e^{cz}-1)\,\nu_2(dz)\big]\\
&= \exp\Big[\lambda_v\tau\Big(\tfrac{c\mu_v}{1-c\mu_v}\Big)\Big].
\end{aligned}$$

The next result which is crucial for the derivation of the pricing formula in the main Theorem 4.1 extends Lemma 4.2 in Ahlip and Rutkowski [22] (see also Duffie *et al.* [8]) where the model without the jump component in the dynamics of v was examined.

Lemma 4.3. *Let the dynamics of processes $v, \widehat{v}$ and r be given by SDEs (2.1) with independent Brownian motions W^v, $\widehat{W}^v$ andW^r . For any complex numbers μ_1, λ_1, μ_2, λ_2, $\widetilde{\mu}$, $\widetilde{\lambda}$, we set*

$$\begin{aligned}
F(\tau, v_t, \widehat{v}_t, r_t) \;=\; \mathbb{E}_t^{\mathbb{P}}\bigg\{&\exp\bigg(-\lambda_1 v_T - \mu_1\int_t^T v_u\,du - \lambda_2\widehat{v}_T - \mu_2\int_t^T \widehat{v}_u\,du\\
&-\widetilde{\lambda}r_T - \widetilde{\mu}\int_t^T r_u\,du\bigg)\bigg\}.
\end{aligned}$$

Then

$$\begin{aligned}
F(\tau, v_t, \widehat{v}_t, r_t) = \;&\exp\big[-G_1(\tau,\lambda_1,\mu_1)v_t - G_2(\tau,\lambda_2,\mu_2)\widehat{v}_t - (G_3(\tau,\widetilde{\lambda},\widetilde{\mu})r_t\big]\\
&\times\exp[-\theta H_1(\tau,\lambda_1,\mu_1) - \widehat{\theta}H_2(\tau,\lambda_2,\mu_2) - aH_3(\tau,\widetilde{\lambda},\widetilde{\mu})]
\end{aligned}$$

where

$$\begin{aligned}
G_1(\tau,\lambda_1,\mu_1) &= \frac{\lambda_1[(\gamma_1+\kappa)+e^{\gamma_1\tau}(\gamma_1-\kappa)]+2\mu_1(e^{\gamma_1\tau}-1)}{\sigma_v^2\,\lambda_1\,(e^{\gamma_1\tau}-1)+\gamma-\kappa+e^{\gamma_1\tau}\,(\gamma_1+\kappa)},\\
G_2(\tau,\lambda_2,\mu_2) &= \frac{\lambda_2[(\gamma_2+\widehat{\kappa})+e^{\gamma_2\tau}(\gamma_2-\widehat{\kappa})]+2\mu_2(e^{\gamma_2\tau}-1)}{\sigma_{\widehat{v}}^2\,\lambda_2\,(e^{\gamma_2\tau}-1)+\gamma_2-\widehat{\kappa}+e^{\gamma_2\tau}\,(\gamma_2+\widehat{\kappa})},\\
G_3(\tau,\widetilde{\lambda},\widetilde{\mu}) &= \frac{\widetilde{\lambda}[(\widetilde{\gamma}+b)+e^{\widetilde{\gamma}\tau}(\widetilde{\gamma}-b)]+2\widetilde{\mu}(e^{\widetilde{\gamma}\tau}-1)}{\sigma_r^2\,\widetilde{\lambda}\,(e^{\widetilde{\gamma}\tau}-1)+\widetilde{\gamma}-b+e^{\widetilde{\gamma}\tau}\,(\widetilde{\gamma}+b)},
\end{aligned}$$

and

$$H_1(\tau,\lambda_1,\mu_1) = -\frac{2}{\sigma_v^2}\ln\left(\frac{2\gamma_1 e^{[(\gamma_1+\kappa)\tau]/2}}{\sigma_v^2\lambda_1(e^{\gamma_1\tau}-1)+\gamma_1-\kappa+e^{\gamma_1\tau}(\gamma_1+\kappa)}\right)$$
$$+\frac{2\lambda_v\mu_v\sigma_v^2}{\theta(\sigma_v^2+2\mu_v\alpha_1)(\sigma_v^2+2\mu_v\beta_1)}\ln\left(\frac{(\sigma_v^2+2\beta_1\mu_v)+\Gamma_1(\sigma_v^2+2\alpha_1\mu_v)e^{\gamma_1\tau}}{(\sigma_v^2+2\beta_1\mu_v)+\Gamma_1(\sigma_v^2+2\alpha_1\mu_v)}\right)$$
$$+\frac{2\lambda_v\mu_v\beta_1}{\theta(\sigma_v^2+2\beta_1\mu_v)}\tau,$$
$$H_2(\tau,\lambda_2,\mu_2) = -\frac{2}{\sigma_{\widehat{v}}^2}\ln\left(\frac{2\gamma_2 e^{[(\gamma_2+\widehat{\kappa})\tau]/2}}{\sigma_{\widehat{v}}^2\lambda_2(e^{\gamma_2\tau}-1)+\gamma_2-\widehat{\kappa}+e^{\gamma_2\tau}(\gamma_2+\widehat{\kappa})}\right),$$
$$H_3(\tau,\widetilde{\lambda},\widetilde{\mu}) = -\frac{2}{\sigma_r^2}\ln\left(\frac{2\widetilde{\gamma}e^{\frac{(\widetilde{\gamma}+b)\tau}{2}}}{\sigma_r^2\widetilde{\lambda}\left(e^{\widetilde{\gamma}\tau}-1\right)+\widetilde{\gamma}-b+e^{\widetilde{\gamma}\tau}(\widetilde{\gamma}+b)}\right),$$

where we denote $\gamma_1 = \sqrt{\kappa^2+2\sigma_v^2\mu_1}$, $\gamma_2 = \sqrt{\widehat{\kappa}^2+2\sigma_{\widehat{v}}^2\mu_2}$, $\widetilde{\gamma} = \sqrt{b^2+2\sigma_r^2\widetilde{\mu}}$,
$\alpha_1 = \frac{-\kappa+\gamma_1}{2}$, $\beta_1 = \frac{-\kappa-\gamma_1}{2}$, $\Gamma_1 = \frac{2\beta_1-\lambda_1\sigma_v^2}{\lambda_1\sigma_v^2-2\alpha_1}$.

Proof. For the reader's convenience, we sketch the proof of the lemma. Let us set, for $t\in[0,T]$,

$$M_t = F(\tau,v_t,\widehat{v}_t,r_t)\exp\left(-\mu_1\int_0^t v_u\,du-\mu_2\int_0^t\widehat{v}_u\,du-\widetilde{\mu}\int_0^t r_u\,du\right). \tag{4.7}$$

Then the process $M=(M_t)_{t\in[0,T]}$ satisfies

$$M_t = \mathbb{E}_t^{\mathbb{P}}\left\{\exp\left(-\lambda_1 v_T-\mu_1\int_0^T v_u\,du-\lambda_2\widehat{v}_T-\mu_2\int_0^T\widehat{v}_u\,du-\widetilde{\lambda}r_T-\widetilde{\mu}\int_0^T r_u\,du\right)\right\}$$

and thus it is an $\mathbb{F}$-martingale under $\mathbb{P}$. By applying the Itô formula to the right-hand side in (4.7) and by setting the drift term in the dynamics of M to be zero, we deduce that the function $F(\tau,v,\widehat{v},r,\widehat{r})$ satisfies the following partial integro-differential equation (PIDE)

$$-\frac{\partial F}{\partial\tau}+\frac{1}{2}\sigma_v^2 v\frac{\partial^2F}{\partial v^2}+\lambda_v\int_0^\infty\big(F(\tau,v+z,r)-F(\tau,v,r)\big)\nu_2(dz)$$
$$+\frac{1}{2}\sigma_{\widehat{v}}^2\widehat{v}\frac{\partial^2F}{\partial\widehat{v}^2}+\frac{1}{2}\sigma_r^2 r\frac{\partial^2F}{\partial r^2}+(\theta-\kappa v)\frac{\partial F}{\partial v}+(\widehat{\theta}-\widehat{\kappa}\widehat{v})\frac{\partial F}{\partial\widehat{v}}$$
$$+(a-br)\frac{\partial F}{\partial r}-(\mu_1 v+\mu_2\widehat{v}+\widetilde{\mu}r)F=0$$

with the initial condition $F(0,v,\widehat{v},r)=\exp(-\lambda_1 v-\lambda_2\widehat{v}-\widetilde{\lambda}r)$. We search for a solution to this PIDE in the form

$$F(\tau,v,r,\widehat{r}) = \exp\big[-G_1(\tau,\lambda_1,\mu_1)v-G_2(\tau,\lambda_2,\mu_2)\widehat{v}-G_3(\tau,\widetilde{\lambda},\widetilde{\mu})r$$
$$-\theta H_1(\tau,\lambda_1,\mu_1)-\widehat{\theta}H_2(\tau,\lambda_2,\mu_2)-aH_3(\tau,\widetilde{\lambda},\widetilde{\mu})\big]$$

with

$$G_1(0,\lambda_1,\mu_1)=\lambda_1,\quad G_2(0,\lambda_2,\mu_2)=\lambda_2,\quad G_3(0,\widetilde{\lambda},\widetilde{\mu})=\widetilde{\lambda},$$

and

$$H_1(0,\lambda_1,\mu_1)=H_2(0,\lambda_2,\mu_2)=H_3(0,\widetilde{\lambda},\widetilde{\mu})=0.$$

By substituting this expression in the PIDE and using part (ii) in Lemma 4.2, we obtain the following system of ODEs for the functions G_1,G_2,G_3,H_1,H_2,H_3 (for brevity, we suppress the last three arguments)

$$\frac{\partial G_1(\tau)}{\partial\tau} = -\frac{1}{2}\sigma_v^2G_1^2(\tau)-\kappa G_1(\tau)+\mu_1,$$
$$\frac{\partial H_1(\tau)}{\partial\tau} = G_1(\tau)+\frac{\lambda_v}{\theta}\left(\frac{\mu_vG_1}{1+\mu_vG_1(\tau)}\right)$$
$$\frac{\partial G_2(\tau)}{\partial\tau} = -\frac{1}{2}\sigma_{\widehat{v}}^2G_2^2(\tau)-\widehat{\kappa}G_2(\tau)+\mu_2,$$
$$\frac{\partial H_2(\tau)}{\partial\tau} = G_2(\tau),$$
$$\frac{\partial G_3(\tau)}{\partial\tau} = -\frac{1}{2}\sigma_r^2G_3^2(\tau)-bG_3(\tau)+\widetilde{\mu}.$$
$$\frac{\partial H_3(\tau)}{\partial\tau} = G_3(\tau),$$

By solving these equations, we obtain the stated formulae. □

Under the assumptions of Lemma 4.3, it is possible to factorise F as a product of two conditional expectations. This means that the functions G_1 (H_1), G_2 (H_2) and G_3 (H_3) are of the same form, except that they correspond to different sets of parameters.
We now introduce a convenient change of the underlying probability measure, from the spot martingale measure $\mathbb{P}$ to the forward martingale measure $\mathbb{P}_T$.

Definition 4.4. The *The T- forward martingale measure* $\mathbb{P}_T$, equivalent to $\mathbb{P}$ on $(\Omega, \mathscr{F}_T)$, is defined by the Radon-Nikodým derivative process $\eta = (\eta_t)_{t\in[0,T]}$ where

$$\eta_t = \frac{d\mathbb{P}_T}{d\mathbb{P}}\Big|_{\mathscr{F}_t} = \exp\left(-\int_0^t \sigma_r n(u,T)\sqrt{r_u}\,dW_u^r - \frac{1}{2}\int_0^t \sigma_r^2 n^2(u,T) r_u\,du\right). \tag{4.8}$$

An application of Girsanov's theorem shows that the process $W^T = (W_t^T)_{t\in[0,T]}$, which is given by the equality

$$W_t^T = W_t^r + \int_0^t \sigma_r n(u,T)\sqrt{r_u}\,du, \tag{4.9}$$

is the Brownian motion under the domestic forward martingale measure $\mathbb{P}_T$. Using the standard change of a numéraire technique, one can check that the price of the European foreign exchange call option admits the following representation under the probability measure $\mathbb{P}_T$

$$C_t(T,K) = B_d(t,T)\,\mathbb{E}_t^{\mathbb{P}_T}\left(F(T,T)\mathbb{1}_{\{F(T,T)>K\}}\right) - KB_d(t,T)\,\mathbb{E}_t^{\mathbb{P}_T}\left(\mathbb{1}_{\{F(T,T)>K\}}\right). \tag{4.10}$$

The following auxiliary result is easy to establish and thus its proof is omitted. Recall that $J^S(t,T)$ is given by equality (4.6).

Lemma 4.5. *Under Assumptions (A.1)–(A.6), the dynamics of the forward stock price dynamics $F(t,T)$ under the forward martingale measure $\mathbb{P}_T$ are given by the SDE*

$$dF(t,T) = F(t,T)\left(dZ_t^S - \lambda_S\mu_S dt + \sqrt{v_t}\,dW_t^S + \sqrt{\widehat{v}_t}\,d\widehat{W}_t^S + \sigma_d n_d(t,T)\sqrt{r_t}\,dW_t^T\right)$$

or, equivalently,

$$F(T,T) = F(t,T)\exp\left(J^S(t,T) - \lambda_S\mu_S(T-t) + \int_t^T \widetilde{\sigma}_F(u,T)\cdot d\widetilde{W}_u^T - \frac{1}{2}\int_t^T \|\widetilde{\sigma}_F(u,T)\|^2\,du\right)$$

where the dot $\cdot$ denotes the inner product in $\mathbb{R}^3$, $(\widetilde{\sigma}_F(t,T))_{t\in[0,T]}$ is the $\mathbb{R}^3$-valued process (row vector) given by

$$\widetilde{\sigma}_F(t,T) = \left[\sqrt{v_t},\, \sqrt{\widehat{v}_t},\, \sigma_r n(t,T)\sqrt{r_t}\right]$$

and $\widetilde{W}^T = (\widetilde{W}_t^T)_{t\in[0,T]}$ is the $\mathbb{R}^3$-valued process (column vector) given by $\widetilde{W}^T = \left[W^S, \widehat{W}^S, W^T\right]^*$.

Under Assumptions (A.1)–(A.6), the process $\widetilde{W}^T$ is the three-dimensional standard Brownian motion under $\mathbb{P}_T$. In view of Lemma 4.5, we have that

$$\begin{aligned}
&B(t,T)\,\mathbb{E}_t^{\mathbb{P}_T}\left(F(T,T)\mathbb{1}_{\{F(T,T)>K\}}\right)\\
&\quad= B(t,T)\,\mathbb{E}_t^{\mathbb{P}_T}\Bigg\{F(t,T)\exp\Bigg(J^S(t,T) - \lambda_S\mu_S(T-t)\\
&\qquad\quad + \int_t^T \widetilde{\sigma}_F(u,T)\cdot d\widetilde{W}_u^T - \frac{1}{2}\int_t^T \|\widetilde{\sigma}_F(u,T)\|^2\,du\Bigg)\mathbb{1}_{\{F(T,T)>K\}}\Bigg\}\\
&\quad= S_t\,\mathbb{E}_t^{\mathbb{P}_T}\Bigg\{\exp\Bigg(J^S(t,T) - \lambda_S\mu_S(T-t)\\
&\qquad\quad + \int_t^T \widetilde{\sigma}_F(u,T)\cdot d\widetilde{W}_u^T - \frac{1}{2}\int_t^T \|\widetilde{\sigma}_F(u,T)\|^2\,du\Bigg)\mathbb{1}_{\{F(T,T)>K\}}\Bigg\}.
\end{aligned}$$

To deal with the first term in the right-hand side of (4.10), we introduce another auxiliary probability measure.

Definition 4.6. The *modified forward martingale measure* $\widehat{\mathbb{P}}_T$, equivalent to $\mathbb{P}_T$ on $(\Omega, \mathscr{F}_T)$, is defined by the Radon-Nikodým derivative process $\widehat{\eta} = (\widehat{\eta}_t)_{t\in[0,T]}$ where

$$\widehat{\eta}_t = \frac{d\widehat{\mathbb{P}}_T}{d\mathbb{P}_T}\Big|_{\mathscr{F}_t} = \exp\left(\int_0^t \widetilde{\sigma}_F(u,T)\cdot d\widetilde{W}_u^T - \frac{1}{2}\int_0^t \|\widetilde{\sigma}_F(u,T)\|^2\,du\right).$$

Using Lemma 4.5 and equation (3.1), we obtain

$$B(t,T)\,\mathbb{E}_t^{\mathbb{P}_T}\left(F(T,T)\mathbb{1}_{\{F(T,T)>K\}}\right) = S_t\,\frac{\mathbb{E}_t^{\mathbb{P}_T}\left(\mathbb{1}_{\{F(T,T)>K\}}\widehat{\eta}_T\right)}{\mathbb{E}_t^{\mathbb{P}_T}\left(\widehat{\eta}_T\right)}$$

and thus the Bayes formula and Definition 4.6 yield

$$B(t,T)\,\mathbb{E}_t^{\mathbb{P}_T}\left(F(T,T)\mathbb{1}_{\{F(T,T)>K\}}\right) = S_t\,\mathbb{E}_t^{\widehat{\mathbb{P}}_T}\left(\mathbb{1}_{\{F(T,T)>K\}}\right).$$

This shows that $\widehat{\mathbb{P}}_T$ is a martingale measure associated with the choice of the price process S_t as a numéraire asset.

Lemma 4.7. *The price of the call option satisfies*

$$C_t(T,K) = S_t\,\widehat{\mathbb{P}}_T\left(S_T > K\,|\,\mathscr{F}_t\right) - KB(t,T)\,\mathbb{P}_T\left(S_T > K\,|\,\mathscr{F}_t\right)$$

or, equivalently,

$$C_t(T,K) = S_t\,\widehat{\mathbb{P}}_T\left(x_T > \ln K\,|\,\mathscr{F}_t\right) - KB(t,T)\,\mathbb{P}_T\left(x_T > \ln K\,|\,\mathscr{F}_t\right). \tag{4.11}$$

To complete the proof of Theorem 4.1, it remains to evaluate the conditional probabilities given in formula (4.11). By another application of Girsanov's theorem, one can check that the process $(S,v,\widehat{v},r)$ has the Markov property under the probability measures $\mathbb{P}_T$ and $\widehat{\mathbb{P}}_T$. In view of Proposition 3.1 and Lemma 3.2, the random variable x_T is a function of S_T and r_T. Hence it follows that

$$C_t(T,K) = S_t\,P_1(t,S_t,v_t,\widehat{v}_t,r_t,K) - KB(t,T)P_2(t,S_t,v_t,\widehat{v}_t,r_t,K) \tag{4.12}$$

where we denote

$$P_1(t,S_t,v_t,\widehat{v}_t,r_t,K) = \widehat{\mathbb{P}}_T(x_T > \ln K\,|\,S_t,v_t,\widehat{v}_t,r_t),$$
$$P_2(t,S_t,v_t,\widehat{v}_t,r_t,K) = \mathbb{P}_T(x_T > \ln K\,|\,S_t,v_t,\widehat{v}_t,r_t).$$

To obtain explicit formulae for the conditional probabilities above, it suffices to derive the corresponding conditional characteristic functions

$$f_1(\phi,t,S_t,v_t,\widehat{v}_t,r_t) = \mathbb{E}_t^{\widehat{\mathbb{P}}_T}\left[\exp(i\phi x_T)\right],$$
$$f_2(\phi,t,S_t,v_t,\widehat{v}_t,r_t) = \mathbb{E}_t^{\mathbb{P}_T}\left[\exp(i\phi x_T)\right].$$

The idea is to use the Radon-Nikodým derivatives in order to obtain convenient expressions for the characteristic functions in terms of conditional expectations under the spot martingale measure $\mathbb{P}$. The following lemma will allow us to achieve this goal.

Lemma 4.8. *The following equality holds*

$$\begin{aligned}\frac{d\widehat{\mathbb{P}}_T}{d\mathbb{P}}\Big|_{\mathscr{F}_t} &= \exp\left(\int_0^t \sqrt{v_u}\,dW_u^S + \int_0^t \sqrt{\widehat{v}_u}\,d\widehat{W}_u^S\right)\\ &\quad\times \exp\left(-\frac{1}{2}\int_0^t (v_u+\widehat{v}_u)\,du\right).\end{aligned}$$

Proof. Straightforward computations show that

$$\begin{aligned}\frac{d\widehat{\mathbb{P}}_T}{d\mathbb{P}}\Big|_{\mathscr{F}_t} &= \frac{d\widehat{\mathbb{P}}_T}{d\mathbb{P}_T}\Big|_{\mathscr{F}_t}\frac{d\mathbb{P}_T}{d\mathbb{P}}\Big|_{\mathscr{F}_t}\\
&= \exp\left(\int_0^t \widetilde{\sigma}_F(u,T)\cdot d\widetilde{W}_u^T - \frac{1}{2}\int_0^t \|\widetilde{\sigma}_F(u,T)\|^2\,du\right)\\
&\quad\times \exp\left(-\int_0^t \sigma_r n(u,T)\sqrt{r_u}\,dW_u^r - \frac{1}{2}\int_0^t \sigma_r^2 n^2(u,T) r_u\,du\right)\\
&= \exp\left(\int_0^t \left(\sqrt{v_u}\,dW_u^S + \sqrt{\widehat{v}_u}\,d\widehat{W}_u^S + \sigma_d n_d(u,T)\sqrt{r_u}\,dW_u^T\right)\right)\\
&\quad\times \exp\left(-\frac{1}{2}\int_t^T \left(v_u+\widehat{v}_u+\sigma_r^2 n^2(u,T) r_u\right)du\right)\\
&\quad\times \exp\left(-\int_0^t \sigma_r n(u,T)\sqrt{r_u}\,dW_u^r - \frac{1}{2}\int_0^t \sigma_r^2 n^2(u,T) r_u\,du\right).\end{aligned}$$

Using (4.9), we now obtain

$$\begin{aligned}\frac{d\widehat{\mathbb{P}}_T}{d\mathbb{P}}\Big|_{\mathscr{F}_t} &= \exp\left(\int_0^t \sqrt{v_u}\,dW_u^S + \sqrt{\widehat{v}_u}\,d\widehat{W}_u^S\right)\\ &\quad\times \exp\left(-\frac{1}{2}\int_0^t (v_u+\widehat{v}_u)\,du\right),\end{aligned}$$

which is the desired expression. □

In view of the formula established in Lemma 4.8 and the abstract Bayes formula, to compute $f_1(\phi) = f_1(\phi,t,S_t,v_t,\widehat{v}_t,r_t)$, it suffices to focus on the following conditional expectation under $\mathbb{P}$

$$\begin{aligned}f_1(\phi) &= \mathbb{E}_t^{\mathbb{P}}\Big\{\exp\left(i\phi x_T\right)\exp\Big(\textstyle\int_t^T \sqrt{v_u}\,dW_u^S + \int_t^T \sqrt{\widehat{v}_u}\,d\widehat{W}_u^S\\ &\qquad - \frac{1}{2}\int_t^T \left(v_u+\widehat{v}_u\right)du\Big)\Big\}.\end{aligned} \tag{4.13}$$

Similarly, in view of formula (4.8), we obtain for $f_2(\phi) = f_2(\phi,t,S_t,v_t,\widehat{v}_t,r_t)$

$$f_2(\phi) = \mathbb{E}_t^{\mathbb{P}}\left\{\exp(i\phi x_T)\exp\left[-\int_t^T \sigma_r n(u,T)\sqrt{r_u}\,dW_u^r - \frac{1}{2}\int_t^T \sigma_r^2 n^2(u,T) r_u\,du\right]\right\}. \tag{4.14}$$

To proceed, we will need the following result, which is an immediate consequence of Lemma 4.5.

Corollary 4.9. *Under Assumptions (A.1)–(A.4), the process $x_t = \ln F(t,T)$ admits the following representation under the forward martingale measure $\mathbb{P}_T$*

$$x_T = x_t + \int_t^T \widetilde{\sigma}_F(u,T)\cdot d\widetilde{W}_u^T - \frac{1}{2}\int_t^T \|\widetilde{\sigma}_F(u,T)\|^2 du + J^S(t,T) - \lambda_S\mu_S(T-t)$$

or, more explicitly,

$$\begin{aligned} x_T = x_t \quad & + \textstyle\int_t^T \sqrt{v_u}\, dW_u^S + \int_t^T \sqrt{\widehat{v}_u}\, d\widehat{W}_u^S + \int_t^T \sigma_r n(u,T)\sqrt{r_u}\, dW_u^T \quad - \displaystyle\frac{1}{2}\int_t^T \left(v_u + \widehat{v}_u + \sigma_r^2 n^2(u,T) r_u\right) du \\ & + \textstyle\sum_{k=N_t^S+1}^{N_T^S} \ln(1+J_k^S) - \lambda_S\mu_S(T-t). \end{aligned}$$

Using equality (4.13) and Corollary 4.9, we obtain

$$\begin{aligned} f_1(\phi) \quad = \quad & \mathbb{E}_t^{\mathbb{P}}\Bigg\{ \exp\left(i\phi x_T\right) \exp\Bigg[\int_t^T \sqrt{v_u}\, dW_u^S + \int_t^T \sqrt{\widehat{v}_u}\, d\widehat{W}_u^S \\ & - \frac{1}{2}\int_t^T \left(v_u + \widehat{v}_u\right) du\Bigg]\Bigg\} \end{aligned}$$

so that

$$\begin{aligned} f_1(\phi) \quad = \quad & \mathbb{E}_t^{\mathbb{P}}\Bigg\{ \exp\left[i\phi\left(x_t + \int_t^T \sqrt{v_u}\, dW_u^S + \int_t^T \sqrt{\widehat{v}_u}\, d\widehat{W}_u^S\right)\right] \\ & \times \exp\left[i\phi\left(\int_t^T \sigma_r n(u,T)\sqrt{r_u}\, dW_u^T\right)\right] \\ & \times \exp\left[-\frac{i\phi}{2}\int_t^T \left(v_u + \widehat{v}_u + \sigma_r^2 n^2(u,T) r_u\right) du\right] \\ & \times \exp\left[\int_t^T \sqrt{v_u}\, dW_u^S + \int_t^T \sqrt{\widehat{v}_u}\, d\widehat{W}_u^S\right] \\ & \times \exp\left[-\frac{1}{2}\int_t^T \left(v_u + \widehat{v}_u\right) du\right] \\ & \times \exp\left[i\phi J^S(t,T) - i\phi\lambda_S\mu_S(T-t)\right]\Bigg\}. \end{aligned}$$

We denote $\alpha = 1 + i\phi$, $\beta = i\phi$ and $c_t = \exp(i\phi x_t)$. After simplifications and rearrangement, the formula above becomes

$$\begin{aligned} f_1(\phi) \quad = \quad & c_t\, \mathbb{E}_t^{\mathbb{P}}\Bigg\{ \exp\left[\alpha\left(\int_t^T \sqrt{v_u}\, dW_u^S + \int_t^T \sqrt{\widehat{v}_u}\, d\widehat{W}_u^S - \frac{1}{2}\int_t^T v_u\, du - \frac{1}{2}\int_t^T \widehat{v}_u\, du\right)\right] \\ & \times \exp\left[\beta\left(\int_t^T \sigma_r n(u,T)\sqrt{r_u}\, dW_u^T - \frac{1}{2}\int_t^T \sigma_r^2 n^2(u,T) r_u\, du\right)\right] \\ & \times \exp\left[\beta J^S(t,T) - \beta\lambda_S\mu_S(T-t)\right]\Bigg\}. \end{aligned}$$

In view of Assumptions (A.1)–(A.6), we may use the following representation for the Brownian motion W^Q

$$W_t^S = \rho_1 W_t^v + \sqrt{1-\rho^2}\, W_t \tag{4.15}$$

where $W = (W_t)_{t\in[0,T]}$ is a Brownian motion under $\mathbb{P}$ independent of the Brownian motions $W^S, W^v, \widehat{W}^v$ and W^r.

$$\widehat{W}_t^S = \rho_2 \widehat{W}_t^{\widehat{v}} + \sqrt{1-\widehat{\rho}^2}\, \widehat{W}_t$$

where $\widehat{W} = (\widehat{W}_t)_{t\in[0,T]}$ is a Brownian motion under $\mathbb{P}$ independent of the Brownian motions $W^v, \widehat{W}^v, W^S$ and W^r . Consequently, the conditional characteristic function $f_1(\phi)$ can be represented in the following way

$$\begin{aligned} f_1(\phi) \quad = \quad & c_t\, \mathbb{E}_t^{\mathbb{P}}\Bigg\{ \exp\left[\alpha\rho\int_t^T \sqrt{v_u}\, dW_u^v + \alpha\sqrt{1-\rho^2}\int_t^T \sqrt{v_u}\, dW_u - \frac{\alpha}{2}\int_t^T v_u\, du\right] \\ & \times \exp\left[\alpha\widehat{\rho}\int_t^T \sqrt{\widehat{v}_u}\, d\widehat{W}_u^{\widehat{v}} + \alpha\sqrt{1-\widehat{\rho}^2}\int_t^T \sqrt{\widehat{v}_u}\, d\widehat{W}_u - \frac{\alpha}{2}\int_t^T \widehat{v}_u\, du\right] \\ & \times \exp\left[\beta\left(\int_t^T \sigma_r n(u,T)\sqrt{r_u}\, dW_u^T - \frac{1}{2}\int_t^T \sigma_r^2 n^2(u,T) r_u\, du\right)\right] \\ & \times \exp\left[\beta J^S(t,T) - \beta\lambda_S(T-t)\mu_S\right]\Bigg\}. \end{aligned} \tag{4.16}$$

By combining Proposition 3.1 with Definition 4.4, we obtain the following auxiliary result, which will be helpful in the proof of Theorem 4.1.

Lemma 4.10. *Given the dynamics (2.1) of processes $v,\widehat{v}$ and r and formula (4.9), we obtain the following equalities*

$$\int_t^T \sqrt{v_u}\,dW_u^v = \frac{1}{\sigma_v}\Big(v_T - v_t - \theta\tau + \kappa\int_t^T v_u\,du - (Z_T^v - Z_t^v)\Big),$$
$$\int_t^T \sqrt{\widehat{v}_u}\,d\widehat{W}_u^{\widehat{v}} = \frac{1}{\sigma_{\widehat{v}}}\Big(\widehat{v}_T - \widehat{v}_t - \widehat{\theta}\tau + \widehat{\kappa}\int_t^T \widehat{v}_u\,du\Big),$$
$$\int_t^T \sigma_r n_d(u,T)\sqrt{r_u}\,dW_u^T - \frac{1}{2}\int_t^T \sigma_r^2 n^2(u,T) r_u\,du = -n(t,T)r_t - \int_t^T an(u,T)\,du + \int_t^T r_u\,du.$$

Proof. The first asserted formula is an immediate consequence of (2.1). For the second, we recall that the function $n(t,T)$ is known to satisfy the following differential equation, for any fixed $T>0$,

$$\frac{\partial n(t,T)}{\partial t} - \frac{1}{2}\sigma_r^2 n^2(t,T) - bn(t,T) + 1 = 0$$

with the terminal condition $n(T,T)=0$. Therefore, using the Itô formula and equality (4.9), we obtain

$$\begin{aligned}
d(n(t,T)r_t) &= r_t\,dn(t,T) + n(t,T)\,dr_t\\
&= r_t\Big(\frac{1}{2}\sigma_r^2 n^2(t,T) + bn(t,T) - 1\Big)dt + n_d(t,T)(a - br_t)\,dt + n(t,T)\sigma_d\sqrt{r_t}\,dW_t^r\\
&= \frac{1}{2}\sigma_r^2 n^2(t,T) r_t\,dt - r_t\,dt + n(t,T)a\,dt + n(t,T)\sigma_r\sqrt{r_t}\,dW_t^r\\
&= -\frac{1}{2}\sigma_r^2 n^2(t,T) r_t\,dt - r_t\,dt + n(t,T)a\,dt + n(t,T)\sigma_r\sqrt{r_t}\,dW_t^T.
\end{aligned}$$

This yields the second asserted formula, upon integration between t and T. The derivation of the last one is based on the same arguments and thus it is omitted. □

4.2. Proof of theorem 4.1

The proof of Theorem 4.1 is split into two steps in which we deal with $f_1(\phi)$ and $f_2(\phi)$, respectively.
Step 1. We will first compute $f_1(\phi)$. By combining (4.16) with the equalities derived in Lemma 4.10, we obtain the following representation for $f_1(\phi)$

$$\begin{aligned}
f_1(\phi) \;=\; & c_t\,\mathbb{E}_t^{\mathbb{P}}\Bigg\{\exp\Big[-\frac{\alpha\rho}{\sigma_v}\Big[(v_t+\theta\tau) + \Big(\widehat{v}_t + \widehat{\theta}\tau\Big)\Big]\\
&\times\exp\Big[\Big(\frac{\alpha\rho\kappa}{\sigma_v} - \frac{\alpha}{2}\Big)\int_t^T v_u\,du + \Big(\frac{\alpha\widehat{\rho}\widehat{\kappa}}{\sigma_{\widehat{v}}} - \frac{\alpha}{2}\Big)\int_t^T \widehat{v}_u\,du\Big]\\
&\times\exp\Big[\alpha\sqrt{1-\rho^2}\int_t^T\sqrt{v_u}\,dW_u + \frac{\alpha\rho}{\sigma_v}v_T\Big]\\
&\times\exp\Big[\alpha\sqrt{1-\widehat{\rho}^2}\int_t^T\sqrt{\widehat{v}_u}\,d\widehat{W}_u + \frac{\alpha\widehat{\rho}}{\sigma_{\widehat{v}}}\widehat{v}_T\Big]\\
&\times\exp\Big[-\beta\Big(n(t,T)r_t + \int_t^T an(u,T)\,du\Big) + \beta\int_t^T r_u\,du\Big]\\
&\times\exp\Big[\beta J^S(t,T) - \beta\lambda_S\mu_S(T-t) - \frac{\alpha\rho}{\sigma_v}(Z_T^v - Z_t^v)\Big]\Bigg\}.
\end{aligned}$$

Recall the well-known property that if ζ has the standard normal distribution then $\mathbb{E}\big(e^{z\zeta}\big) = e^{z^2/2}$ for any complex number $z\in\mathbb{C}$. Consequently, by conditioning first on the sample path of the process $(v,\widehat{v},r)$ and using the independence of the processes $(v,\widehat{v},r)$ and W under $\mathbb{P}$ and Lemma 4.2, we obtain

$$\begin{aligned}
f_1(\phi) \;=\; & c_t\exp\Big[\lambda_S\tau\Big((1+\mu_S)^{\beta}e^{-\frac{1}{2}\beta\gamma\sigma_S^2} - 1\Big)\Big]\\
&\times\exp\Big[-\Big(\beta\lambda_S\mu_S\tau + \lambda_v\tau\frac{\rho\alpha\mu_v}{\sigma_v + \rho\alpha\mu_v} + \frac{\alpha\rho}{\sigma_v}(v_t+\theta\tau) + \frac{\alpha\widehat{\rho}}{\sigma_{\widehat{v}}}(\widehat{v}_t + \widehat{\theta}\tau)\Big)\Big]\\
&\times\exp\Big[-\beta\Big(n(t,T)r_t + \int_t^T an(u,T)\,du\Big)\Big]\\
&\times\mathbb{E}_t^{\mathbb{P}}\Bigg\{\exp\Big[\frac{\alpha\rho}{\sigma_v}v_T + \Big(\frac{\alpha^2(1-\rho^2)}{2} + \frac{\alpha\rho\kappa}{\sigma_v} - \frac{\alpha}{2}\Big)\int_t^T v_u\,du\Big]\\
&\times\exp\Big[\frac{\alpha\widehat{\rho}}{\sigma_{\widehat{v}}}\widehat{v}_T + \Big(\frac{\alpha^2(1-\widehat{\rho}^2)}{2} + \frac{\alpha\widehat{\rho}\widehat{\kappa}}{\sigma_{\widehat{v}}} - \frac{\alpha}{2}\Big)\int_t^T \widehat{v}_u\,du\Big]\\
&\times\exp\Big[\beta\int_t^T r_u\,du\Big]\Bigg\}.
\end{aligned}$$

where we denote $\gamma = 1 - i\phi$. This in turn implies that the following equality holds

$$\begin{aligned} f_1(\phi) &= c_t \exp\left[\lambda_S \tau\left((1+\mu_S)^\beta e^{-\frac{1}{2}\beta\gamma\sigma_S^2} - 1\right)\right] \\ &\times \exp\left[-\left(\beta\lambda_S\mu_S\tau + \lambda_v \tau \frac{\rho\alpha\mu_v}{\sigma_v + \rho\alpha\mu_v} + \frac{\alpha\rho}{\sigma_v}(v_t + \theta\tau) + \frac{\alpha\widehat{\rho}}{\sigma_{\widehat{v}}}(\widehat{v}_t + \widehat{\theta}\tau)\right)\right] \\ &\times \exp\left[-\beta\left(n(t,T)r_t + \int_t^T an(u,T)\,du\right)\right] \\ &\times \mathbb{E}_t^{\mathbb{P}}\left\{\exp\left[-s_1 v_T - s_2\int_t^T v_u\,du - s_3\widehat{v}_T - s_4\int_t^T \widehat{v}_u\,du\right]\right. \\ &\times \left.\exp\left[-s_5 r_T - s_6\int_t^T r_u\,du\right]\right\} \end{aligned}$$

where the constants $s_1, s_2, s_3, s_4, s_5, s_6$ are given by (4.4). A direct application of Lemma 4.3 furnishes an explicit formula for $f_1(\phi)$, as reported in the statement of Theorem 4.1.

Step 2. In order to compute the conditional characteristic function

$$f_2(\phi) = f_2(\phi, t, S_t, v_t, \widehat{v}_t, r_t) = \mathbb{E}_t^{\mathbb{P}_T}\left[\exp(i\phi x_T)\right]$$

we proceed in an analogous manner as for $f_1(\phi)$. We first recall that (see (4.14))

$$f_2(\phi) = \mathbb{E}_t^{\mathbb{P}}\left\{\exp(i\phi x_T)\exp\left[-\int_t^T \sigma_r n(u,T)\sqrt{r_u}\,dW_u^r - \frac{1}{2}\int_t^T \sigma_r^2 n^2(u,T) r_u\,du\right]\right\}.$$

Therefore, using Corollary 4.9, we obtain

$$\begin{aligned} f_2(\phi) &= c_t\,\mathbb{E}_t^{\mathbb{P}}\left\{\exp\left[i\phi\left(\int_t^T \sqrt{v_u}\,dW_u^S + \int_t^T \sqrt{\widehat{v}_u}\,d\widehat{W}_u^S + J^S(t,T)\right)\right]\right. \\ &\times \exp\left[i\phi\left(\int_t^T \sigma_r n(u,T)\sqrt{r_u}\,dW_u^T\right)\right] \\ &\times \exp\left[-i\phi\left(\frac{1}{2}\int_t^T (v_u + \sigma_r^2 n^2(u,T) r_u)\,du\right)\right] \\ &\times \left.\exp\left[-\int_t^T \sigma_r n(u,T)\sqrt{r_u}\,dW_u^r - \frac{1}{2}\int_t^T \sigma_r^2 n^2(u,T) r_u\,du\right]\right\}. \end{aligned}$$

Consequently, using formulae (4.9), (4.15) and Lemma 4.2, we obtain the following expression for $f_2(\phi)$

$$\begin{aligned} f_2(\phi) &= c_t \exp\left[\lambda_S\tau\left((1+\mu_S)^\beta e^{-\frac{1}{2}\beta\gamma\sigma_S^2} - 1\right) - \beta\lambda_S\mu_S\tau\right] \\ &\times \mathbb{E}_t^{\mathbb{P}}\left\{\exp\left[\beta\left(\rho\int_t^T \sqrt{v_u}\,dW_u^v + \sqrt{1-\rho^2}\int_t^T \sqrt{v_u}\,dW_u\right)\right]\right. \\ &\times \exp\left[\beta\left(\widehat{\rho}\int_t^T \sqrt{\widehat{v}_u}\,d\widehat{W}_u^v + \sqrt{1-\widehat{\rho}^2}\int_t^T \sqrt{\widehat{v}_u}\,d\widehat{W}_u\right)\right] \\ &\times \exp\left[-\beta\left(\frac{1}{2}\int_t^T (\widehat{v}_u + \widehat{v}_u)\,du\right)\right] \\ &\times \left.\exp\left[-\gamma\left(\int_t^T \sigma_r n(u,T)\sqrt{r_u}\,dW_u^r + \frac{1}{2}\int_t^T \sigma_r^2 n^2(u,T) r_u\,du\right)\right]\right\}. \end{aligned}$$

Similarly as in the case of $f_1(\phi)$, we condition on the sample path of the process $(v, \widehat{v}, r)$ and we use the postulated independence of the processes $(v, \widehat{v}, r)$ and W under $\mathbb{P}$. By invoking also Lemma 4.2, we obtain

$$\begin{aligned} f_2(\phi) &= c_t \exp\left[\lambda_S\tau\left((1+\mu_S)^\beta e^{-\frac{1}{2}\beta\gamma\sigma_S^2} - 1\right) - \beta\lambda_S\mu_S\tau\right] \\ &\mathbb{E}_t^{\mathbb{P}}\left\{\exp\left[\beta\rho\int_t^T \sqrt{v_u}\,dW_u^v + \frac{\beta^2(1-\rho^2) - \beta}{2}\int_t^T v_u\,du\right]\right. \\ &\times \exp\left[\beta\widehat{\rho}\int_t^T \sqrt{\widehat{v}_u}\,d\widehat{W}_u^v + \frac{\beta^2(1-\widehat{\rho}^2) - \beta}{2}\int_t^T \widehat{v}_u\,du\right] \\ &\times \left.\exp\left[-\gamma\left(\int_t^T \sigma_r n(u,T)\sqrt{r_u}\,dW_u^r + \frac{1}{2}\int_t^T \sigma_r^2 n(u,T) r_u\,du\right)\right]\right\}. \end{aligned}$$

Using Lemma 4.10, we conclude that

$$
\begin{aligned}
f_2(\phi) \quad = \quad & c_t \exp\left[\lambda_S \tau \left((1+\mu_S)^{\beta} e^{-\frac{1}{2}\beta\gamma\sigma_S^2} - 1\right)\right] \\
& \times \exp\left[-\left(\beta\lambda_S\mu_S\tau + \lambda_v\tau\frac{\rho\beta\mu_v}{\sigma_v+\rho\beta\mu_v} + \frac{\beta\rho}{\sigma_v}(v_t+\theta\tau) + \frac{\beta\widehat{\rho}}{\sigma_{\widehat{v}}}(\widehat{v}_t+\widehat{\theta}\tau)\right)\right] \\
& \times \exp\left[-\gamma\left(n(t,T)r_t + \int_t^T an(u,T)\,du\right)\right] \\
& \times \mathbb{E}_t^{\mathbb{P}}\left\{\exp\left[-q_1 v_T - q_2\int_t^T v_u\,du - q_3\widehat{v}_T - q_4\int_t^T \widehat{v}_u\,du\right]\right. \\
& \left.\times \exp\left[-q_5 r_T - q_6\int_t^T r_u\,du\right]\right\}
\end{aligned}
$$

with the coefficients $q_1, q_2, q_3, q_4, q_5, q_6$ reported in formula (4.5). Another straightforward application of Lemma 4.3 yields the closed-form expression (4.3) for the conditional characteristic function $f_2(\phi)$.
To complete the proof of Theorem 4.1, it suffices to combine formula (4.12) with the standard inversion formula (4.1) providing integral representations for the conditional probabilities

$$P_1(t, S_t, v_t, \widehat{v}_t, r_t, K) = \widehat{\mathbb{P}}_T(x_T > \ln K \,|\, S_t, v_t, \widehat{v}_t, r_t)$$

and

$$P_2(t, S_t, v_t, \widehat{v}_t, , r_t, K) = \mathbb{P}_T(x_T > \ln K \,|\, S_t, v_t, \widehat{v}_t, r_t).$$

This ends the derivation of the pricing formula for the call option. The price of the corresponding put option is readily available as well, due to the put-call parity relationship (4.17).

$$C_t(T,K) - P_t(T,K) = S_t - KB(t,T) \tag{4.17}$$

where $C_t(T,K)$ and $P_t(T,K)$ are prices of the call and put options, respectively. □

5. Model calibration and empirical analysis

In this section we estimate the parameters for DHJDH model considered in this paper using Dow Jones Industrial implied volatilities(IV) quoted May 10, 2012 [26] and compare the model's empirical performance with that of the Double Heston Model considered by Christoffersen et.al [2] and the Heston model. In this analysis we have assumed constant interest rates. Calibration of DHJDH model parameters

$$\Theta = \{\lambda_S, \mu_S, \lambda_V, \mu_V, \theta, \widehat{\theta}, \kappa, \widehat{\kappa}, \sigma_v, \sigma_{\widehat{v}}, \rho, \widehat{\rho}, \sigma_S, v_1, v_2\}$$

was performed using Interior Point optimisation. Further, the US treasury yield curve rates for one, three, six and twelve -months have been used as a proxy for the initial interest rates for the different maturities. To fit the model to market implied volatilities we use the approximation implied volatility root mean squared error(`IVRMSE`) loss function considered by Christoffersen et.al.[2], also Carr and Wu [13] and Trolle and Schwartz [27].

$$\texttt{IVRMSE} \approx \sqrt{\frac{1}{N}\sum_{t,k}\left(\frac{C_{t,k}^M - C_{t,k}^{\Theta}}{\texttt{BSVega}_{t,k}}\right)^2} \tag{5.1}$$

where $C_{t,k}^M$ is the market price, $C_{t,k}^{\Theta}$ is the model price,and BSVega(t,k) is the Black Scholes sensitivity of the option computed using the implied volatility from the market price of the option, $C_{t,k}^M$. Interior point optimization is used to obtain the set of parameters that minimise the objective function in equation (5.1).
Using the data from Table 1, the parameter estimates Θ for the univariate, double Heston and Double Heston Jump-Diffusion Hybrid models, along with their estimation error are found in Table 2. If we compare the calibrated parameters for the Double Heston and DHJDH models, we notice that κ, σ and v_0 are similar, implying that the calibrated Double Heston parameters can be used as a seed for when calibrating the DHJDH Model. One practical consequence of this is that the Double Heston parameters can be fitted fairly robustly using longer dated options and then jump parameters can be found to generate the extra skew for short-dated options.
The panels in figure 5.1 show the implied volatility surfaces for the double Heston and DHJDH Models for all strikes and across all times to maturities. These figures show that theoretical implied volatilities of the DHJDH model provide satisfactory approximation for the observed implied volatilities across all maturities and across all strikes but particularly outperforms out-of-sample calls for the double Heston Model across all expiries ranging from 37 to 226 days(short dated options). This improvement is achieved through the inclusion of jumps in the dynamics of the stock price and the volatility processes and using only one set of model parameters.
To visualise how well the DHJDH fits the market IV, we have provided contour plots in Figure 5.2, of the Market IV and the predicted market IV using the DHJDH model. Note that the market IV contour plot was generated using the data from Table 1 and the model contour plot was generated using the DHJDH model, therefore the resolution of the model contour is much finer since we can compute many points of the contour, while the resolution of the market contour is coarse since we are only able to use the provided data points. The difference in resolution can be seen from the straight contour lines in the market IV contour plot, while the model contour lines are much smoother due to the abundance of generated contour points from the model. Other than this, the contour plots are very similar, implying that the DHJDH model provides a good fit to the market data.

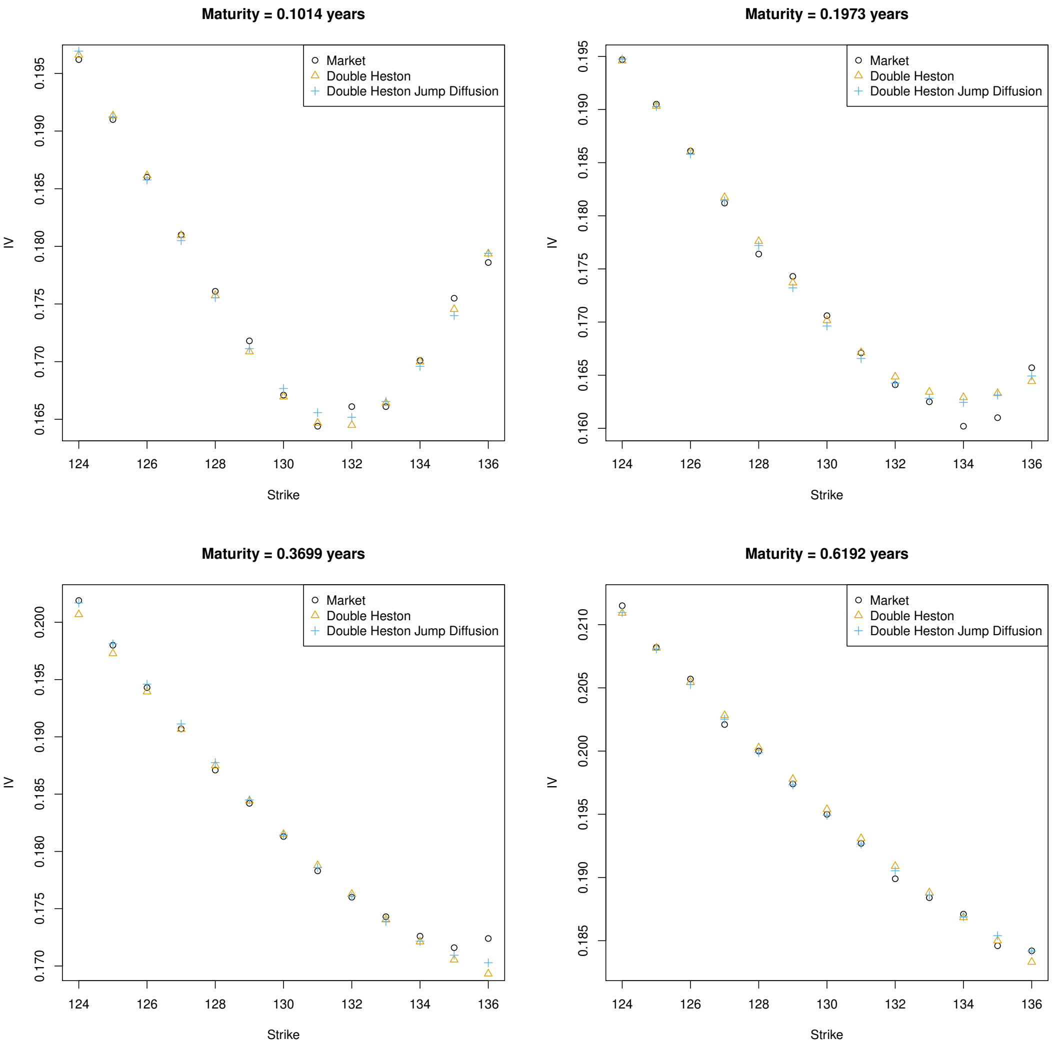

Figure 5.1: The implied volatility for various strike prices at four maturity times. Each plot shows the market IV, the calibrated Double Heston IV and the calibrated DHJDH IV.

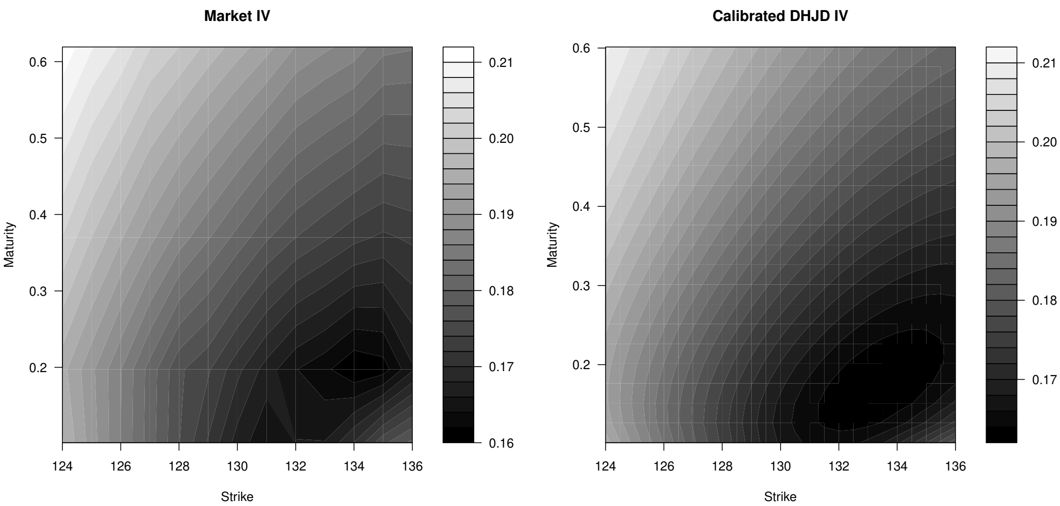

Figure 5.2: Contour plots showing the implied volatility for the given strike prices and maturities from market data (left) and the calibrated DHJDH Model (right).

Strike	Maturity			
	37	72	135	226
124	19.62	19.47	20.19	21.15
125	19.10	19.05	19.8	20.82
126	18.60	18.61	19.43	20.57
127	18.10	18.12	19.07	20.21
128	17.61	17.64	18.71	20.00
129	17.18	17.43	18.42	19.74
130	16.71	17.06	18.13	19.50
131	16.44	16.71	17.83	19.27
132	16.61	16.41	17.60	18.99
133	16.61	16.25	17.43	18.84
134	17.01	16.02	17.26	18.71
135	17.55	16.10	17.16	18.46
136	17.86	16.57	17.24	18.42

Table 1: S&P 500 index Implied Volatilities for strike prices ranging from 124 to 136 and maturities from 37 to 226 days.

Method	κ	θ	σ	v_0	ρ	IVMSE
Univariate	0.8998	0.1721	1.3390	0.0325	-0.3716	3.951×10^{-4}
Double Heston	2.7994	0.0716	0.9565	0.0179	-0.8510	1.227×10^{-4}
	18.4552	0.0074	1.8167	0.0221	0.7557	
DHJDH	2.2336	0.1642	0.5424	0.0092	-0.8372	1.039×10^{-4}
	18.9014	0.0179	1.8764	0.0287	0.1547	
	λ_V	λ_S	μ_S	μ_V	σ_S	
	0.0047	0.0617	2.0541	0.7108	2.2827	

Table 2: Calibrated parameters of the Double Heston Jump-Diffusion Hybrid Model, along with the Single and Double Heston model calibrated parameters. The last column shows the model mean square error.

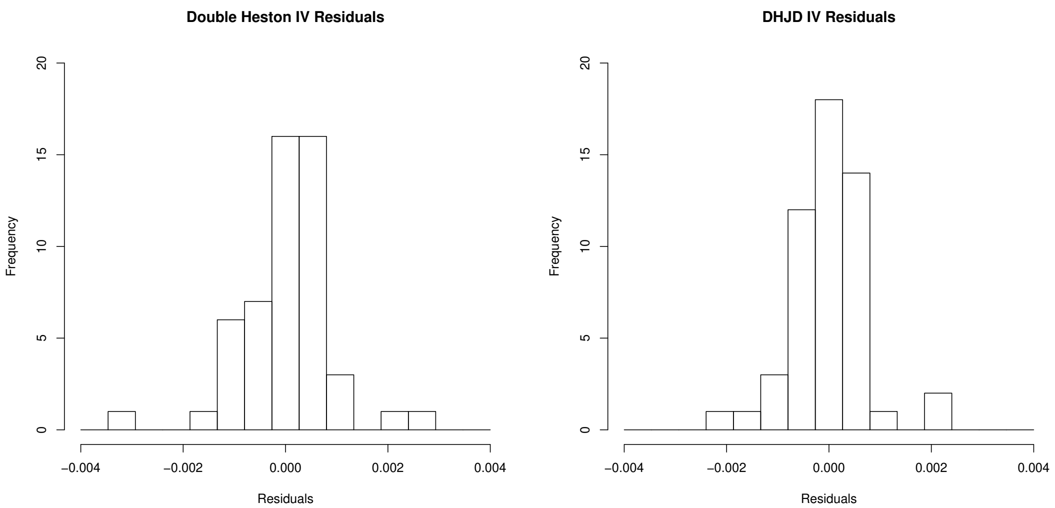

Figure 5.3: Histogram of the residuals of the Double Heston (left) and DHJDH (right) models.

Finally, we will examine the model residuals. Figure 5.3 contains the histograms of the Double Heston residuals and the Double DHJDH residuals. We can see from the histograms that the majority of the residuals for the Double DHJDH model are located near zero, with only a few residuals located further than ± 0.001, while the Double Heston residuals are more widely spread between -0.002 and 0.002. The smaller residuals from the DHJDH model is a clear indication it having a smaller IVRMSE then the Double Heston model.

References

[1] S.L. Heston, *A closed-form solution for options with stochastic volatility with applications to bond and currency options*, Rev. Fin. Stud., **6** (1993), 327–343.
[2] P. Christoffersen, S. Heston, C. Jacobs, *The shape and term structure of the index option smirk: Why multifactor stochastic volatility models work so well*, Management Sci., **55** (2009), 1914–1932.
[3] J. C. Cox, J. E. Ingersoll, S. A Ross, *A theory of term structure of interest rates*, Econometrica, **53** (1985), 385–408.
[4] J. Gatheral, *The Volatility Surface*, John Wiley, 2006.
[5] M. C. Recchioni, Y. Sun, *An explicitly solvable Heston model with stochastic interest rates*, European J. Oper. Res., **249** (2016), 359–377.
[6] G. Bakshi, C. Cao, Z. Chen, *Empirical performance of alternative option pricing models*, J. Finance, **5** (1997), 2003–2049.
[7] D. Bates, *Jumps and stochastic volatility: exchange rate processes implicit in Deutsche Mark options*, Rev. Fin. Stud., **9** (1996), 69–107.
[8] D. Duffie, J. Pan, K. Singleton, *Transform analysis and asset pricing for affine jump-diffusions*, Econometrica, **68** (2000), 1343–1376.
[9] T. Andersen, J. Andreasen, *Jump-diffusion processes: Volatility smile fitting and numerical methods*, J. Fin. Econ., **4** (2000), 231–262.
[10] B. Eraker, M. Johannes, N. Polson, *The impacts of jumps in volatility and returns*, J. Finance, **58** (2003), 1269–1300.
[11] A. L. Lewis, *Option Valuation under Stochastic Volatility II*, Finance Press, New Port Beach, California, USA 2016.
[12] R. Cont, T. Kokholm, *A consistent pricing model for index options and volatility derivatives*, Math. Finance, **23** (2013), 248–274.
[13] P. Carr, L. Wu, *Stochastic skewness in currency options*, J. Fin. Econ., **86** (2007), 213–244.
[14] A. Van Haastrecht, R. Lord, A. Pelsser, D. Schrager, *Pricing long-maturity equity and FX derivatives with stochastic interest rates and stochastic volatility*, Insurance Math. Econom., **45** (2009), 436–448.
[15] R. Schöbel, J. Zhu, *Stochastic volatility with an Ornstein-Uhlenbeck process: An extension*, Europ. Finance Rev., **3** (1999), 23–46.
[16] O. Vasicek, *An equilibrium characterisation of the term structure*, J. Fin. Econ., **5** (1977), 177–188.
[17] A. Van Haastrecht, A. Pelsser, *Generic pricing of FX, inflation and stock options under stochastic interest rates and stochastic volatility*, Quant. Fin., **11** (2011), 665–691.
[18] L. A. Grzelak, C. W. Oosterlee, *On the Heston model with stochastic interest rates*, SIAM J. Fin. Math., **2** (2011), 255–286.
[19] L. A. Grzelak, C. W. Oosterlee, *On the Heston model with stochastic interest rates*, Appl. Math. Finance, **19** (2012), 1–35.
[20] L. A. Grzelak, C. W. Oosterlee, S. Van Weeren, *Extension of stochastic volatility models with Hull-White interest rate process*, Quant. Finance, **12** (2012), 89–105.
[21] A. Cozma, C. Reisinger, *Convergence of an Euler discretisation scheme for the Heston stochastic-local volatility model with CIR interest rates*, available at http://ideas.repec.org/p/arx/papers/1501.06084.html
[22] R. Ahlip, M. Rutkowski, *Semi-analytical pricing of currency options in the Heston/CIR jump-diffusion Hybrid model*, Appl. Math. Finance, **22** (2015), 1–27.
[23] B. Wong, C. C. Heyde, *On the martingale property of stochastic exponentials*, J. Appl. Probab., **41** (2004), 654–664.
[24] M. Musiela, M. Rutkowski, *Martingale Methods in Financial Modelling*, Springer, Berlin, 2005.
[25] M. Jeanblanc, M. Yor, M. Chesney, *Mathematical Methods for Financial Markets*, Springer, Berlin, 2009.
[26] R. Ahlip, M. Rutkowski, *Pricing of foreign exchange options under the Heston stochastic volatility model and the CIR interest rates*, Quant. Finance, **13** (2013), 955–966.
[27] A. S. Trolle, *Unspanned stochastic volatility and the pricing of commodity derivatives*, Rev. Financ. Stud., **22** (2009), 4423–4461.
[28] C. Bernard, Z. Cui, C. McLeish, *Nearly exact option price simulation using characteristic functions*, Int. J. Theor. Appl. Finance, 2012, 1250047, 29 pages.
[29] D. Brigo, A. Alfonsi, *Credit default swaps calibration and option pricing with the SSRD stochastic intensity and interest-rate model*, Finance Stochast., **9** (2005), 29–42.
[30] P. Carr, D. Madan, *Option valuation using the fast Fourier transform*, J. Comput. Finance, **2** (1999), 61–73.
[31] P. Carr, D. Madan, *Saddlepoint methods for option pricing*, J. Comput. Finance, **13** (2009), 49–61.
[32] P. Carr, L. Wu, *Time-changed Levy Processes and option pricing*, J. Financ. Econ., **17** (2004), 113–141.
[33] S. Levendorskiĭ, *Efficient pricing and reliable calibration in the Heston model*, Int. J. Theor. Appl. Finance, **15** (2012), 1250050, 44 pages.
[34] R. Lord, C. Kahl, *Optimal Fourier inversion in semi-analytical option pricing*, J. Comput. Finance, **10** (2007), 1–30.
[35] R. Lord, C. Kahl, *Complex logarithms in Heston-like models*, Math. Finance, **20** (2010), 671–694.
[36] F.D. Rouah, *The Heston model: And it's extensions in Matlab and C*, J. Wiley & Sons, 2013.

Journal of Mathematical Sciences and Modelling, 1 (3) (2018) 153-157
Research Article

Journal of Mathematical Sciences and Modelling

Journal Homepage: www.dergipark.gov.tr/jmsm
ISSN: 2636-8692

A New Generalization of Non-Unique Fixed Point Theorems of Ćirić for Akram-Zafar-Siddiqui Type Contraction

Memudu O. Olatinwo[a*]

[a]*Department of Mathematics, Faculty of Science, Obafemi Awolowo University, Ile-Ife, Nigeria*
[*]*Corresponding author*

Article Info

Keywords: *Non-unique fixed point, Ćirić's type, Akram-Zafar-Siddiqui type contractions*
2010 AMS: *47H10, 54H25, 55M20*
Received: *18 April 2018*
Accepted: *14 September 2018*
Available online: *30 December 2018*

Abstract

In this article, we establish some fixed point theorems of Ćirić's type for Akram-Zafar-Siddiqui type contractive mappings having non-unique fixed points. Our results generalize, extend and improve several ones in the literature.

1. Introduction

Let (X,d) be a complete metric space and $T : X \to X$ a self-mapping of X. Suppose that $F(T) = \{x \in X \mid Tx = x\}$ is the set of fixed points of T.
The following definitions shall be required in the sequel: $O(x,T) = \{x, Tx, T^2x, \cdots, T^nx, \cdots\}$ =orbit of T at x.

Definition 1.1. *Ćirić [1]: A metric space (X,d) is said to be $T-$orbitally complete if $T : X \to X$ is a selfmapping and if any Cauchy subsequence $\{T^{n_i}x\}$ in orbit $O(x,T)$, with $x \in X$, converges in X.*

Definition 1.2. *An operator $T : X \to X$ is orbitally continuous if*

$$\lim_{i\to\infty} d(T^{n_i}x, x^*) = 0 \implies \lim_{i\to\infty} d(T(T^{n_i}x), Tx^*) = 0.$$

Definition 1.2 was originally stated in the following equivalent form in Ćirić [1]:
An operator $T : X \to X$ is said to be *orbitally continuous* if $T^{n_i}x \to x^* \implies T(T^{n_i}x) \to Tx^*$ as $i \to \infty$.
Indeed, the notions in both Definition 1.1 and Definition 1.2 were first introduced by Ćirić [1] in 1971 to obtain some fixed point theorems. The definitions are also contained in Ćirić [2].
There are non-linear equations which may arise in applications and whose fixed points are not necessarily unique. Ćirić [3] established some results pertaining to this notion of non-unique fixed points. The classical Banach's fixed point theorem was established by Banach [4], using the following contractive definition: there exists $c \in [0,1)$ (fixed) such that $\forall\, x,\ y \in X$,

$$d(Tx,Ty) \le c\, d(x,y). \tag{1.1}$$

However, it is crucial to say that the mappings satisfying the contractive condition (1.1) are necessarily continuous. In order to have a wider class of contractive mappings than those satisfying (1.1), Kannan [5] generalized the Banach's fixed point theorem by employing the following contractive definition: there exists $a \in [0, \frac{1}{2})$ such that

$$d(Tx,Ty) \le a[d(x,Tx) + d(y,Ty)],\ \forall\, x,\ y \in X. \tag{1.2}$$

So, the mappings satisfying (1.2) need not be continuous and this is a very nice initiative by the author [5]. Several authors have generalized and extended Banach's fixed point theorem using similar notion as in (1.2). Interested readers may also consult Chatterjea [6], Zamfirescu [7] and a host of others in the literature.

Email address and ORCID number: **memudu.olatinwo@gmail.com/molaposi@yahoo.com/polatinwo@oauife.edu.ng ???????????(M. O. Olatinwo)**

However, it is noteworthy to say that several contractive conditions including Banach's contractive condition (1.1) have always been concerned with establishing the existence and uniqueness of the fixed point of the mapping. Therefore, in order to include mappings whose fixed points may be not unique, Ćirić [3] introduced a new technique involving contractive conditions for such mappings, realizing the fact that there are also nonlinear equations with more than one fixed point as aforementioned. In particular, Ćirić [3] introduced, amongst others, the following two contractive conditions: For a mapping $T: X \to X$, there exists $\lambda \in (0,1)$ such that $\forall\, x,\ y \in X$,

$$\min\{d(Tx,Ty),d(x,Tx),d(y,Ty)\}-\min\{d(x,Ty),d(y,Tx)\} \leq \lambda d(x,y), \tag{1.3}$$

where T is orbitally continuous; and also there exists $\lambda \in (0,1)$ such that $\forall\, x,\ y \in X$,

$$\min\{d(Tx,Ty),\max\{d(x,Tx),d(y,Ty)\}\}-\min\{d(x,Ty),d(y,Tx)\} \leq \lambda d(x,y). \tag{1.4}$$

Another contractivity condition worthy of note is the following:

Definition 1.3. *(Akram et al. [8]): A selfmap $T: X \to X$ of a metric space (X,d) is said to be A-contraction if it satisfies the condition:*

$$d(Tx,Ty) \leq \beta(d(x,y),d(x,Tx),d(y,Ty)),\ \forall\, x,\ y \in X, \tag{1.5}$$

and some $\beta \in A$, where A is the set of all functions $\beta: \boldsymbol{R}_+^3 \to \boldsymbol{R}_+$ satisfying
(i) β is continuous on the set $\boldsymbol{R}_+^3$ (with respect to the Euclidean metric on $\boldsymbol{R}^3$);
(ii) $a \leq kb$ for some $k \in [0,1)$ whenever $a \leq \beta(a,b,b)$, or $a \leq \beta(b,a,b)$, or, $a \leq \beta(b,b,a)$, $\forall\, a,\ b \in \boldsymbol{R}_+$.

Akram *et al.* [8] employed the contractive condition (1.5) to prove that if X is a complete metric space, then the mapping T has a unique fixed point.
Olatinwo [9] generalized the results of Akram et al. [8] by employing the following more general contractive condition:

Definition 1.4. *(Olatinwo [9]): A selfmap $T: X \to X$ of a metric space (X,d) is said to be a generalized A-contraction* or G_A-contraction *if it satisfies the condition:*

$$d(Tx,Ty) \leq \alpha(d(x,y),d(x,Tx),d(y,Ty),[d(x,Tx)]^r[d(y,Tx)]^p d(x,Ty),d(y,Tx)[d(x,Tx)]^m),$$

$\forall\, x,\ y \in X,\ r,\ p,\ m \in \boldsymbol{R}_+$ and some $\alpha \in G_A$, where G_A is the set of all functions $\alpha: \boldsymbol{R}_+^5 \to \boldsymbol{R}_+$ satisfying
(i) α is continuous on the set $\boldsymbol{R}_+^5$ (with respect to the Euclidean metric on $\boldsymbol{R}^5$);
(ii) if any of the conditions $a \leq \alpha(b,b,a,c,c)$, or, $a \leq \alpha(b,b,a,b,b)$, or, $a \leq \alpha(a,b,b,b,b)$ holds for some $a,\ b,\ c \in \boldsymbol{R}_+$, then there exists $k \in [0,1)$ such that $a \leq kb$.

The contractive mappings of both Akram *et al.* [8] and Ćirić [3] are our motivation for the present article. Therefore, in this paper, we prove various and more general non-unique fixed point theorems by employing on a complete metric space for selfmappings by using Akram-Zafar-Siddiqui type contractive conditions which are hybrids of those used in [3, 8, 9]. Our results are generalizations, extensions and improvemens of the results of Ćirić [3] and those of the author [10, 11, 12]. Many unique fixed point theorems in the literature involving those of Akram *et al.* [8] are also special cases of the results of the present article. One can consult the reference section for detail on unique fixed point theorems. For excellent study of mappings having non-unique fixed points, we refer to Achari [13, 14, 15], Ćirić [2, 3, 16], Karapinar [17] and Pachpatte [18].
To prove our results, we shall employ the following more general contractive conditions than those stated in (1.3) and (1.4)
(a) For a mapping $T: X \to X$, there exists a function $\beta: \mathbf{R}_+^5 \to \mathbf{R}_+$ such that $\forall\, x,\ y \in X$, we have

$$\begin{gathered}\min\{d(Tx,Ty),d(x,Tx),d(y,Ty)\}-\min\{d(x,Ty),d(y,Tx)\} \leq \\ \beta(d(x,y),d(x,Tx),d(y,Ty),[d(x,Tx)]^r[d(y,Tx)]^p d(x,Ty),d(y,Tx)[d(x,Tx)]^m);\end{gathered} \tag{1.6}$$

$\forall\, x,\ y \in X,\ r,\ p,\ m \in \mathbf{R}_+$, where the function β satisfies:
(i) β is continuous on the set $\mathbf{R}_+^5$ (with respect to the Euclidean metric on $\mathbf{R}^5$);
(ii) there exists some $\lambda \in [0,1)$, such that $a \leq \lambda b$ whenever $a \leq \beta(b,b,a,c,c)$, $\forall\, a,\ b,\ c \in \mathbf{R}_+$.
(b) For a mapping $T: X \to X$, there exists a function $\beta: \mathbf{R}_+^5 \to \mathbf{R}_+$ such that $\forall\, x,\ y \in X$, we have

$$\begin{gathered}\min\{d(Tx,Ty),\max\{d(x,Tx),d(y,Ty)\}\}-\min\{d(x,Ty),d(y,Tx)\} \leq \\ \beta(d(x,y),d(x,Tx),d(y,Ty),[d(x,Tx)]^r[d(y,Tx)]^p d(x,Ty),d(y,Tx)[d(x,Tx)]^m),\end{gathered} \tag{1.7}$$

$\forall\, x,\ y \in X,\ r,\ p,\ m \in \mathbf{R}_+$, where the function β satisfies:
(i) β is continuous on the set $\mathbf{R}_+^5$ (with respect to the Euclidean metric on $\mathbf{R}^5$);
(ii) there exists some $\lambda \in [0,1)$, such that $a \leq \lambda b$ whenever $a \leq \beta(b,b,a,c,c)$, or, $a \leq \beta(b,b,a,b,b)$, $\forall\, a,\ b,\ c \in \mathbf{R}_+$.

Remark 1.5. *Each of the contractive conditions (1.6) and (1.7) can be reduced to several other ones in the literature. In particular, we have the following:*
(i) It is obvious that both contractive conditions (1.3) and (1.4) are special cases of contractive conditions (1.6) and (1.7) respectively if $\beta(t_1,t_2,t_3,t_4,t_5) = \lambda t_1,\ \forall\, (t_1,t_2,t_3) \in \boldsymbol{R}_+^5,\ \lambda \in (0,1)$.

2. Main results

Theorem 2.1. *Let (X,d) be a complete metric space and $T : X \to X$ an orbitally continuous mapping satisfying contractive condition (1.6). For $x_0 \in X$, let $\{x_n\}_{n=0}^{\infty}$ defined by $x_n = Tx_{n-1} = T^n x_0,\ n = 0,1,2,\cdots$, be the Picard iteration associated with T. Then, T has a fixed point.*

Proof. We have that $x_n = Tx_{n-1} = T^n x_0,\ x_0 \in X\ (n = 0,1,2,\cdots)$. If $d(x_q, x_{q+1}) = 0$ for some $q \geq 0$, then x_0 is the limit point of $\{T^n x_0\}$ and x_q is a fixed point of T. Suppose that $d(x_n, x_{n+1}) > 0,\ n = 0,1,2,\cdots$. Using condition (1.6) with $x = x_n,\ y = x_{n+1}$, we have

$$\begin{aligned} &\min\{d(Tx_n, Tx_{n+1}), d(x_n, Tx_n), d(x_{n+1}, Tx_{n+1})\} - \min\{d(x_n, Tx_{n+1}), d(x_{n+1}, Tx_n)\} \\ &\leq \beta(d(x_n, x_{n+1}), d(x_n, Tx_n), d(x_{n+1}, Tx_{n+1}), [d(x_n, Tx_n)]^r [d(x_{n+1}, Tx_n)]^p d(x_n, Tx_{n+1}), d(x_{n+1}, Tx_n)[d(x_n, Tx_n)]^m), \end{aligned}$$

from which we obtain that

$$\min\{d(x_{n+1}, x_{n+2}), d(x_n, x_{n+1})\} \leq \beta(d(x_n, x_{n+1}), d(x_n, x_{n+1}), d(x_{n+1}, x_{n+2}), 0, 0). \tag{2.1}$$

Since $\lambda < 1$, we choose $\min\{d(x_{n+1}, x_{n+2}), d(x_n, x_{n+1})\} = d(x_{n+1}, x_{n+2})$ and apply Property (ii) of β so that from (2.1) we get

$$d(x_{n+1}, x_{n+2}) \leq \beta(d(x_n, x_{n+1}), d(x_n, x_{n+1}), d(x_{n+1}, x_{n+2}), 0, 0) \leq \lambda d(x_n, x_{n+1}),$$

which yields

$$d(x_{n+1}, x_{n+2}) \leq \lambda d(x_n, x_{n+1}) \leq \lambda^2 d(x_{n-1}, x_n) \leq \cdots \leq \lambda^{n+1} d(x_0, x_1). \tag{2.2}$$

Using (2.2) inductively in the repeated application of the triangle inequality yields, for $p \in \mathbb{N}$,

$$d(x_n, x_{n+p}) \leq \frac{\lambda^n (1-\lambda^p)}{1-\lambda} d(x_0, x_1) \to\ 0 \text{ as n} \to \infty. \tag{2.3}$$

Hence, from (2.3) we have that $\{x_n\}$ is a Cauchy sequence in X. Since (X,d) is a complete metric space, there exists $u \in X$ such that $\lim\limits_{n\to\infty} d(x_n, u) = 0$, that is, $\lim\limits_{n\to\infty} x_n = u$. Therefore, since $x_n = T^n x_0$ and T is orbitally continuous, we have

$$0 = d(\lim_{n\to\infty} T(T^n x_0), Tu) = \lim_{n\to\infty} d(T(T^n x_0), Tu) = \lim_{n\to\infty} d(Tx_n, Tu) = \lim_{n\to\infty} d(x_{n+1}, Tu) = d(u, Tu).$$

Thus, proving that $Tu = u$, that is, $u \in X$ is a fixed point of T. □

Theorem 2.2. *Let (X,d) be a complete metric space and $T : X \to X$ a mapping satisfying contractive condition (1.7) For $x_0 \in X$, let $\{x_n\}_{n=0}^{\infty}$ defined by $x_n = Tx_{n-1} = T^n x_0,\ n = 0,1,2,\cdots$, be the Picard iteration associated with T. Then, T has a fixed point.*

Proof. We have that $x_n = Tx_{n-1} = T^n x_0,\ x_0 \in X\ (n = 0,1,2,\cdots)$. If $d(x_q, x_{q+1}) = 0$ for some $q \geq 0$, then x_0 is the limit point of $\{T^n x_0\}$ and x_q is a fixed point of T. Suppose that $d(x_n, x_{n+1}) > 0,\ n = 0,1,2,\cdots$. Using condition (1.7) with $x = x_n,\ y = x_{n+1}$, we have

$$\begin{aligned} &\min\{d(Tx_n, Tx_{n+1}), \max\{d(x_n, Tx_n), d(x_{n+1}, Tx_{n+1})\}\} - \min\{d(x_n, Tx_{n+1}), d(x_{n+1}, Tx_n)\} \leq \\ &\beta(d(x_n, x_{n+1}), d(x_n, Tx_n), d(x_{n+1}, Tx_{n+1}), [d(x_n, Tx_n)]^r [d(x_{n+1}, Tx_n)]^p d(x_n, Tx_{n+1}), d(x_{n+1}, Tx_n)[d(x_n, Tx_n)]^m), \end{aligned}$$

which reduces to

$$\begin{aligned} &\min\{d(x_{n+1}, x_{n+2}), \max\{d(x_n, x_{n+1}), d(x_{n+1}, x_{n+2})\}\} \leq \\ &\qquad \beta(d(x_n, x_{n+1}), d(x_n, x_{n+1}), d(x_{n+1}, x_{n+2}), 0, 0). \end{aligned} \tag{2.4}$$

Since

$$\min\{d(x_{n+1}, x_{n+2}), \max\{d(x_n, x_{n+1}), d(x_{n+1}, x_{n+2})\}\} = \max\{d(x_n, x_{n+1}), d(x_{n+1}, x_{n+2})\},$$

we obtain from (2.4) that

$$\max\{d(x_{n+1}, x_{n+2}), d(x_n, x_{n+1})\} \leq \beta(d(x_n, x_{n+1}), d(x_n, x_{n+1}), d(x_{n+1}, x_{n+2}), 0, 0). \tag{2.5}$$

Again, since $\lambda < 1$, we choose $\max\{d(x_{n+1}, x_{n+2}), d(x_n, x_{n+1})\} = d(x_{n+1}, x_{n+2})$, so that from (2.5) we obtain

$$d(x_{n+1}, x_{n+2}) \leq \beta(d(x_n, x_{n+1}), d(x_n, x_{n+1}), d(x_{n+1}, x_{n+2}), 0, 0) \leq \lambda d(x_n, x_{n+1}),$$

which inductively leads again (as in the proof of Theorem 2.1) to

$$d(x_n, x_{n+1}) \leq \lambda^n d(x_0, x_1).$$

For $p \in \mathbb{N}$, we therefore, have again as in the proof of Theorem 2.1 that $d(x_n, x_{n+p}) \to 0$ as $n \to \infty$.
Hence, we have that $\{x_n\}$ is a Cauchy sequence in X. Since (X,d) is complete, there exists $u \in X$ such that $\lim\limits_{n\to\infty} x_n = u$.
Using (1.7) again with $x = x_n,\ y = u$ we obtain

$$\begin{aligned} &\min\{d(Tx_n, Tu), \max\{d(x_n, Tx_n), d(u, Tu)\}\} - \min\{d(x_n, Tu), d(u, Tx_n)\} \leq \\ &\beta(d(x_n, u), d(x_n, Tx_n), d(u, Tu), [d(x_n, Tx_n)]^r [d(u, Tx_n)]^p d(x_n, Tu), d(u, Tx_n)[d(x_n, Tx_n)]^m), \end{aligned}$$

which reduces to

$$\min\{d(x_{n+1},Tu),\max\{d(x_n,x_{n+1}),d(u,Tu)\}\}-\min\{d(x_n,Tu),d(u,x_{n+1})\}\leq \\ \beta(d(x_n,u),d(x_n,x_{n+1}),d(u,Tu),[d(x_n,x_{n+1})]^r[d(u,x_{n+1})]^p d(x_n,Tu),d(u,x_{n+1})[d(x_n,x_{n+1})]^m). \tag{2.6}$$

As $n\to\infty$, we obtain from (2.6) that

$$\min\{d(u,Tu),d(u,Tu)\}\leq\beta(0,0,d(u,Tu),0,0). \tag{2.7}$$

Using Property(ii) of β in (2.7) yields

$$d(u,Tu)\leq\beta(0,0,d(u,Tu),0,0)\leq\lambda.0=0,$$

from which it follows that $d(u,Tu)\leq 0$.
Therefore, due to nonnegativity of the metric, we obtain $d(Tu,u)=0\iff Tu=u$. Thus, T has a fixed point $u\in X$. □

The next two results are Maia type (see [19]) which extend both Theorem 2.1 and Theorem 2.2

Theorem 2.3. *Let X be a non-empty set, d and ρ two metrics on X and $T\colon X\to X$ a mapping. For $x_0\in X$, let $\{x_n\}_{n=0}^{\infty}$ defined by $x_{n+1}=Tx_n,\ n=0,1,2,\cdots$, be the Picard iteration associated with T. Suppose that*
(i) there exists $M>0$ such that $\rho(Tx,Ty)\leq Md(x,y),\ \forall\, x,\ y\in X$;
(ii) (X,ρ) is a complete metric space;
(iii) $T\colon (X,\rho)\to(X,\rho)$ is orbitally continuous;
(iv) $T\colon (X,d)\to(X,d)$ is a mapping satisfying (Δ).
Then, $T\colon (X,\rho)\to(X,\rho)$ has a fixed point.

Proof. By condition (iv), we obtain as in Theorem 2.1 that, for $p\in\mathbb{N}, d(x_n,x_{n+p})\to 0$ as n $\to\infty$. That is, $\{x_n\}$ is a Cauchy sequence in (X,d).
We now show that $\{x_n\}$ is a Cauchy sequence in (X,ρ) as follows: By condition (i), we have, for $p\in\mathbb{N}$,

$$\rho(x_n,x_{n+p})=\rho(Tx_{n-1},Tx_{n+p-1})\leq Md(x_{n-1},x_{n+p-1})\to 0 \text{ as } n\to\infty,$$

that is, $\rho(x_n,x_{n+p})\to 0$ as n $\to\infty$. Thus, $\{x_n\}$ is a Cauchy sequence in (X,ρ) too.
By condition (ii), (X,ρ) is a complete metric space implies that there exists $u\in X$ such that $\lim\limits_{n\to\infty}\rho(x_n,u)=0$, that is, $\lim\limits_{n\to\infty}x_n=u$.
By condition (iii), since $x_n=T^nx_0$ and $T\colon (X,\rho)\to(X,\rho)$ is orbitally continuous, we have

$$0=\rho(\lim_{n\to\infty}T(T^nx_0),Tu)=\lim_{n\to\infty}\rho(T(T^nx_0),Tu)=\lim_{n\to\infty}\rho(Tx_n,Tu)=\lim_{n\to\infty}\rho(x_{n+1},Tu)=\rho(u,Tu).$$

Therefore, $\rho(u,Tu)=0\iff Tu=u$. So, T has a fixed point u. □

Theorem 2.4. *Let X be a non-empty set, d and ρ two metrics on X and $T\colon X\to X$ a mapping. For $x_0\in X$, let $\{x_n\}_{n=0}^{\infty}$ defined by $x_{n+1}=Tx_n,\ n=0,1,2,\cdots$, be the Picard iteration associated with T. Suppose that*
(i) there exists $M>0$ such that $\rho(Tx,Ty)\leq Md(x,y),\ \forall\, x,\ y\in X$;
(ii) (X,ρ) is a complete metric space;
(iii) $T\colon (X,\rho)\to(X,\rho)$ is continuous;
(iv) $T\colon (X,d)\to(X,d)$ is a mapping satisfying $(\Delta\star)$.
Then, $T\colon (X,\rho)\to(X,\rho)$ has a fixed point.

Proof. By condition (iv), we obtain as in Theorem 2.2 that $\{x_n\}$ is a Cauchy sequence in (X,d).
By condition (i), we have as in Theorem 2.3 that $\{x_n\}$ is a Cauchy sequence in (X,ρ) too.
By condition (ii), (X,ρ) is a complete metric space implies that there exists $u\in X$ such that $\lim\limits_{n\to\infty}\rho(x_n,u)=0$, that is, $\lim\limits_{n\to\infty}x_n=u$.
By condition (iii), since $T\colon (X,\rho)\to(X,\rho)$ is continuous, we have

$$0=\lim_{n\to\infty}\rho(x_{n+1},u)=\lim_{n\to\infty}\rho(Tx_n,u)=\rho(T(\lim_{n\to\infty}x_n),u)=\rho(Tu,u).$$

Therefore, $\rho(u,Tu)=0\iff Tu=u$. So, T has a fixed point u. □

Remark 2.5. *Our results generalize and extend several classical results in the literature, involving unique and nonunique fixed points. In particular, both Theorem 2.1 and Theorem 2.2 are generalizations and extensions of the corresponding results of Ćirić [3, 2]. Both Theorem 2.3 and Theorem 2.4 extend both Theorem 2.1 and Theorem 2.2 respectively as well as the corresponding results of Ćirić [3, 2]. Both Theorem 2.3 and Theorem 2.4 also generalize the result of Maia [19]. Indeed, the results of our present paper generalize the corresponding results of Olatinwo [10, 11, 12], but independent of the corresponding results of the author [20]. We also observe that the unique fixed point theorems of Akram et al. [8] are special cases of the results contained in this paper.*

Remark 2.6. *We also employ this medium to announce that while proving the existence of the fixed point of T, the term "$d(T\lim\limits_{n\to\infty}(T^nx_0),Tu)$" that appeared was a typographical misprint in Theorem 2.1 and Theorem 2.3 of [10] as well as in Theorem 2.1 and Theorem 2.4 of [20]. Since T is orbitally continuous in those Theorems (rather than being continuous), the misprint should change to "$d(\lim\limits_{n\to\infty}T(T^nx_0),Tu)$" (which is now correctly expressed in the present article). Our interested readers can also see the correct term "$d(\lim\limits_{n\to\infty}T(T^nx_0),Tu)$" in the articles [11, 12] (which invariably becomes "$\lim\limits_{n\to\infty}d(T(T^nx_0),Tu)$" since metric is continuous).*

3. Conclusion

So far, the results obtained in the present article are the most general results in non-unique fixed point theory.

Acknowledgement

This paper is dedicated to the late Professor Ljubomir Ćirić (one of my great mentors) who was born on Tuesday, 13th August, 1935 and whose demise occurred on Saturday, 23rd July, 2016. He was a pioneering expert of Fixed Point Theory in Serbia.

References

[1] Lj. B. Ćirić, *On contraction type mappings,* Math. Balkanica, **1** (1971), 52-57.
[2] Lj. B. Ćirić, *Some Recent Results in Metrical Fixed Point Theory,* University of Belgrade, 2003.
[3] Lj. B. Ćirić, *On some maps with a nonunique fixed point*, Publ. Inst. Math., **17** (31) (1974), 52-58.
[4] S. Banach, *Sur les operations dans les ensembles abstraits et leur applications aux equations integrales*, Fund. Math., **3** (1922), 133-181.
[5] R. Kannan, *Some results on fixed points*, Bull. Calcutta Math. Soc., **10** (1968), 71-76.
[6] S. K. Chatterjea, *Fixed-point theorems,* C. R. Acad. Bulgare Sci., **10** (1972), 727-730.
[7] T. Zamfirescu, *Fix point theorems in metric spaces*, Arch. Math., **23** (1972), 292-298.
[8] M. Akram, A. A. Zafar, A. A. Siddiqui, *A general class of contractions: $A-$contractions*, Novi Sad J. Math., **38**(1) (2008), 25-33.
[9] M. O. Olatinwo, *Some new fixed point theorems in complete metric spaces*, Creat. Math. Inf. **21**(2) (2012), 189-196.
[10] M. O. Olatinwo, *Non-unique fixed point theorems of Ćirić's type for rational hybrid contractions*, Nanjing Univ. J. Math. Biquarterly, **31**(2) (2014), 140-149.
[11] M. O. Olatinwo, *Some Ćirić's type non-unique fixed point theorems and rational type contractive conditions*, Kochi J. Math., **10** (2015), 1-9.
[12] M. O. Olatinwo, *Some non-unique fixed point theorems of Ciric's type using rational type contractive conditions*, Georgian Math. J., **24**(3) (2017), 455-461.
[13] J. Achari, *On Ciric's nonunique fixed points*, Mat. Vesnik, **13**(28) (1976), 255-257.
[14] J. Achari, *Results on nonunique fixed points*, Publ. Inst. Math. Nouvelle Serie, **26**(40) (1979), 5-9.
[15] J. Achari, *On the generalization of Pachpatte's nonunique fixed point theorem*, Indian J. Pure Appl. Math., **13**(3) (1982), 299-302.
[16] Lj. B. Ćirić, N. Jotić, *A further extension of maps with nonunique fixed points*, Mat. Vesnik, **50** (1998), 1-4.
[17] E. Karapinar, *Some nonunique fixed point theorems of Ciric type on cone metric spaces*, Abstr. Appl. Anal., **2010**, Article ID 123094, 14 pages.
[18] B. G. Pachpatte, *On Ciric type maps with a non-unique fixed point*, Indian J. Pure Appl. Math., **10**(8) (1979), 1039-1043.
[19] M. G. Maia, *Un'osservazione sulle contrazioni metriche*, Rend. Sem. Mat. Univ. Padova, **40** (1968), 139-143.
[20] M. O. Olatinwo, *Non-unique fixed point theorems of Achari and Ciric-Jotic types for hybrid contractions*, J. Adv. Math. Stud., **9**(2) (2016), 226-234.
[21] R. P. Agarwal, M. Meehan, D. O'Regan, *Fixed Point Theory and Applications*, Cambridge University Press, 2004.
[22] T. Basu, *Extension of Ciric's fixed point theorem in a uniform space*, Ranchi Univ. Math. J., **11** (1980), 109-115.
[23] V. Berinde, *Iterative Approximation of Fixed Points,* Editura Efemeride, 2002.
[24] V. Berinde, *Approximating Fixed Points of Weak Contractions using Picard Iteration*, Nonlinear Anal. Forum, **9**(1) (2004), 43-53.
[25] V. Berinde, *Iterative Approximation of Fixed Points*, Springer-Verlag Berlin Heidelberg (2007).
[26] D. S. Jaggi, *Some unique fixed point theorems,* Indian J. Pure Appl. Math., **8**(2) (1977), 223-230.
[27] M. A. Khamsi, W. A. Kirk, *An Introduction to Metric Spaces and Fixed Point Theory*, John Wiley & Sons, Inc. (2001).
[28] A. R. Khan, V. Kumar, N. Hussain, *Analytical and numerical treatment of Jungck-type iterative scheme,* Appl. Math. Comput., **231** (2014), 521-535.
[29] M. O. Olatinwo, *Some stability and convergence results for Picard, Mann, Ishikawa and Jungck type iterative algorithms for Akram-Zafar-Siddiqui type contraction mappings,* Nonlinear Anal. Forum, **21**(1) (2016), 65-75.
[30] I. A. Rus, *Generalized Contractions and Applications,* Cluj Univ. Press, Cluj Napoca, 2001.
[31] I. A. Rus, A. Petrusel, G. Petrusel; *Fixed Point Theory, 1950-2000, Romanian contributions,* House of the Book of Science, Cluj Napoca, 2002.
[32] E. Zeidler, *Non-Linear Functional Analysis and Its Applications-Fixed Point Theorems*, Springer-Verlag, New York, Inc., 1986.

Journal of Mathematical Sciences and Modelling, *1 (3) (2018) 158-180*
Research Article

Journal of Mathematical Sciences and Modelling

Journal Homepage: www.dergipark.gov.tr/jmsm
ISSN: 2636-8692

Computational Enumeration of Colorings of Hyperplanes of Hypercubes for all Irreducible Representations and Applications

Krishnan Balasubramanian[a*]

[a]*School of Molecular Sciences, Arizona State University, Tempe, AZ 85287-1604*
[*]*Corresponding author*

Article Info

Keywords: *Combinatorial Enumerations, Colorings of hypercubes, Character Tables of hypercubes, Pólya Theory for all charters, Character cycle indices for all hyperplanes*
2010 AMS: *15A03, 15A63, 15A72.*
Received: *18 October 2018*
Accepted: *29 November 2018*
Available online: *30 December 2018*

Abstract

We obtain the generating functions for the combinatorial enumeration of colorings of all hyperplanes of hypercubes for all irreducible representations of the hyperoctahedral groups. The computational group theoretical techniques involve the construction of generalized character cycle indices of all irreducible representations for all hyperplanes of the hypercube using the Möbius function, polynomial generators for all cycle types and for all hyperplanes. This is followed by the construction of the generating functions for colorings of all (n-q)-hyperplanes of the hypercube, for example, vertices (q=5), edges (q=4), faces (q=3), cells (q=2) and tesseracts (q=4) for a 5D-hypercube. Tables are constructed for the combinatorial numbers for coloring all hyperplanes of 5D-hypercubes for 36 irreducible representations. Applications to chirality, chemistry and biology are also pointed out.

1. Introduction

Hypercubes [1]-[29] and related combinatorics of wreath product groups [30]-[54] have been the focus of a number of research investigations owing to their importance in numerous applications in a variety of disciplines. Hypercubes are natural representations of Boolean functions, as 2n possible Boolean functions from a set of n entities that take binary values can be represented by the vertices of a hypercube. Thus hypercubes find applications in chemistry, biology, finite automata, electrical circuits, genetics, enumeration of isomers, isomerization reactions, visualization and computer graphics, chirality, protein-protein interactions, intrinsically disordered proteins, partitioning of massively large databases, and parallel computing [1]-[11], [19]-[29], [41]-[55], [56]-[59]. The automorphism groups of hypercubes which are hyperoctahedral wreath products find applications in enumerative combinatorics, isomerization reactions, chirality, nuclear spin statistics, weakly-bound non-rigid water clusters, non-rigid molecules, and in proteomics [41]-[55], [56]-[59]. The hypercubes have also been connected to Goldbach conjecture, last Fermat's theorem, Erdös discrepancy conjecture, modern multi-dimensional representation of time measures, quantum similarity measures, [1]-[5], biochemical imaging [6], multi-dimensional imaging [19],[20], [22]-[26], classification of large data, Quantitative Shape-Activity Relations (QShAR)etc. [7]-[10].

Combinatorial enumeration of colorings of different hyperplanes, especially vertices of hypercubes has been the topic of several studies for the past two centuries. In fact, subsequent to publication of his classic 1937 [15] paper on combinatorics of groups, graphs and chemical compounds, Pólya in a subsequent work [17] has pointed out the errors in previous enumeration of colorings of vertices hypercubes. As pointed out recently by Banks et al. [19],[20] in the context of computer visualization, in 1877, Clifford [12],[13] has enumerated the number of equivalence classes for 2-colorings of a 4D-hypercube vertices as 396 which was subsequently shown to be incorrect by Pólya [17] in 1940 who obtained 402 equivalence classes for 2-colorings of a 4d-hypercube. Historically Pólya's theorem was anticipated in Redfield's paper on superposition theorem [16]. Although in more recent mathematical literature, cycle indices of hypercubes and enumerations of colorings of the vertices of hypercubes have been considered [17]-[29], [34] these studies have been restricted only to the totally symmetric irreducible representations of the hyperoctahedral groups. Moreover in the most recent work on the 5D-hypercube enumeration [29] of vertex colorings there are errors, as we show here. Pólya's theorem and its variation [1]-[6], [17]-[21] have been applied extensively which generate equivalence classes for different distribution of colors called the pattern inventory and also the total number of colorings. However, several chemical and spectroscopic applications require more powerful and generalized enumeration techniques that span all the irreducible representations of the groups where Pólya's theorem becomes a special case for the totally symmetric representation. Furthermore in the

Email address: **kbalu@asu.edu (K. Balasubramanian)**

case of hypercubes, most of the previous combinatorics is restricted to the enumeration of vertex colorings. The vertices of hypercubes are only one of several possible hypercube's hyperplanes. The present author [39]-[40] has generalized Pólya's theorem, De Bruijn's theorem [60] and Harary-Palmer power group theorem [31] to characters of all irreducible representations of a group cast into the form of generalized character cycle indices or GCCIs. Such combinatorial and graph theoretical methods have several applications to rovibronic spectroscopy, non-rigid molecules, water clusters, nuclear spin statistics, multiple-quantum NMR spectroscopy, dynamic NMR, enumeration of isomerization reactions, chirality, ESR spectroscopy, topological indices in QSAR [36]-[58], [61]-[63].

The n-dimensional hypercube's automorphism group is comprised of $2^n \times n!$ operations, and thus the order of this group increases both exponentially and factorially. For example, the automorphism group of a 6D-hypercube consists of 46, 080 operations spanning 65 irreducible representation. In ordinary Pólya's theory, different conjugacy classes that give rise to the same cycle types under group action on a given set are combined into a single term, as they give rise to the same monomial for patterns, and in general with the exception of full symmetric group S_n, multiple conjugacy classes often contribute to the same cycle type. This poses a problem when one needs to consider all irreducible representation, as character values in general are based on conjugacy classes and not cycle types. Furthermore there is no one-to-one correspondence between cycle types and conjugacy classes for hyperoctahedral wreath product groups of hypercubes. Thus we need both cycle types of each conjugacy class and the character table of the group unlike the ordinary Pólya cycle index which only needs the cycle types that compose the cycle index of a group. The other computational challenge that arises for hypercube colorings is that the cycle types of induced permutation for different hyperplanes need to be obtained. In general there are n hyper planes for an nD-hypercube represented by q values ranging from 1 to n with of course q=0 being the trivial single vertex and hence is not considered. When q=n we obtain the vertices of the hypercube, q=n-1 we obtain the edges, q=n-2 yields faces, and in general q represents (n-q)-hyperplanes of an nD-hypercube. Each such hyperplane generates a set of cycle types for each conjugacy class. Thus computing the equivalence classes of the colorings of various hyperplanes requires the computation of the cycle types of different (n-q)-hyperplanes of the hypercube with q=1 through n. Previous works in the mathematical literature [17]-[29] have focused on the total number of equivalence classes rather than the inventory of patterns or a generating function that yields number of colorings for a given number of colors of various kinds. Such a distribution of patterns for various colors is quite important for a number of practical applications, and thus we focus in the present study the computational techniques to obtain such generating functions for all hyperplanes and all irreducible representations of the hypercube. Moreover none of the previous studies [17]-[29] has dealt with irreducible representations other than totally symmetric representation in their enumerations. The present author [11] has previously considered multinomial colorings of 4D-hypercube for different hyperplanes, and with chemical applications to water pentamer in mind, the present author has considered colorings of tesseracts [64] of the 5D-hypercube, and recently vertices (q=4) and tesseracts q=1 for all irreducible representations and 2-colorings of (q=2) 3-faces only for the totally symmetric irreducible representation of the 5D-hypercube [61]. The present work considers for the first time enumeration of colorings for all hyperplanes (q=1 through q=5) of the 5D-hypercube for all 36 irreducible representations.

2. Mathematical and computational techniques

In general, the automorphism group of an nD-hypercube is the wreath product $S_n[S_2]$ where S_n is the full permutation group of n objects comprising of $n!$ permutations. The order of the nD-hypercube wreath product group is $2^n \times n!$ and hence it grows in astronomical proportion as a function of n. For example, the automorphism group of a 10D-hypercube consists of $2^{10} \times 10!$ permutations that give rise to 481 conjugacy classes, and 481 irreducible representations, 10 hyperplanes, thus demonstrating the combinatorial complexity of the problem of enumerating colorings of different hyperplanes of an nD-hypercube for all irreducible representations. Coxeter [65] has discussed in depth hypercubes and various other regular polytopes and their mathematical characterizations using various projections and graph theory. An nD-hypercube is comprised of (n-q)-hyperplanes where q goes from 0 to n. The largest value of q = n represents the vertices, q=n-1 represents the edges, q=n-2 represents the faces, q=n-3 represents the cells, q=n-4 represents tesseracts, and so on. The induced permutation of the automorphism group of the nD-hypercube on each of these hyperplanes is quite different and it cannot be deduced from a simple inspection with the exception of a 2D-hypercube (square) and a 3D-hypercube (a regular cube). Thus the first step is to construct the cycle types for each conjugacy class of the hypercube's wreath product group for the induced permutations of all hyperplanes of the hypercube. We note that although for ordinary Pólya enumeration one needs only the cycle index which can be constructed by other methods as cycle types of several conjugacy classes become degenerate for wreath products, the enumerations that involve all irreducible representations require the cycle types of each conjugacy class, as there is no one-to-one correspondence between the conjugacy classes and cycle types for wreath product groups. The cycle types of q=1 or (n-1)-hyperplanes are the ones that can be readily constructed as they are natural representations of the hypercube permutations.

The techniques to construct the conjugacy class cycle types of q=1 or (n-1)-hyperplanes and the character table for all irreducible representations of the hypercube group involve matrix generating functions and we shall consider this first. We use the 5D-hypercube as not only an illustrative example but also to carry out all of the needed computations. For a 5D-hypercube the special case of q=1 enumerates the various tesseracts of the hypercube, and Fig.1 shows a graph that exemplifies the underlying relationship between the tesseracts of the 5D-hypercube. In Fig. 1 the vertices represent the tesseracts while the edges represent the underlying connectivity among the ten tesseracts of the 5D-hypercube. The cycle types of the permutations of q=1 tesseracts are isomorphic with the permutations of vertices of the automorphism group of the graph in Fig. 1.

In general, let a permutation $g \in S_n$ upon its action on the set Ω of $q = 1$ hyperplanes of the hypercube generate a_1 cycles of length 1, a_2 cycles of length 2, a_3 cycles of length 3, ..., a_n cycles of length n, which can be represented by $1^{a_1}2^{a_2}3^{a_3}\ldots n^{a_n}$. Alternatively, the cycle type T_g of g χ can be denoted as $T_g = (a_1, a_2, a_3, \ldots, a_n)$. As the composing group in $S_n[S_2]$, S_2 of the wreath product has only two conjugacy classes, the conjugacy class of the wreath product $S_n[S_2]$ and he cycle types of action on q=1 hyperplanes can be expressed as a cycle type comprised of a $2 \times n$ matrix, where the first row corresponds to the action of $\{(g;\pi)\}$permutations where $\pi = e \in S_2$ and $g \in S_n$ and the second row represents the permutations $\{(g;\pi)\}$, for $\pi = (12) \in S_2$. The cycle type of any conjugacy class, $T(g;\pi)$, where $(g;\pi)$ is any representative in then a $2 \times n$ matrix is obtained using the orbit structure of $g \in S_n$ and the corresponding conjugacy class of S_2. For the particular case of $S_5[S_2]$ under consideration, the cycle type of $(g;\pi)$ for a conjugacy class of $S_5[S_2]$ is given by

$$T(g;\pi) = a_{ik} \quad (1 \le i \le 2), (1 \le k \le 5) \tag{2.1}$$

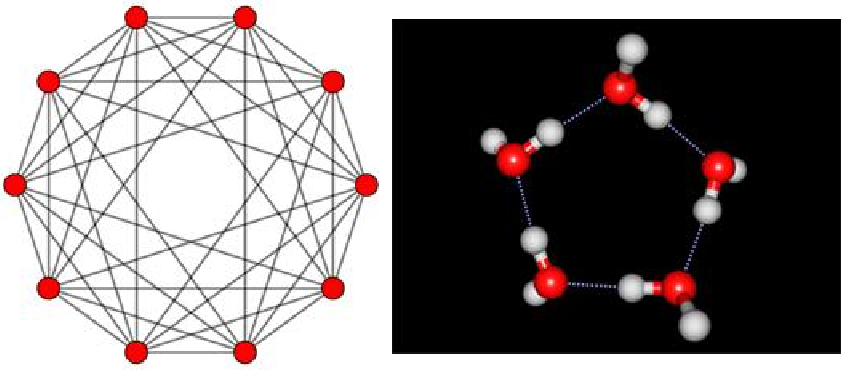

Figure 2.1: Ten tesseracts of the 5D-hypercube are represented by the vertices of the graph shown in this figure (reproduced from ref.[59]). Right: Water Pentamer. The automorphism group of this graph is also the automorphism group of the 5D-hypercube and fully non-rigid water pentamer or S5[S2] comprising of 3840 permutations that span 36 conjugacy classes.

To illustrate, the conjugacy class $\{(1)(2)(345);(12)\}$ of $S_5[S_2]$ given by (2.2)

$$T[\{(1)(2)(345);(12)\}] = \begin{bmatrix} 2\,0\,0\,0\,0 \\ 0\,0\,1\,0\,0 \end{bmatrix} \tag{2.2}$$

Likewise the conjugacy class of $\{(12)(34)(5);(12)\}$(1234)(5); (12) is given by (2.3):

$$T[\{(12)(34)(5);(12)\}] = \begin{bmatrix} 1\ 0\ 0\ 0\ 0 \\ 0\ 0\ 0\ 1\ 0 \end{bmatrix} \tag{2.3}$$

In this manner all conjugacy classes of $S_n[S_2]$ are obtained and for the simplest example of $S_3[S_2]$ which represents the permutations of the six faces of the cube, Table 1 shows all as 2×3 matrices thus constructed for the 3D-cube. In Table 1 we have also shown the corresponding rotations or mirror planes of the cube, as the cycle types of the cube's faces can also be directly obtained by applying these operations on a regular cube and collecting the induced orbits of the permutations of the faces of the cube under the action of these operations. It can be seen from Table 1 that there is no one-to-one correspondence between the cycle types and conjugacy classes of the 3D-cube, as orbit structures of two different matrix types can be the same, for example, for matrices 3 and 5 in Table 1 have the same cycle types of $1^2 2^2$ for the six faces of the cube (q=1). However these two matrices belong to different conjugacy classes with different character values for the various irreducible representations of the octahedral (cubic) group or $S_3[S_2]$. Thus the matrices are important for the enumerations involving all irreducible representations while only the cycle types are needed for the ordinary Pólya enumeration of equivalence classes, as such enumeration becomes a special case of our formalism applied to the totally symmetric A_1 irreducible representation.
We can obtain the orders of the conjugacy classes and the cycle types for the q=1 or (n-1)hyper planes of the hypercube directly from their $2\times n$ matrices. Suppose $P(m)$ denotes the number of partitions of integer m with $P(0)=1$. Then all ordered partitions of n into pairs or compositions of n into two parts, denoted by (n_1,n_2) such that $\sum n_i = n$, yields the number of conjugacy classes of $S_n[S_2]$. That is, the total number of conjugacy classes of $S_n[S_2]$is given by

$$N_C = \sum\nolimits_{(n)} P(n_1)\,P(n_2) \tag{2.4}$$

where the sum is over all ordered pairs of partitions of n. Furthermore, the order any conjugacy class of $S_n[S_2]$ with the matrix type $T(g;\pi) = a_{ik}$ can be obtained with Eq (2.5):

$$|T(g;\pi)| = \frac{n!}{\prod_{i,k} a_{ik}!(2k)^{a_{ik}}} \tag{2.5}$$

For example, for the 6-D hyperoctahedral group, $S_6[S_2]$, the ordered partitions of 6 into 2 parts are given by $\{(6,0),(0,6),(5,1),(1,5),(4,2),(2,4),(3,3)$ and hence the number of conjugacy classes of the $S_6[S_2]$ group is

$$2P(6)P(0) + 2P(5)P(1) + 2P(4)P(2) + P(3)^2 = 65 \tag{2.6}$$

The number of elements in any particular conjugacy class of $S_n[S_2]$ can also be readily computed from the corresponding matrix cycle type. For example, application of (2.5) to the conjugacy class 6 in table 1 gives:

$$\left|\begin{pmatrix} 1\,0\,0 \\ 0\,1\,0 \end{pmatrix}\right| = \frac{3!2^3}{1!(2.1)^1 1!(2.2)^1} = 6 \tag{2.7}$$

The orders of conjugacy classes thus obtained for the cube are shown in Table 1 for each conjugacy class. The cycle types for the permutations induced on the $q=1$ or $(n-1)-$ hyperplanes are also obtained readily from the $2\times n$ matrices by mapping place values for the non-zero entries in the matrix type. That is, assign a cycle of length $\left(k^2\right)^{a_1 k}$ for each non-zero entry column k in the first row while for the second row the contribution is $2k$ for nonzero entries. Thus the above matrix yields the overall cycle type $1^2 2^2$ for the regular cube's 6 faces. The cycle types thus obtained for $q=1$ or tesseracts of the 5D-hypercubeand for all conjugacy classes of the cubic group, $S_3[S_2]$ group are shown in Tables 2 and 1 together with the orders of each conjugacy class.

The above process for finding the cycle types of conjugacy classes and their orders can be likewise applied to the 5D-hypercube and the results are shown in Table 2. The next step is to compute the cycle types of the induced permutations for each conjugacy class for all of the remaining (n-q)-hyperplanes. For the 5d-hypercube this corresponds to $q = 2$ (cells), $q = 3$ (faces), $q = 4$ (edges) and $q = 5$ (vertices). Although there are previous studies [17]-[29] that have discussed the techniques for obtaining the cycle indices of the hypercube including the 5D-hypercube, these previous works have been predominantly restricted to the Pólya cycle indices of the vertices of a hypercube with the exception of Lemmis [23] who has explicitly considered other cycle types for a 4D-hypercube even though Lemmis [23] does not compute or report any results for the equivalence classes even for the totally symmetric irreducible representation . The explicit expressions have also been constructed for the ordinary cycle indices of hypercubes up to six dimensions [26], [28], [29]. In the present study we outline techniques for constructing the generalized character cycle indices for all irreducible representations and all cycle types of the various (n-q)-hyperplanes of the hypercube.

The process of computing the generating functions for the cycle types of various $(n-q)-$ hyperplanes of the hypercube involve the Möbius function, a fundamental enumerative combinatorial technique that encompasses generalization of the fundamental combinatorial principle of inclusion and exclusion that has been applied to many disciplines [66], [67] including music theory [35] and isomers with nearest neighbor exclusions [63]. The Möbius functions appear in a natural way, as the construction of various cycle types for the $(n-q)-$hyperplanes is related to the divisors of the set of all hyperplanes and it relates to the simplest cycle types of $q = 1$. Thus the technique involves computing the polynomial generating functions via Möbius sums. We accomplish this from the matrix types of the conjugacy classes of the $S_n[S_2]$ groups to generate all of the cycle types for all $(n-q)-$hyperplanes through polynomial generating functions. The techniques employed are similar to the ones outlined in Krishnamurthy's book [67] and the work of Lemmis [24] who has made use of the enumerative Möbius inversion technique. That is, the generating functions for all cycle types for all values of q representing $(n-q)-$hyperplanes are generated as coefficient of x^q in the polynomial generating function $Q_p(x)$ obtained using the Möbius functions shown below:

$$Q_p(x) = \frac{1}{p}\sum_{d/p}\mu(p/d)F_d(x) \tag{2.8}$$

where the sum is strictly over all divisors d of p, and $\mu(p/d)$ is the Möbius function which takes values

$1,\ -1,\ -1,\ 0,\ -1,\ 1,\ -1,\ 0,\ 0,\ 1\ \ldots$

for arguments 1 to 10; in general, the Möbius function is obtained as follows for any number:
$\mu(m) = 1$ if one of m's prime factors is not a perfect square and m contains even number of prime factors,
$\mu(m) = -1$ if m satisfies the same perfect-square condition as before but m contains odd number of prime factors,
$\mu(m) = 0$ if m has a perfect square as one of its factors.
$F_d(x)$ in the above Eq (2.8) is defined as a polynomial in x constructed from the matrix cycle types shown in the first column of Table 1 or Table 2. Consider the non-zero columns of the matrix cycle types of $S_n[S_2]$ (see Tables 1 and 2) . Recall that the first row of these elements are represented by a1k while the second rows are denoted by $a_{2k}(k = 1,n)$. Then if p is the period of the matrix type shown in the first column of Table 1 or 2, and define, $g = \gcd(k;p)$, $p' = \frac{k}{g}$, $h = \gcd(2k;p)$; $p'' = \frac{2k}{h}$ and define the polynomial $F_p(x)$ in terms of these divisors of the cycle type as

$$aaa \tag{2.9}$$

where the product is taken only over nc, non-zero columns of the $2\times n$ matrix cycle type shown in Tables 1 or 2. The coefficient of x^q in $Q_p(x)$ obtained from the Möbius sums of various F_d polynomials where d's are strictly divisors of p generate the various cycle types for $(n-q)-$ hyperplanes of the nD-hypercube. We shall illustrate this by one of the matrix cycle types in Table 2. Consider the 31st matrix shown in Table 2 for $S_5[S_2]$:

$$\begin{pmatrix} 0\ 1\ 1\ 0\ 0 \\ 0\ 0\ 0\ 0\ 0 \end{pmatrix} \tag{2.10}$$

As only 2^{nd} and 3^{rd} columns contain non-zero values, hence we need to consider only these two columns. Thus the maximum period to consider is 6 and hence the possible F polynomials are F_6, F_3, F_2 and F_1 as divisors of 6 are 1, 2, 3, and 6. Applying the GCD followed by the use of Eq (2.9), we obtain each of these polynomials as

$$F_1(x) = \left(1+2x^2\right)\left(1+2x^3\right) \tag{2.11}$$

$$F_2(x) = (1+2x)^2\left(1+2x^3\right) \tag{2.12}$$

$$F_3(x) = \left(1+2x^2\right)(1+2x)^3 \tag{2.13}$$

$$F_6(x) = (1+2x)^5. \tag{2.14}$$

From the F_d polynomials thus constructed above, we obtain the Q_p polynomials using the Möbius sum, shown in Eq (2.8). Thus we obtain

$$Q_1 = F_1 = 1+2x^2+2x^3+4x^5 \tag{2.15}$$

$$Q_2=\frac{m(2)F_1+m(1)F_2}{2}=\frac{F_2--F_1}{2}=\frac{(1+2x)^2\left(1+2x^3\right)--\left(1+2x^2\right)\left(1+2x^3\right)}{2}=2x+x^2+4x^4+2x^5 \tag{2.16}$$

$$Q_3=\frac{m(1)F_3+m(3)F_1}{3}=\frac{F_3--F_1}{3}=\frac{\left(1+2x^2\right)(1+2x)^3-\left(1+2x^2\right)\left(1+2x^3\right)}{3}=2x+4x^2+6x^3+8x^4+4x^5 \tag{2.17}$$

$$Q_6=\frac{m(1)F_6+m(2)F_3+m(3)F_2+m(6)F_1}{6}=\frac{F_6--F_3--F_2+F_1}{6}=4x^2+10x^3+8x^4+2x^5 \tag{2.18}$$

The coefficients of $x^q s$ are tabulated below for all possible Q_p polynomials which yield the cycle types for various $(n-q)$ −perplanes as shown below:

Table 1

Q_p	x	x^2	x^3	x^4	x^5
Q_1		2	2		4
Q_2	2	1		4	2
Q_3	2	4	6	8	4
Q_6		4	10	8	2
Cycle type	$2^2 3^2$	$1^2 2^1 3^4 6^4$	$1^2 3^6 6^{10}$	$2^4 3^8 6^8$	$1^4 2^2 3^4 6^2$
Hyperplane	$q=1$ (tesseracts)	$q=2$ (cells)	$q=3$ (faces)	$q=2$ (edges)	$q=5$ (vertices)

The results thus obtained for all cycle types of the hyperplanes of 5D-hypercube are shown in Table 2. We believe this is the first time that these cycle types have been tabulated for all hyperplanes of the 5D-hypercube. Although previously the cycle index for the vertices of the 5D-hypercube have been reported in the literature [24]-[26], [28], [29] using different techniques, and our results agree with those results, Table 2 is exhaustive as it includes all hyperplanes, not just $q=5$ (vertices). Moreover, as outlined below we consider all irreducible representations for coloring the $(n-q)-$ hyperplanes, and not just the totally symmetric A1 representation. In our previous studies [51],[52] we have shown how the character tables of the $S_n[S_2]$ groups can be obtained from matrix generating functions and thus we shall not repeat the techniques in detail. Instead we shall focus on the colorings of the hyperplanes using the character table of $S_5[S_2]$, and the cycle types obtained for various hyperplanes of the 5D-hypercube shown in Table 2.
The character table of $S_5[S_2]$ containing 36 irreducible representations have been constructed before and thus we employ the GCCIs of the irreducible representation with character of the group $S_5[S_2]$. In general, the GCCI for the character χ of a group G' is defined as

$$P_{G'}^{\chi}=\frac{1}{|G'|}\sum_{g\in G'}\chi(g)S_1^{b_1}S_2^{b_2}\ldots S_n^{b_n} \tag{2.19}$$

where the sum is over all permutation representations of $g\in G'$ that generate b1 cycles of length 1, b_2 cycles of length 2, ..., b_n cycles of length n upon its action on the set Ω of the $(n-q)-$ hyperplanes of the 5D-hypercube. Upon construction of the GCCIs for each irreducible representation and each of the $(n-q)$ −hyperplane's cycle types shown in Table 2, one can carry out generalized Pólya substitution in the GCCIs for each representation of $S_5[S_2]$ with a multinomial expansion. Let[n] be an ordered partition, also called the composition of n into p parts such that $n_1\geq 0,\ n_2\geq 0,\ \ldots,\ n_p\geq 0,\ \sum_{i=1}^{p}n_i=n$. A multinomial generating function in λs is obtained as

$$(\lambda_1+\lambda_2+\ldots..+\lambda_p)^n=\sum_{[n]}^{p}\begin{pmatrix} & & n & & \\ n_1 & n_2 & . & . & n_p\end{pmatrix}\lambda_1{}^{n_1}\lambda_2{}^{n_2}\ldots\ldots..\lambda_{p-1}{}^{n_{p-1}}\lambda_p{}^{n_p} \tag{2.20}$$

where $\begin{pmatrix} & & n & & \\ n_1 & n_2 & . & . & n_p\end{pmatrix}$ are multinomials given by

$$\begin{pmatrix} & & n & & \\ n_1 & n_2 & . & . & n_p\end{pmatrix}=\frac{n!}{n_1!n_2!\ldots\ldots n_{p-1}!n_p!} \tag{2.21}$$

Define two sets, the set D which contains a set of $(n-q)$ −hyperplanes for a given q to be colored and the set R which contains different colors. Let wi be the weight of each color r in R . The weight of a function f from D to R is defined as

$$W(f)=\prod_{i=1}^{|R|}w(f(d_i)) \tag{2.22}$$

The generating function for each irreducible representation of the nD-hyperoctahedral group is obtained by the substitution as

$$GF^{\chi}(\lambda_1,\lambda_2\ldots.\lambda_p)=P_G^{\chi}\left\{s_k\to\left(w_1^k+w_1^k+\ldots.+w_{p-1}^k+w_p^k\right)\right\} \tag{2.23}$$

The above GFs are computed for each irreducible representation of the 5D-hyperoctahedral group. The coefficient of each term ${w_1}^{n1}{w_2}^{n2}\ldots{w_p}^{np}$ generates the number of functions in the set R^D that transform according to the irreducible representation Γ with character χ . For the special case of the totally symmetric irreducible representation A_1 , the GF becomes the ordinary Pólya's theorem, thus enumerating the number of equivalence classes of colorings.

In the case of hyperplanes of nD-hypercubes the number of $(n-q)-$hyperplanes for a given value of q increase as $\binom{n}{q}2^q$ and thus, for example, a 10D-hypercube would have 13,440 4-hyperplanes (q=6) and 15,360 3-hyperplanes (q=7). Consequently, as the multinomial generators explode in astronomical proportions for such large sets, it is practically not possible to consider more than 2 colors in the set R or only 2-colorings for larger hypercubes are feasible. We have developed Fortran '95 codes that compute the cycle types for all hyperplanes using the Möbius method, the character tables and then finally the generating functions for 2-colorings of various $(n-q)-$hyperplanes of the hypercube. All of the arithmetic were carried out in Real*16 quadruple precision arithmetic and thus we can rely on an accuracy of up to 32 digits, which appears to suffice for 2-colorings for all possible distribution of colors up to six-dimensional cases. However, for larger cases either only first k coefficients that contain 32 or fewer digits be considered for colorings or the codes have to be enhanced with multiple arrays to store beyond 32 digits as presently most compilers handle at most quadruple precision for real numbers. The special cases of multinomials for 2 colorings were computed in a single step for 2-colorings recursively, and stored in memory for computations of each of the monomials, sorting and collection of the coefficients for the final GF without computation of any factorials to save time. Moreover the expansion of multinomials, sorting and collection of coefficients is done only for the A_1 IR and for the remaining IRs the computed terms for each cycle type of A_1 are used. For the present case of the 5D-hypercube we were able to compute all of the possible 2-colorings for all $(n-q)-$hyperplanes as discussed in the next section within real quadruple precision or REAL*16 precision.

3. Results and discussions

As seen from Table 2, the 5D-hypercube contains 5 different hyperplanes, where $q=1$ to 5, represent tesseracts, cells, 3-faces, edges and vertices, respectively. Owing to the simplicity of $q=1$which yields only 10 tesseracts that can be represented by 10 vertices of a graph (Fig. 1) and as these 10 vertices also represent the protons of the fully nonrigid water pentamer $(H_2O)_5$, colorings of these ten vertices have been considered previously [64] and thus we shall not repeat the results. However for other q values with the exception of $q=5$ (vertices) restricted to A_1 , complete enumeration results for all IRs have not been considered previously. We note that the problem of coloring the vertices of the hypercube is equivalent to generating the equivalence classes of 2^n Boolean functions of a $n-$ dimensional hypercube which is of considerable interest [24]-[**?**], [28], [29]. Previous exhaustive combinatorial enumerations for the 4d-hypercube for all irreducible representations have been considered by the current author recently [11].

Tables 3-6 show the unique terms for 2-colorings of $(5-q)-$ hyperplanes $q=2-5$, respectively for the 5D-hypercube. In all these tables irreducible representations of the $S_5[S_2]$ group are denoted as A_1 to A_{36}, respectively. We note that only A_1 to A_4 are one-dimensional, A_5-A_8 are 4-dimensional, A_9-A_{16} are five-dimensional, $A_{17}-A_{18}$ are 6-dimensional, A19-A28 are 10-dimensional, $A_{29}-A_{32}$ are 15-dimensional, $A_{33}-A_{36}$ are 20-dimensional IRs of the 5d-hypercube. The number of colorings that transform according to the irreducible representation $A_i\,(i=1-36)$ are shown in Tables 3-6 for unique partition of colors. For example, the number of colorings which transform as the given irreducible representation in a row and contain 35 red colors and 5 green colors for coloring the cells $(q=2)$ of the 5D-hyercube are shown in Table 3 in the fifth column. We use the notation $[\lambda]$ to denote the unique partitions for the colorings and in order to save space, owing to the symmetry of binomial numbers the results are shown only for $[\,n_1,n_2]$ where n_1 GE n_2 as the other case $(n_2,\,n_1)$ is equivalent to $(n_1,\,n_2)$. As can be seen from Table 3, there are 1, 1, 5, 18, 84, and 362 colorings that transform as A_1 for 40 reds, 39 reds, 38 reds, 37 reds, 36 reds, and 35 reds (remaining 40-red = greens), respectively. The number of colorings that transform as A_1 irreducible representation is simply the number of equivalence classes under the action of the 5D-hyperoctahedal group on the cells for Table 3. Thus from Table 3, there are 36,600,432 ways to color the cells of the 5D-hypercube with 20 red colors and 20 green colors.- a result that is not known up to now. In the mathematics literature, the focus has been often on the total number of equivalence classes for the vertex colorings as opposed to the detailed enumeration for each possible distribution of colors $(n_1,\,n_2)$ that we show in Table 3. The results in Tables 3-5 have not been obtained before.

As can be seen from Table 4 the number of equivalence classes for coloring faces $(q=3)$ of the 5D-hypercube are 1, 8, 54, 633 and 7287 for 1, 2, 3, 4, 5 green colors (remaining being red colors), respectively. The fact that the number of equivalence classes for 79 red and 1 green colors for the face colorings is one implies all the faces of the hypercube are equivalent, a result that is expected. As seen from table 4, the number of equivalence classes (A_1 colorings) for 40 red and 40 green colors is a result that is unknown up to now. The numbers for other 35 irreducible representations (A_2-A_{36}) correspond to the number of functions out of 280 functions in the set R^D4 that transform as the corresponding irreducible representation. Consequently, the numbers in each row multiplied by the dimensions of the corresponding irreducible representations for all 36 IRs and all color distributions, that is, doubling each number in Table 4 for $[\lambda]$ with the exception [40 40] we obtain 2^{80} which is the total number of functions in the set of all maps. Likewise the sum of twice all numbers for the A1 representation with the exception that [40 40] is added only once, generates the total number of equivalence classes. This result can also be directly obtained from the cycle index for the A_1 IR by replacing every x_k by 2. That is, for the results in Table 3, total equivalence classes count is given by

$$
\begin{aligned}
I(faces;2) &= \left\{\begin{array}{l}
2^{80}+5\times2^{56}+10\times2^{44}+10\times2^{40}+5\times2^{40}+1\times2^{40}+20\times2^{50}+20\times2^{26}\\
+60\times2^{44}+60\times2^{22}+60\times2^{42}+60\times2^{22}+20\times2^{40}+20\times2^{22}+80\times2^{28}\\
+80\times2^{14}+160\times2^{20}+160\times2^{14}+80\times2^{16}+80\times2^{14}+60\times2^{44}+120\times2^{24}\\
+60\times2^{40}+120\times2^{22}+60\times2^{20}+60\times2^{20}+240\times2^{22}+240\times2^{10}+240\times2^{22}\\
+240\times2^{10}+160\times2^{18}+160\times2^{14}+160\times2^{10}+160\times2^{8}+384\times2^{16}+384\times2^{8}
\end{array}\right\}\\
&= 314,824,532,572,147,370,464
\end{aligned}
$$

The result thus obtained agrees with the computer code that independently computed the sum of all coefficients in the generating function, thus providing independent validation of our results. Consequently, the total number of equivalence classes for the face colorings of 5D-hypercube with 2 colors is 314,824,532,572,147,370,464.

As seen from Table 5, there are also 80 edges for the 5D-hypercube, which happens to be coincidentally same as the number of faces. We have provide all 2-coloring distributions in Table 5 and as these numbers contain less than 32-33, digits all results are computed accurately within the quadruple precision arithmetic. Once again from Table 5, we infer there are 1, 8, 50, 608, 7092 colorings for 1, 2, 3, 4, 5 green colors (remaining reds) for the edge colorings of the 5D-cube.Although the first two numbers coincide with the face coloring distribution from the third number onwards all the results differ. In general, the number of face colorings is larger than the number of edge colorings for the same color distribution. Thus we obtain $27,996,670,589,987,902,014$ as the number of equivalence classes for edge colorings with 40 red colors and 40 green colors while the corresponding number for face colorings is with 40 reds and 40 greens. The total number of equivalence classes for edge colorings of the 5D-hypercube with 2 colors is 314,824,456,456,819,827,136 which can be obtained in two independent ways as demonstrated for the face colorings.
Table 6 shows the vertex colorings for all irreducible representations for the 5D-hypercube. The results for the vertex colorings of the 5D-hypercube have been obtained previously by Chen and Guo [29] using a completely different method of generating the cycle index of the group. The results obtained by Chen and Guo [29] for the equivalence classes correspond to our numbers in Table 6 for the A1 IR. Chen and Guo [29] obtain these numbers as 1, 1, 5, 29, 47, 131, 472, 1326, 3779, 9013, 19,963, 38,073, 65,664, 98,804, 133,576, 158,658, for greens varying from 0 to 17 (remaining red). The corresponding results that we obtain in Table 6 for the same color distribution for the vertex colorings of the 5D-hypercube are 1, 1, 5, 10, 47, 131, 472, 1326, 3779, 9013, 19,963, 38,073, 65,664, 98,804, 133,576, 158,658, respectively. In addition we obtain the number of equivalence classes for 40 red and 40 green as 169,112 that Chen and Guo [29] did not report. Evidently the number of equivalence classes reported for 3 green colors by Chen and Guo [29] as 29 is not correct, and it disagrees with our result of 10 equivalence classes for the same color distribution. Furthermore the total number of equivalence classes that we obtain by adding doubles of all the numbers for A_1 in Table 6 except that [16 16] is counted once, is 1,228,158 which clearly does not agree with the results of Chen and Guo [29] although the total number directly obtained from their cycle index by replacing every x_k with 2 agrees with our result of 1,228,158. Therefore we conclude that only the number reported for 3 green colors as 29 by Chen and Guo [29] must be incorrect. Moreover, our result of 1,228,158 for the total number of equivalence classes for 2 colors agrees with the number reported by Perez-Agulia [26] but differs from the result of Aichholzer [25] who has obtained it as 1,226,525. The difference was reconciled by Perez-Agulia [26] with the explanation that vertices with 0 to 4 polytopes were treated differently by Aichholzer [25].

4. Chiral and alternating colorings, chemical and biological applications

As discussed in the previous section the numbers enumerated for the A1 representation (totally symmetric) for the partition $[n_1, n_2]$ of colors enumerates the number of Pólya equivalence classes for the coloring of $(n-q)-$ hyperplanes with n1 colors of one kind and n2 colors of another kind. A geometrical or physical interpretation for the numbers enumerated for other irreducible representations in Tables is that these numbers enumerate the number of functions that transform as the IR among the set of all R^D functions from the set D to R. That is, for hypercube's binary colorings there are 2^n such functions where n is the number of $(n-q)-$hyperplanes for a given q . Thus the number of irreducible representations in Tables 3 to 6 for a given color partition $[n_1 n_2]$ gives the number of possible symmetry-adapted orthogonal functions generated from the set R^D of 2^n functions. In addition to this interpretation the numbers enumerated for irreducible representations other than A_1 can yield information on different aspects of colorings such as chirality, alternation and various other applications.
Chirality arises in a coloring if the mirror image of the coloring is not superimposable on the original coloring. Objects are chiral when they have handedness such as shoes, hands, feet, gloves, etc. In such cases, the mirror images of the object cannot be converted into the original object by any proper rotations in the physical space. The term proper rotation refers to a rotation by an angle $2p/m$ for a natural number m around a specified axis of rotation denoted by a C_m axis of rotation. The set of such proper rotations that leave the object in the set D invariant constitute a subgroup that we call the rotational subgroup of the nD-hyperoctahedral group and it is comprised of $2^{(n-1)}x\ n!$ operations for the nD-hypercube. While such rotational operations are readily identified for a regular three-dimensional square or a cube shown in Table 1, this is less transparent for the higher dimensional hypercubes. As seen from Table 1, for each conjugacy class we can assign a rotational operation or mirror plane or a composite improper rotation by simply applying the operation on the vertices or edges or faces of the cube and gathering the various orbits generated upon the action of the operation. An improper axis of rotation, denoted is defined as the product $C_n\sigma_h$, or σ_h, C_n where the σ_h operation is a mirror plane perpendicular to the C_n axis. For a cube these operations are assigned to the various matrix conjugacy classes in Table 1 based on the permutation's orbits it generates upon its action on the vertices or edges or faces of the 3D cube. The proper rotations for an nD-hypercube can be obtained from the $2\times n$ matrix of the corresponding conjugacy class by considering the non-zero column's place values. That is, a conjugacy class with matrix $[a_{ik}]$ is a proper rotation if and only if

$$\sum_{k}^{even} a_{1k} + \sum_{k}^{odd} a_{2k}$$

is even, where the first sum is restricted to even ks while the second to odd ks. If the above sum is odd then the operation corresponding to the $2\times n$ matrix of the conjugacy class is an improper axis of rotation, where a special case of an improper axis may also be a mirror plane of symmetry or a center of inversion. This procedure can be applied to higher dimensional cubes, and thus in Table 2 we have identified each proper rotation of the 5D-hypercube by placing the label R next to the conjugacy class. If the label R is absent it means that the conjugacy class represents an improper axis of rotation. Chirality can then be determined by the definition that an object is chiral if it does not possess an improper axis of rotation. Evidently uncolored 5D-hypercube or a 3D-cube is not chiral because of the presence of improper axes of rotations. However, once the (n-q)-hyperplanes are colored some of the colorings for certain distribution of colors may become chiral. Tables 3-6 that we have constructed enumerate and identify these chiral colorings. The chiral colorings are obtained by stipulating that the functions in R^D for the coloring distribution $[n_1\ n_2]$ must transform in accord to the irreducible representation of chirality. This irreducible representation for chirality of the nD-hypercube is rigorously identified as the uni-dimensional IR that has +1 character values for all proper rotations of the nD-hyperoctahedral group and -1 for all improper rotations. By examining the character values for the uni-dimensional representations for the 5D-hypercube we identify this IR as A2 representation, and thus in Tables 3-5 they are identified with * in these tables. Consequently, the number of chiral colorings for a given distribution of colors $[n_1\ n_2]$is enumerated by the numbers for the $A2$ row in Tables 3-6 for various $(n-q)-$ hyperplanes.

As seen from Table 3, the first few numbers or the A2 representation are $0,0,0,0,6,84,657,3750,16,898,63,366,203,095,565,964,...$ suggesting that coloring 40 cells of the 5D-hypercube do not produce any chiral colorings for 40 reds $\delta0$ greens, 39 reds $\delta1$ green, 38 reds $\delta2$ green, 37 reds $\delta3$ greens, and in order to produce a chiral coloring one needs at least 4 green colors and remaining 36 red, and there are exactly 6 such colorings which are chiral. That is, among the 84 equivalence classes of cell colorings for [36 4] partition of colors there are exactly six chiral pairs in that mirror images of a chiral coloring is not superimposable on the original coloring. In order to illustrate this further consider a regular 3D cube. Among the total of 14 equivalence classes produced for all 2-colorings of the vertices of a 3D cube, only one coloring is chiral and all remaining colorings are achiral. The chiral coloring is shown in Figure 2.

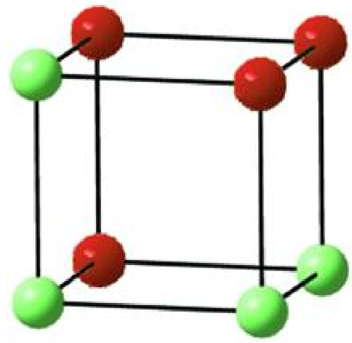

Figure 4.1: The only chiral coloring among 14 equivalence classes of 2-colorings of vertices of a cube. This is enumerated as the number of A_{1u} irreducible representations for the 2-colorings. For the 5D-hypercube the first chiral coloring appears for 4 greens and 28 reds. There are 2, 26, 148, 653, 2218, 6300, 14972, 30,730, and 54,528 such chiral colorings for 4, 5, 6, 7, 8, 9, 10, 11, and 12 green colors (remaining red), respectively for the 2-colorings of the vertices of the 5D-hypercube as enumerated by the A2 chiral representation of the 5D-hypercube..

The numbers of chiral colorings for face-colorings of the 5D-hypercube are given by the numbers of the A_2 IR in Table 4, and it can be seen as 14, 326, 5722, 74973, 811,527, 7, 477, 975 and 60,113,621 for 3, 4, 5, 6, 7, 8, and 9 greens (remaining reds), respectively. The corresponding results for the edge 2-colorings are 12, 330, 5782, 75,369, 815,762, 60, 219, 494 and 428, 191, 237 for 3, 4, 5, 6, 7, 8, and 9 greens (remaining reds), respectively. Finally as can be seen from Table 6, 2-colorings of the vertices of the 5D-hypercube produce 2, 26, 148, 653, 2218, 6300, 14,972, 30,730, and 54,528 chiral colorings for 4, 5, 6, 7, 8, 9, 10, 11, and 12 green colors (remaining red), respectively. Thus in order to produce a chiral coloring of 2-coloring of the vertices of a 5D-hypercube one needs at least 4 colors of one kind and 28 colors of another kind, and there are 2 such chiral colorings for [28 4] color distribution.

The alternating irreducible representation is defined as the one that exhibits +1 character values for even permutations of q=1 (n-1)hyperplanes and -1 for the odd permutations. The set of all even permutations form the alternating subgroup of the hypercube group. The alternating representation plays an important role in the quantum chemical classification of the rovibronic total wave functions of fermions as such wave functions for fermions must transform as the alternating IR in order to comply with the Pauli Principle. For the 5D-hypercube the uni-dimensional alternating IR is the A3 representation in Table 3-6. Thus the 2-colorings enumerated for the A3representationprovidesimportant information on the nuclear spin functions of rovibronic levels and nuclear spin statistical weights of fermionic particles of molecules, for example, water pentamer. We thus point out that these combinatorial enumerations aid in the analysis of experimental spectroscopic studies of weakly-bound van der waals clusters and molecular clusters of polar molecules such as ammoniated ammonia, $(H_2O)_n$, $(NH_3)_n$ [50], [64], [62] etc., as such clusters exhibit potential energy surfaces with multiple valleys separated by surmountable mountains, and consequently, these molecular clusters undergo rapid tunneling motions. Hence these tunneling motions that occur rapidly at higher room temperatures result in the splittings of the rovibronic levels to tunneling levels. Consequently, the interpretation of the rovibronic spectra of these molecular clusters requires hypercube colorings and detailed analysis for all IRs.

Finally we would like to point out applications to biology in the context of genetic regulatory network and phylogeny. The phylogenic trees are recursive in nature and they are special cases of Cayley trees and thus the automorphism groups and colorings of phylogenic trees require nested nD-hypergroups and wreath products. Likewise, in genetics it has been shown that canalization or control of one genetic trait by another trait of genetic regulatory networks is important in evolutionary processes, and such networks are represented by nD-hypercubes where the vertices of the nD-hypercube represent the 2^n possible Boolean functions for n traits. Reichhardt and Bassler [34] have shown the connection between 2-colorings of an nD-hypercube and genetic regulatory pathways, and the necessity to classify the 2-colorings of the vertices into equivalence classes in order to generate a smaller clustering subsets on the basis of equivalence classes thus enumerated for the 2-colorings of the vertices of the nD-hypercube. Thus the properties of any representative function in a class would have the same genetic expression as any other function in the equivalence class thereby reducing the amount of computations. The question of if chirality in colorings would have any implication in the probability of producing chiral traits and thus biological evolutionary implication of chirality has not been visited thus far.

5. Conclusion

Combinatorial enumeration of 2-colorings for all irreducible representations and all hyperplanes for were considered for a 5D-hypercube. The techniques involved Möbius inversion combined with generalized character cycle indices for all 36 irreducible representations of the 5D-hypercube. We also discussed applications chirality, alternation of colorings in the equivalence class. Applications to genetics and molecular spectroscopy were pointed out. As nD-hypercube colorings explode combinatorially in astronomical proportions, it remains to be seen how well the techniques will computationally scale and work for higher dimensional hypercubes.

Table 2: Conjugacy Classes, polynomials, cycle types of a regular cube or 3D-cube with group $S_3[S_2]$

CC	$\|CC\|$	O	$F_d(x)$	$q=1$ (face)	$q=2$ (edge)	$q=3$ (Vert)
$\begin{pmatrix}3&0&0\\0&0&0\end{pmatrix}$	1	E	$F_1(x)=(1+2x)^3$	1^6	1^{12}	1^8
$\begin{pmatrix}2&0&0\\1&0&0\end{pmatrix}$	3	σ_h	$F_1(x)=(1+2x)^2$ $F_2(x)=(1+2x)^3$	$1^4 2$	$1^4 2^4$	2^4
$\begin{pmatrix}1&0&0\\2&0&0\end{pmatrix}$	3	C_4^2	$F_1(x)=(1+2x)$ $F_2(x)=(1+2x)^3$	$1^2 2^2$	2^6	2^4
$\begin{pmatrix}0&0&0\\3&0&0\end{pmatrix}$	1	i	$F_1(x)=1$ $F_2(x)=(1+2x)^3$	2^3	2^6	2^4
$\begin{pmatrix}1&1&0\\0&0&0\end{pmatrix}$	6	σ_d	$F_1(x)=(1+2x)(1+2x^2)$ $F_2(x)=(1+2x)^3$	$1^2 1^2$	$1^2 2^5$	$1^4 2^2$
$\begin{pmatrix}1&0&0\\0&1&0\end{pmatrix}$	6	C_4	$F_1(x)=(1+2x)$ $F_2(x)=(1+2x)$ $F_4(x)=(1+2x)^3$	$1^2 4$	4^3	4^2
$\begin{pmatrix}0&1&0\\1&0&0\end{pmatrix}$	6	C_2	$F_1(x)=(1+2x^2)$ $F_2(x)=(1+2x)^3$	2^3	$1^2 2^5$	2^4
$\begin{pmatrix}0&0&0\\1&1&0\end{pmatrix}$	6	S_4	$F_1(x)=1$ $F_2(x)=(1+2x)$ $F_4(x)=(1+2x)^3$	$2^1 4^1$	4^3	4^2
$\begin{pmatrix}0&0&1\\0&0&0\end{pmatrix}$	8	C_3	$F_1(x)=(1+2x^3)$ $F_3(x)=(1+2x)^3$	3^2	3^4	$1^2 3^2$
$\begin{pmatrix}0&0&0\\0&0&1\end{pmatrix}$	8	S_3	$F_1(x)=1$ $F_2(x)=(1+2x^3)$ $F_3(x)=1$ $F_6(x)=(1+2x)^3$	6	6^2	26

Table 3: Conjugacy Classes of $S_5[S_2]$, their orders, F_d polynomials and cycle types generated using Möbius inversion for the 5D-hypercube's five hyperplanes*.

Conj Class C	$\lvert C\rvert$	$F_d(x)$	$q=1$ tes	$q=2$ Cel	$q=3$ fac	$q=4$ ed	$q=5$ Ver
$\begin{pmatrix}5&0&0&0&0\\0&0&0&0&0\end{pmatrix}$	1E	$F_1(x)=(1+2x)^5$	1^{10}	1^{40}	1^{80}	1^{80}	1^{32}
$\begin{pmatrix}4&0&0&0&0\\1&0&0&0&0\end{pmatrix}$	5	$F_1(x)=(1+2x)^4$ $F_2(x)=(1+2x)^5$	$1^8 2$	$1^{24}2^8$	$1^{32}2^{24}$	$1^{16}2^{32}$	2^{16}
$\begin{pmatrix}3&0&0&0&0\\2&0&0&0&0\end{pmatrix}$	10R	$F_1(x)=(1+2x)^3$ $F_2(x)=(1+2x)^5$	$1^8 2^2$	$1^{12}2^{14}$	$1^8 2^{36}$	2^{40}	2^{16}
$\begin{pmatrix}2&0&0&0&0\\3&0&0&0&0\end{pmatrix}$	10	$F_1(x)=(1+2x)^2$ $F_2(x)=(1+2x)^5$	$1^4 2^3$	$1^4 2^{18}$	2^{40}	2^{40}	2^{16}
$\begin{pmatrix}1&0&0&0&0\\4&0&0&0&0\end{pmatrix}$	5R	$F_1(x)=(1+2x)$ $F_2(x)=(1+2x)^5$	$1^2 2^4$	2^{20}	2^{40}	2^{40}	2^{16}
$\begin{pmatrix}0&0&0&0&0\\5&0&0&0&0\end{pmatrix}$	1	$F_1(x)=1$ $F_2(x)=(1+2x)^5$	2^5	2^{20}	2^{40}	2^{40}	2^{16}
$\begin{pmatrix}3&1&0&0&0\\0&0&0&0&0\end{pmatrix}$	20	$F_1(x)=(1+2x)^3(1+2x^2)$ $F_2(x)=(1+2x)^5$	$1^6 2^2$	$1^{14}2^{13}$	$1^{20}2^{30}$	$1^{24}2^{28}$	$1^{16}2^8$
$\begin{pmatrix}3&0&0&0&0\\0&1&0&0&0\end{pmatrix}$	20R	$F_1(x)=(1+2x)^3$ $F_2(x)=(1+2x)^3$ $F_4(x)=(1+2x)^5$	$1^6 4$	$1^{12}4^7$	$1^8 4^{18}$	4^{20}	4^8
$\begin{pmatrix}2&1&0&0&0\\1&0&0&0&0\end{pmatrix}$	60R	$F_1(x)=(1+2x)^2(1+2x^2)$ $F_2(x)=(1+2x)^5$	$1^4 2^3$	$1^{16}2^{17}$	$1^8 2^{36}$	$1^8 2^{36}$	2^{16}
$\begin{pmatrix}2&0&0&0&0\\1&1&0&0&0\end{pmatrix}$	60	$F_1(x)=(1+2x)^2$ $F_2(x)=(1+2x)^3$ $F_4(x)=(1+2x)^5$	$1^4 2 4$	$1^4 2^4 4^7$	$2^4 4^{18}$	4^{20}	4^8
$\begin{pmatrix}1&1&0&0&0\\2&0&0&0&0\end{pmatrix}$	60	$F_1(x)=(1+2x)(1+2x^2)$ $F_2(x)=(1+2x)^5$	$1^2 2^4$	$1^2 2^{19}$	$1^4 2^{38}$	2^{40}	2^{16}
$\begin{pmatrix}1&0&0&0&0\\2&1&0&0&0\end{pmatrix}$	60R	$F_1(x)=(1+2x)$ $F_2(x)=(1+2x)^3$ $F_4(x)=(1+2x)^5$	$1^4 2^2 4$	$2^6 4^7$	$2^4 4^{18}$	4^{20}	4^8
$\begin{pmatrix}0&1&0&0&0\\3&0&0&0&0\end{pmatrix}$	20R	$F_1(x)=(1+2x^2)$ $F_2(x)=(1+2x)^5$	2^5	$1^2 2^{19}$	2^{40}	2^{40}	2^{16}
$\begin{pmatrix}0&0&0&0&0\\3&1&0&0&0\end{pmatrix}$	20	$F_1(x)=1$ $F_2(x)=(1+2x)^3$ $F_4(x)=(1+2x)^5$	$2^3 4$	$2^6 4^7$	$2^4 4^{18}$	4^{20}	4^8
$\begin{pmatrix}2&0&1&0&0\\0&0&0&0&0\end{pmatrix}$	80R	$F_1(x)=(1+2x)^2(1+2x^3)$ $F_3(x)=(1+2x)^5$	$1^4 3^2$	$1^4 3^{12}$	$1^2 2^{26}$	$1^8 3^{24}$	$1^8 3^8$
$\begin{pmatrix}2&0&0&0&0\\0&0&1&0&0\end{pmatrix}$	80	$F_1(x)=(1+2x)^2$ $F_2(x)=(1+2x)^2(1+2x^3)$ $F_3(x)=(1+2x)^2$ $F_6(x)=(1+2x)^5$	$1^4 6$	$1^4 6^6$	$2 6^{13}$	$2^4 6^{12}$	$2^4 6^4$
$\begin{pmatrix}1&0&1&0&0\\1&0&0&0&0\end{pmatrix}$	160	$F_1(x)=(1+2x)(1+2x^3)$ $F_2(x)=(1+2x)^2(1+2x^3)$ $F_3(x)=(1+2x)^4$ $F_6(x)=(1+2x)^5$	$1^2 2 3^2$	$2^2 3^{10} 6^8$	$1^2 3^8 6^2$	$1^4 2^2 3^4 6^{10}$	$2^4 6^4$

Table 4: Conjugacy Classes of $S_5[S_2]$, their orders, F_d polynomials and cycle types generated using Möbius inversion for the 5D-hypercube's five hyperplanes*, (Cont.).

Conj Class C	$\lvert C\rvert$	$F_d(x)$	$q=1$ tes	$q=2$ Cel	$q=3$ fac	$q=4$ ed	$q=5$ Ver
$\begin{pmatrix}1&0&0&0&0\\1&0&1&0&0\end{pmatrix}$	160R	$F_1(x)=(1+2x)$ $F_2(x)=(1+2x)^2(1+2x^3)$ $F_3(x)=(1+2x)$ $F_6(x)=(1+2x)^5$	$1^2 2 6$	$2^2 6^6$	$2 6^{13}$	$2^4 6^{12}$	$2^4 6^4$
$\begin{pmatrix}0&0&1&0&0\\2&0&0&0&0\end{pmatrix}$	80R	$F_1(x)=(1+2x^3)$ $F_2(x)=(1+2x)^2(1+2x^3)$ $F_3(x)=(1+2x)^3$ $F_6(x)=(1+2x)^5$	$2^2 3^2$	$2^2 3^4 6^4$	$1^2 3^2 6^{12}$	$2^4 6^{12}$	$2^4 6^4$
$\begin{pmatrix}0&0&0&0&0\\2&0&1&0&0\end{pmatrix}$	80	$F_1(x)=1$ $F_2(x)=(1+2x)^2(1+2x^3)$ $F_3(x)=1$ $F_6(x)=(1+2x)^5$	$2^2 6$	$2^2 6^6$	$2 6^{13}$	$2^4 6^{12}$	$2^4 6^4$
$\begin{pmatrix}1&2&0&0&0\\0&0&0&0&0\end{pmatrix}$	60R	$F_1(x)=(1+2x)(1+2x^2)^2$ $F_2(x)=(1+2x)^5$	$1^2 2^4$	$1^4 2^{18}$	$1^8 2^{36}$	$1^4 2^{38}$	$1^8 2^{12}$
$\begin{pmatrix}1&1&0&0&0\\0&1&0&0&0\end{pmatrix}$	120	$F_1(x)=(1+2x)(1+2x^2)$ $F_2(x)=(1+2x)^3$ $F_4(x)=(1+2x)^5$	$1^2 2^2 4$	$1^2 2^5 4^7$	$1^4 2^2 4^{18}$	4^{20}	4^8
$\begin{pmatrix}0&2&0&0&0\\1&0&0&0&0\end{pmatrix}$	60	$F_1(x)=(1+2x^2)^2$ $F_2(x)=(1+2x)^5$	2^5	$1^4 2^{18}$	2^{40}	$1^4 2^{38}$	2^{16}
$\begin{pmatrix}0&1&0&0&0\\1&1&0&0&0\end{pmatrix}$	120R	$F_1(x)=(1+2x^2)$ $F_2(x)=(1+2x)^3$ $F_4(x)=(1+2x)^5$	$2^3 4$	$1^2 2^5 4^7$	$2^4 4^{18}$	4^{20}	4^8
$\begin{pmatrix}1&0&0&0&0\\0&2&0&0&0\end{pmatrix}$	60R	$F_1(x)=(1+2x)$ $F_2(x)=(1+2x)$ $F_4(x)=(1+2x)^5$	$1^2 4^2 4$	4^{10}	4^{20}	4^{20}	4^8
$\begin{pmatrix}0&0&0&0&0\\1&2&0&0&0\end{pmatrix}$	60	$F_1(x)=1$ $F_2(x)=(1+2x)$ $F_4(x)=(1+2x)^5$	$2 4^2$	4^{10}	4^{20}	4^{20}	4^8
$\begin{pmatrix}1&0&0&1&0\\0&0&0&0&0\end{pmatrix}$	240	$F_1(x)=(1+2x)(1+2x^4)$ $F_2(x)=(1+2x)(1+2x^2)^2$ $F_4(x)=(1+2x)^5$	$1^2 4^2 4$	$2^2 4^9$	$2^4 4^{18}$	$1^2 2 4^{19}$	$1^4 2^2 4^6$
$\begin{pmatrix}1&0&0&0&0\\0&0&0&1&0\end{pmatrix}$	240R	$F_1(x)=(1+2x)$ $F_2(x)=(1+2x)$ $F_4(x)=(1+2x)$ $F_8(x)=(1+2x)^5$	$1^2 8$	8^5	8^{10}	8^{10}	8^4
$\begin{pmatrix}0&0&0&1&0\\1&0&0&0&0\end{pmatrix}$	240R	$F_1(x)=(1+2x)(1+2x^4)$ $F_2(x)=(1+2x)(1+2x^2)^2$ $F_4(x)=(1+2x)^5$	$2 4^2$	$2^2 4^9$	$2^4 4^{18}$	$1^2 2 4^{19}$	$2^4 4^6$
$\begin{pmatrix}0&0&0&0&0\\1&0&0&1&0\end{pmatrix}$	240	$F_1(x)=1$ $F_2(x)=(1+2x)$ $F_4(x)=(1+2x)$ $F_8(x)=(1+2x)^5$	$2 8$	8^5	8^{10}	8^{10}	8^4
$\begin{pmatrix}0&1&1&0&0\\1&0&0&1&0\end{pmatrix}$	160	$F_1(x)=(1+2x^2)(1+2x^3)$ $F_2(x)=(1+2x)^2(1+2x^3)$ $F_3(x)=(1+2x^2)(1+2x)^3$ $F_6(x)=(1+2x)^5$	$2^3 3^2$	$1^2 2 3^4 6^4$	$1^2 3^6 6^{10}$	$2^4 3^8 6^8$	$1^4 2^2 3^4 6^2$

Table 5: Conjugacy Classes of $S_5[S_2]$, their orders, F_d polynomials and cycle types generated using Möbius inversion for the 5D-hypercube's five hyperplanes*, (Cont.).

Conj Class C	$\|C\|$	$F_d(x)$	$q=1$ tes	$q=2$ Cel	$q=3$ fac	$q=4$ ed	$q=5$ Ver
$\begin{pmatrix} 0 & 1 & 0 & 0 & 0 \\ 0 & 0 & 1 & 0 & 0 \end{pmatrix}$	160R	$F_1(x)=(1+2x^2)$ $F_2(x)=(1+2x)^2(1+2x^3)$ $F_3(x)=(1+2x^2)$ $F_6(x)=(1+2x)^5$	$2^2 6$	$1^2 2 6^6$	$2 6^{13}$	$2^4 6^{12}$	$2^4 6^4$
$\begin{pmatrix} 0 & 0 & 1 & 0 & 0 \\ 0 & 1 & 0 & 0 & 0 \end{pmatrix}$	160R	$F_1(x)=(1+2x^3)$ $F_2(x)=(1+2x^3)$ $F_3(x)=(1+2x)^3$ $F_4(x)=(1+2x)^2(1+2x^3)$ $F_6(x)=(1+2x)^3$ $F_{12}(x)=(1+2x)^5$	$4 3^2$	$3^4 4 12^2$	$1^2 3^2 12^6$	$4^2 12^6$	$4^2 12^2$
$\begin{pmatrix} 0 & 0 & 0 & 0 & 0 \\ 0 & 1 & 1 & 0 & 0 \end{pmatrix}$	160	$F_1(x)=1$ $F_2(x)=(1+2x^3)$ $F_3(x)=1$ $F_4(x)=(1+2x)^2(1+2x^3)$ $F_6(x)=(1+2x)^3$ $F_{12}(x)=(1+2x)^5$	$4 6$	$4 6^2 12^2$	$2 6 12^6$	$4^2 12^6$	$4^2 12^2$
$\begin{pmatrix} 0 & 0 & 0 & 0 & 1 \\ 0 & 0 & 0 & 0 & 0 \end{pmatrix}$	384R	$F_1(x)=(1+2x^5)$ $F_5(x)=(1+2x)^5$	5^2	5^8	5^{16}	5^{16}	$1^2 5^6$
$\begin{pmatrix} 0 & 0 & 0 & 0 & 0 \\ 0 & 0 & 0 & 0 & 1 \end{pmatrix}$	384	$F_1(x)=1$ $F_2(x)=(1+2x^5)$ $F_5(x)=1$ $F_{10}(x)=(1+2x)^5$	10	10^4	10^8	10^8	$2^1 10^3$

*Label R identifies proper rotations.

Table 6: 2-colorings of $q = 2$ or 3-hyerplnes (cells) of 5D-hhypercube*

$[\lambda]$	40	39 1	38 2	37 3	36 4	35 5
A_1	1	1	5	18	84	362
A_2*	0	0	0	0	6	84
$A_3\dagger$	0	0	0	1	17	130
A_4	0	0	0	3	29	218
A_5	0	0	0	14	132	912
A_6	0	1	8	41	234	1198
A_7	0	0	0	1	33	376
A_8	0	0	0	3	53	466
A_9	0	0	3	28	211	1266
A_{10}	0	1	7	43	261	1410
A_{11}	0	0	0	2	46	502
A_{12}	0	0	0	3	57	548
A_{13}	0	0	1	11	105	753
A_{14}	0	0	0	4	59	570
A_{15}	0	1	5	36	217	1247
A_{16}	0	0	0	10	130	958
A_{17}	0	0	3	34	253	1534
A_{18}	0	0	0	3	63	632
A_{19}	0	0	1	20	225	1705
A_{20}	0	0	0	19	231	1741
A_{21}	0	1	7	48	335	2060
A_{22}	0	10	2	30	266	1853
A_{23}	0	0	0	11	161	1394
A_{24}	0	0	1	16	181	1454
A_{25}	0	0	2	27	237	1684
A_{26}	0	0	1	22	217	1624
A_{27}	0	0	1	14	158	1315
A_{28}	0	0	4	44	341	2197
A_{29}	0	0	0	11	191	1808
A_{30}	0	0	0	18	232	1991
A_{31}	0	0	4	54	471	3155
A_{32}	0	1	9	80	558	3444
A_{33}	0	0	3	50	489	3556
A_{34}	0	0	6	66	562	3797
A_{35}	0	0	1	32	376	3012
A_{36}	0	0	3	40	414	3130
$[\lambda]$	34 6	33 7	32 8	31 9	30 10	29 11
A_1	1608	6549	24447	81523	243027	645920
A_2*	657	3750	16898	63366	203095	565964
$A_3\dagger$	820	4201	18036	65883	208248	575519
A_4	1196	5575	22187	76923	234085	630118
A_5	4957	22752	89932	310271	941691	2530274
A_6	5764	24690	94419	319457	959523	2561868
A_7	2788	15437	68714	255963	817470	2273349
A_8	3112	16337	70988	260991	827766	2292449
A_9	6548	29276	114337	391745	1184645	3176086
A_{10}	6951	30250	116572	396345	1193551	3191888
A_{11}	3603	19622	86732	321822	1025657	2848796
A_{12}	3766	20073	87870	324339	1030810	2858351
A_{13}	4505	22424	94334	340422	1066636	2931379
A_{14}	3902	20774	90308	331592	1048890	2898671

Table 7: 2-colorings of $q = 2$ or 3-hyerplnes (cells) of 5D-hhypercube*, (Cont.)

$[\lambda]$	40	39 1	38 2	37 3	36 4	35 5
A_{15}	6315	28332	111060	382756	1162511	3128715
A_{16}	5519	26226	106192	372241	1142010	3091274
A_{17}	7917	35318	137717	471282	1424118	3816104
A_{18}	4423	23823	104768	387705	1233905	3424315
A_{19}	10100	49179	202674	719261	2225769	6060963
A_{20}	10246	49608	203802	721773	2231003	6070695
A_{21}	11143	51877	209058	732893	2252661	6109809
A_{22}	10559	50479	205914	726505	2240491	6088449
A_{23}	8893	45231	191440	690879	2161351	5928638
A_{24}	9081	45720	192650	693498	2166648	5938361
A_{25}	9791	47669	197270	703613	2186655	5975122
A_{26}	9603	47180	196060	700994	2181358	5965399
A_{27}	8394	43167	184598	671959	2115409	5829890
A_{28}	11821	54521	217202	754936	2304404	6219829
A_{29}	12097	63479	273932	1001661	3160917	8722835
A_{30}	12691	65129	277938	1010491	3178627	8755543
A_{31}	17340	80747	323394	1127177	3446414	9311103
A_{32}	18136	82853	328262	1137692	3466915	9348544
A_{33}	20657	99644	408572	1445748	4466210	12149350
A_{34}	21383	101463	412836	1454636	4483602	12180432
A_{35}	18488	92296	387472	1391838	4342653	11893939
A_{36}	18860	93370	389890	1397068	4353235	11913375
$[\lambda]$	28 12	27 13	26 14	25 15	24 16	20 20
A_{1}	1534959	3268238	6253840	10780533	16780905	36600432
$A_{2}*$	1387615	3018198	5860684	10206958	16001831	35267044
$A_{3}\dagger$	1404093	3044481	5899917	10261735	16073555	35382134
A_{4}	1508474	3227163	6193673	10698058	16674124	36432620
A_{5}	6051057	12935884	24815540	42849105	66771193	145850208
A_{6}	6103944	13018005	24935767	43014020	66984612	146185674
A_{7}	5566873	12098955	23481819	40882439	64078845	141182942
A_{8}	5599815	12151509	23560277	40991977	64222269	141413110
A_{9}	7585897	16203956	31069136	53629419	83551831	182450208
A_{10}	7612322	16245031	31129219	53711894	83658502	182617894
A_{11}	6970887	15143304	29381578	51144016	80152173	176564772
A_{12}	6987365	15169587	29420811	51198793	80223897	176679862
A_{13}	7122810	15401876	29787455	51737069	80956494	177940894
A_{14}	7066962	15313232	29655841	51554067	80717484	177559178
A_{15}	4793096	16040561	30802821	53232534	83001076	181479598
A_{16}	7430012	15940878	30655982	53029221	82736568	181059380
A_{17}	9111568	19458488	37303794	64384562	100300776	219002868
A_{18}	8374980	18187785	35281495	61405751	96225728	211946906
A_{19}	14630010	31481747	60673483	105113023	164178470	359867382
A_{20}	14646966	31508798	60714034	105169696	164252800	359986806
A_{21}	14712710	31612100	60865880	105379320	164525016	360417862
A_{22}	14677526	31557917	60787385	105272259	164387422	360203692
A_{23}	14381627	31054027	59993215	104112178	162809521	357499270
A_{24}	14398357	31080628	60032854	104167367	162881749	357614990
A_{25}	14460573	31179079	60178307	104369056	163144521	358033038
A_{26}	14443843	31152478	60138668	104313867	163072293	357917318
A_{27}	14189604	30714843	59442940	103290802	161673524	355499400
A_{28}	14922940	31981159	61458432	106261406	165737190	362538286
A_{29}	21247566	46014649	89080019	154819871	242359594	533011478
A_{30}	21303354	46103293	89211549	155002873	242598504	533393068
A_{31}	22352952	47922037	92114414	159290627	248473758	543597666
A_{32}	22416036	48021720	92261253	159493940	248738266	544017884
A_{33}	29307474	63039544	121460718	210385140	328565692	720070782
A_{34}	29359594	63120751	121579741	210548843	328777586	720404344
A_{35}	28825377	62206368	120131677	208425861	325881583	715416208
A_{36}	28858823	62259556	120210947	208536219	326026015	715647636

$*$Identifies Chiral Representation, $\dagger$Identifies Alternating Representation

Table 8: 2-colorings of 5D-hypercube: q=3 or 2-hyperplanes(faces)

$[\lambda]$	80 0	79 1	78 2	77 3	76 4	75 5
A_1	1	1	8	54	633	7287
A_2*	0	0	0	14	326	5722
$A_3\dagger$	0	0	1	2	408	699
A_4	0	0	0	19	418	661
A_5	0	0	1	86	1724	25905
A_6	0	1	14	154	2138	27755
A_7	0	0	0	48	1329	22923
A_8	0	0	2	71	1491	23876
A_9	0	0	8	136	2349	33188
A_{10}	0	1	14	171	2552	34114
A_{11}	0	0	1	73	1735	29121
A_{12}	0	0	2	85	1817	29598
A_{13}	0	0	6	110	2060	30896
A_{14}	0	0	1	73	1771	29392
A_{15}	0	1	10	168	2435	33702
A_{16}	0	0	3	106	2090	31741
A_{17}	0	0	7	167	2811	40020
A_{18}	0	0	1	79	2086	34886
A_{19}	0	0	7	201	4067	62428
A_{20}	0	0	6	213	4117	62905
A_{21}	0	1	18	275	4557	64866
A_{22}	0	0	6	220	4201	6500
A_{23}	0	0	4	173	3807	60718
A_{24}	0	0	4	165	3833	60755
A_{25}	0	1	11	245	4232	6148
A_{26}	0	0	8	210	4090	62222
A_{27}	0	0	7	180	3825	60285
A_{28}	0	1	13	271	4519	65440
A_{29}	0	0	4	233	5451	89243
A_{30}	0	0	7	270	5728	90747
A_{31}	0	0	14	354	6550	96726
A_{32}	0	1	21	416	6895	98687
A_{33}	0	0	13	421	8268	125928
A_{34}	0	1	24	487	8672	127770
A_{35}	0	0	12	381	7893	122938
A_{36}	0	0	15	406	8057	123899
$[\lambda]$	74 6	73 7	72 8	71 9	70 10	69 11
A_1	83555	849445	7641565	60729304	429970617	2732388768
A_2*	74973	811527	7477975	60113621	427758604	2725189869
$A_3\dagger$	77230	821376	7515124	60245702	428179564	2726468083
A_4	79347	833673	7583400	60540511	429376647	2730690404
A_5	319235	3344486	30366992	242293889	1717899937	10924039594
A_6	327603	3376017	30483176	242671455	1719087495	10927436302
A_7	301055	3250060	29935770	240529874	1711337285	10901617831
A_8	305566	3269746	30010065	240794016	1712179165	10904174239
A_9	402754	4193869	38008521	303022994	2147870156	13656428163
A_{10}	406924	4209641	38066550	303211787	2148463784	13658126527
A_{11}	378269	4071401	37450878	300775427	2139516551	13628085765
A_{12}	380526	4081250	37488027	300907508	2139937511	13629363979

Table 9: 2-colorings of 5D-hypercube: q=3 or 2-hyperplanes(faces)

$[\lambda]$	80 0	79 1	78 2	77 3	76 4	75 5
A_{13}	388244	4115896	37642667	301493236	2142078579	13636348861
A_{14}	380718	4085029	37522094	301081473	2140734613	13632382149
A_{15}	403325	4194147	37983313	302887223	2147152220	13653690659
A_{16}	394699	4157315	37849447	302418655	2145690306	13649303434
A_{17}	483936	5037385	45625203	363695529	2577640232	16388396724
A_{18}	454418	4886903	44952736	360964567	2567578338	16354134118
A_{19}	782696	8276912	75522353	604085534	4288538040	27288670143
A_{20}	784537	8286761	75555698	604217615	4288931526	27289948357
A_{21}	794398	8323593	75700964	604686183	4290475691	27294335582
A_{22}	787906	8301941	75618251	604440771	4289681978	27292217431
A_{23}	772614	8226772	75295921	603175242	4285167659	27277249393
A_{24}	773790	8230741	75319810	603250704	4285470842	27278107820
A_{25}	783478	8273411	75466888	603775798	4287050362	27282914469
A_{26}	780121	8257639	75416431	603587005	4286511454	27281216105
A_{27}	768923	8200847	75164722	602574387	4282812548	27268730688
A_{28}	797985	8351384	75832721	605305556	4292841882	27302993771
A_{29}	1147363	12280002	112662231	903599298	6423347475	40900693107
A_{30}	1154851	12310869	112782678	904011061	6424691099	40904659819
A_{31}	1191584	12502770	113668866	907667442	6438414240	40951876998
A_{32}	1200210	12539602	113802732	908136010	6439876154	40956264223
A_{33}	1570592	16578830	151140594	1208526176	8578219760	54580887445
A_{34}	1578916	16610319	151256643	1208903649	8579406919	54584283790
A_{35}	1552712	16484362	150712329	1206762068	8571678755	54558465319
A_{36}	1557242	16504090	150786672	1207026303	8572520806	54561022090

Table 10

$[\lambda]$	44 36	43 37	42 38	41 39	40 40
A_1	18847863525339251552	22413675116856521554	25362842575806673932	27313830262039356344	27996675954790045648
A_2*	18847852585019852784	22413662952649979772	25362829447471548304	27313816527678832042	27996662005552559820
$A_3\dagger$	18847853190803004294	22413663622117296124	25362830164050160934	27313817276349083728	27996662763315380740
A_4	18847862859627984748	22413674384398836626	25362841789323193438	27313829443562144630	27996675123446791678
A_5	75391452039570414338	89654698207061418894	101451367868400802692	109255318522918146262	111986701245805189142
A_6	75391453370992774196	89654699671976785110	101451369441367576670	109255320159872567790	111986702908491503538
A_7	75391410895382419988	89654652417075817924	101451318447499755284	109255266789578133400	111986648717878780904
A_8	75391412106948721622	89654653756010447008	101451319880656979158	109255268286918634892	111986650233404418984
A_9	94239315564909056836	112068373323916723632	126814210444206867570	136569148784956847548	139983377200593924674
A_{10}	94239316230620152144	112068374056374408560	126814211230690163308	136569149603434059262	139983378031936988900
A_{11}	94239264086184823660	112068316039191912380	126814148611549315596	136569084065926569990	139983311481192867368
A_{12}	94239264691967975170	112068316708659228732	126814149328127928226	136569084814596821676	139983312238955688288
A_{13}	94239275611010301062	112068328846778722822	126814162431677508060	136569098520092612896	139983326162116863420
A_{14}	94239273757571746680	112068326806566039966	126814160239766081968	136569096238736595918	139983323844407910574
A_{15}	94239306532959553232	112068363268005984602	126814199571879555474	136569137407356432010	139983365636539659632
A_{16}	94239304629041322386	112068361164802814868	126814197321003585678	136569135056193326978	139983363256737576052
A_{17}	113087179025595952234	134482048377782845824	152177052944638511992	163882978977189213078	167980053076059861824
A_{18}	113087117226508284532	134481979598318989036	152176978716635025204	163882901272468852522	167979974182415265728
A_{19}	188478589300930046414	224136700109485934928	253628370658848001576	273138245000424414272	279966701018560496814
A_{20}	188478589901989013044	224136700778953251280	253628371369956483346	273138245749094665958	279966701770579703858
A_{21}	188478591820079755620	224136702882156421014	253628373637242754192	273138248100257770990	279966704167612580446
A_{22}	188478591089716591170	224136702086708485832	253628372775384675292	273138247211973727294	279966703256945725386
A_{23}	188478568698399675330	224136677182998016880	253628345912898114958	273138219098850995800	279966674717232831548
A_{24}	188478569253703298004	224136677789475082978	253628346570512276262	273138219777714415504	279966675412902686308
A_{25}	188478571208100940998	224136679955668384664	253628348880352605006	273138222198684224492	279966677854797606408
A_{26}	188478570551838143964	224136679223210699736	253628348104809448672	273138221380207012778	279966677034941689648
A_{27}	188478549368580840744	224136655653342348792	253628322671442383030	273138194758827908970	279966650006522174306
A_{28}	188478611161999668620	224136724432806385474	253628396892881934154	273138272463548459144	279966728893274635996
A_{29}	282717823061500661778	336204982396918169290	380442482835833897378	409707290927757703692	419949973771606452858
A_{30}	282717824914939044664	336204984437130852146	380442485027745138714	409707293209113720670	419949976089315216212
$A_{31}1$	282717915740561360068	336205085534618800980	380442594154920976128	409707407449934795308	419950092087919132428
A_{32}	282717917644479590914	336205087637821970714	380442596405796945924	409707409801097900340	419950094467721216008
A_{33}	376957180390646038772	448273402196193222712	507256743434232078056	546276492212397496308	559933404275504931684
A_{34}	376957181722068167618	448273403661108470626	507256745007198636492	546276493849351789810	559933405938190990028
A_{35}	376957139250237212918	448273356406207503440	507256694017706957254	546276440479057355420	559933351752173214880
A_{36}	376957140461803631240	448273357745142250826	507256695450864273506	546276441976397984938	559933353267698982600

*Identifies Chiral Representation

†Identifies Alternating Representation

Table 11: 2-colorings of 5D-hypercube for q=4 or 1-hyperplanes (edges) of 5D-hypercube

[λ]	80 0	79 1	78 2	77 3	76 4	75 5
A_1	1	1	8	50	608	7092
A_2*	0	0	0	12	330	5782
$A_3\dagger$	0	0	2	30	488	6690
A_4	0	0	0	10	319	5730
A_5	0	0	0	55	1426	23866
A_6	0	1	13	132	1990	26563
A_7	0	0	1	64	1465	23992
A_8	0	0	5	98	1781	25800
A_9	0	0	3	97	2010	30903
A_{10}	0	0	10	136	2289	32246
A_{11}	0	0	2	90	1940	30638
A_{12}	0	0	4	108	2098	31546
A_{13}	0	1	10	148	2345	32892
A_{14}	0	0	2	74	1808	29722
A_{15}	0	1	10	162	2385	33253
A_{16}	0	0	1	67	1795	29648
A_{17}	0	0	5	127	2489	37615
A_{18}	0	0	4	120	2428	37328
A_{19}	0	0	4	171	3786	60625
A_{20}	0	0	6	191	3952	61607
A_{21}	0	1	19	284	4598	65138
A_{22}	0	0	6	225	4204	63415
A_{23}	0	0	3	157	3735	60286
A_{24}	0	0	5	175	3893	61194
A_{25}	0	1	14	270	4483	64799
A_{26}	0	1	12	252	4325	63891
A_{27}	0	0	9	212	4121	62523
A_{28}	0	0	8	219	4148	62810
A_{29}	0	0	6	267	5820	91884
A_{30}	0	0	13	340	6347	95035
A_{31}	0	0	9	286	5943	92458
A_{32}	0	1	18	381	6533	96063
A_{33}	0	0	10	394	7978	124004
A_{34}	0	1	23	471	8536	126701
A_{35}	0	0	13	403	8041	124130
A_{36}	0	0	17	437	8357	125938
[λ]	74 6	73 7	72 8	71 9	70 10	69 11
A_1	82379	843038	7611823	60601324	429479585	2730645204
A_2*	75639	815762	7501366	60219494	428191237	2726763270
$A_3\dagger$	80615	837606	7592170	60547288	429312879	2730230168
A_4	75477	815283	7500045	60216779	428185149	2726758252
A_5	307123	3284074	30095715	241209472	1713913625	10910627650
A_6	320894	3339553	30319122	241978353	1716502254	10918401261
A_7	307440	3284670	30095732	241204688	1713884368	10910515598
A_8	317386	3328346	30277316	241860238	1716127616	10917449272
A_9	389378	4126847	37706909	301809609	2143390868	13641268215
A_{10}	396261	4154583	37818587	302193983	2144685133	13645154996
A_{11}	387957	4122042	37687342	301750856	2143195045	13640741264
A_{12}	392933	4143886	37778146	302078650	2144316687	13644208162
A_{13}	399267	4171384	37884523	302461562	2145574281	13648094476
A_{14}	383245	4099953	37598806	301421467	2142091443	13637273850
A_{15}	400355	4177159	37900610	302525641	2145738361	13648631429
A_{16}	383252	4099836	37601654	301428966	2142137746	13637390920
A_{17}	470161	4965306	45302969	362369722	2572751209	16371625455
A_{18}	468572	4959648	45279512	362298144	2572507924	16370971432

*Identifies Chiral Representation

†Identifies Alternating Representation

Table 12: 2-colorings of 5D-hypercube for q=4 or 1-hyperplanes (edges) of 5D-hypercube

$[\lambda]$	80 0	79 1	78 2	77 3	76 4	75 5
A_{19}	772214	8226800	75301905	603231076	4285454906	27278542065
A_{20}	777520	8249976	75397983	603574410	4286630098	27282141053
A_{21}	795119	8325967	75699273	604655545	4290232009	27293249472
A_{22}	786640	8293652	75571959	604229960	4288818500	27289074727
A_{23}	771209	8221878	75288996	603179822	4285332791	27278132184
A_{24}	776185	8243722	75379800	603507616	4286454433	27281599082
A_{25}	793288	8321045	75678756	604604291	4290055048	27292839591
A_{26}	788312	8299201	75587952	604276497	4288933406	27289372693
A_{27}	782308	8270850	75482201	603880760	4287661270	27285359307
A_{28}	783403	8276508	75501136	603952338	4287871653	27286013330
A_{29}	1163976	12366243	113065434	905261187	6429633640	40922345364
A_{30}	1179979	12437655	113351061	906301111	6433116307	40933165819
A_{31}	1166655	12376344	113102790	905381304	6430009399	40923404250
A_{32}	1183758	12453667	113401746	906477979	6433610014	40934644759
A_{33}	1558766	16520230	150873340	1207459954	8574271258	54567612412
A_{34}	1572537	16575709	151096684	1208228835	8576859887	54575386023
A_{35}	1559415	16520826	150876380	1207455170	8574263945	54567500360
A_{36}	1569361	16564502	151057964	1208110720	8576507193	54574434034

*Identifies Chiral Representation

†Identifies Alternating Representation

Table 13: 2-colorings of 5D-hypercube for q=4 or 1-hyperplanes (edges) of 5D-hypercube (Cont.)

$[\lambda]$	44 36	43 37	42 38	41 39	40 40
A_1	18847859334620010456	22413670446997972838	25362837531743140240	27313824978896887460	27996670589987902014
A_2*	18847856749898064896	22413667593567098448	25362834461344949584	27313821778724903160	27996667338560535196
$A_{3\dagger}$	18847859257885780852	22413670364841246912	25362837441865001528	27313824887601341100	27996670495254082980
A_4	18847856766704295498	22413667612733468770	25362834481318343144	27313821800213507326	27996667359714049916
A_5	75391429606157432796	89654673254005600786	101451340942485322288	109255290345061834468	111986672634212247242
A_6	75391434741988768948	89654678922534504952	101451347043334813206	109255296702428492698	111986679094759845390
A_7	75391429507567646082	89654673145529299732	101451340825886267878	109255290223762071580	111986672510921365600
A_8	75391434523543070266	89654678688077585068	101451346786926363114	109255296441514937800	111986678824308450416
A_9	94239288940765094724	112068343700990309476	126814178474214859414	136569115323944723314	139983343224185808696
A_{10}	94239291508680725702	112068346535254721166	126814181524639564132	136569118502628011070	139983346454459568290
A_{11}	94239288765441089748	112068343510357292528	126814178267737678352	136569115111349424020	139983343006161121260
A_{12}	94239291273428805704	112068346281631440992	126814181248257730296	136569118220225861960	139983346162854669044
A_{13}	94239293852494038614	112068349135075557906	126814184312105381812	136569121420411825260	139983349407403993730
A_{14}	94239286278051269304	112068340758262768502	126814175311580690928	136569112023975578906	139983339875230284004
A_{15}	94239293986646838254	112068349287375751864	126814184469883533380	136569121590029833798	139983349573931817500
A_{16}	94239286361724523754	112068340847572699234	126814175410394391170	136569112123786737628	139983339979665122900
A_{17}	113087148246821895790	134482014116808664130	152177015972758652110	163882940268379932380	167980013779270147172
A_{18}	113087148023326870600	134482013875198539440	152177015709602679880	163882939998950765120	167980013501415204240
A_{19}	188478575214092180140	224136684459253077978	253628353780325450740	273138227347920302220	279966683093672480502
A_{20}	188478577753444741688	224136687262337963862	253628356797550900292	273138230492142003960	279966686289042830634
A_{21}	188478585356450552428	224136695670330279072	253628365831274846342	273138239923039836330	279966695856119919142
A_{22}	188478582759971824040	224136692804886249198	253628362747650794080	273138236709894870180	279966692590942719194
A_{23}	188478575127165613502	224136684357929991762	253628353678132069522	273138227235136161648	279966682985826244160
A_{24}	188478577635153329458	224136687129204140226	253628356658652121466	273138230344012599588	279966686142519791944
A_{25}	188478585260075643958	224136695569007192856	253628365718141263676	273138239810255695758	279966695736786486544
A_{26}	188478582752087928002	224136692797733044392	253628362737621211732	273138236701379257818	279966692580092938760
A_{27}	188478580130520633006	224136689893311819736	253628359623658890590	273138233444359426552	279966689282605624774
A_{28}	188478580348346687096	224136690134921944426	253628359880250742400	273138233713788593812	279966689553568287440
A_{29}	282717866380008860880	336205030620395062432	380442534902040326352	409707345433873419442	419950029122932529996
A_{30}	282717873954451546210	336205038997207759458	380442543902564924858	409707354830309573418	419950038655106147470
A_{31}	282717866710071210850	336205030982494643660	380442535290645133570	409707345837575331440	419950029533233410340
A_{32}	282717874334993525350	336205039422297696290	380442544350134275780	409707355303818427610	419950039127500104940
A_{33}	376957157974051675740	448273377264126084652	507256716527962663540	546276464057801193400	559933375684600884504
A_{34}	376957163109882955912	448273382932654988818	507256722628812154458	546276470415167851630	559933382145148421080
A_{35}	376957157879241203778	448273377155649783598	507256716415739690158	546276463936501430512	559933375565904857280
A_{36}	376957162895216627962	448273382698198068934	507256722376779785394	546276470154254296732	559933381879291942096

*Identifies Chiral Representation

†Identifies Alternating Representation

Table 14: Table 6: Two-Colorings of Vertices or q=5-hyperplanes of 5D-hypercube.

$[\lambda]$	32 0	31 1	30 2	29 3	28 4	27 5	26 6	25 7	24 8
A_1	1	1	5	10	47	131	472	1326	3779
A_2*	0	0	0	0	2	26	148	653	2218
$A_3\dagger$	0	1	2	10	33	131	421	1326	3616
A_4	0	0	0	0	1	26	144	653	2210
A_5	0	0	0	0	8	120	664	2870	9511
A_6	0	0	4	13	82	310	1281	4174	12576
A_7	0	0	0	0	13	120	690	2870	9600
A_8	0	0	2	13	67	310	1215	4174	12360
A_9	0	0	0	4	39	228	1092	4135	13189
A_{10}	0	0	2	11	77	324	1399	4789	14718
A_{11}	0	0	0	4	35	228	1073	4135	13128
A_{12}	0	0	1	11	64	324	1339	4789	14514
A_{13}	0	1	5	23	105	441	1657	5500	16038
A_{14}	0	0	0	0	17	146	852	3523	11868
A_{15}	0	1	4	23	100	441	1636	5500	15976
A_{16}	0	0	0	0	15	146	838	3523	11818
A_{17}	0	0	0	3	42	276	1335	5068	16098
A_{18}	0	0	0	3	45	276	1342	5068	16126
A_{19}	0	0	0	4	52	374	1922	7658	24982
A_{20}	0	0	0	3	56	396	2021	7938	25690
A_{21}	0	1	7	34	176	765	3034	10289	30678
A_{22}	0	0	0	16	100	586	2498	9242	28298
A_{23}	0	0	0	4	50	374	1911	7658	24946
A_{24}	0	0	0	3	58	396	2032	7938	25726
A_{25}	0	1	5	34	164	765	2975	10289	30490
A_{26}	0	0	2	16	112	586	2557	9242	28486
A_{27}	0	0	2	15	106	552	2447	8924	27754
A_{28}	0	0	1	15	99	552	2412	8924	27642
A_{29}	0	0	0	7	91	624	3091	12073	38804
A_{30}	0	0	2	27	171	910	3875	14031	42938
A_{31}	0	0	0	7	93	624	3105	12073	38854
A_{32}	0	0	3	27	176	910	3896	14031	43000
A_{33}	0	0	0	18	148	948	4398	16862	53220
A_{34}	0	0	4	31	220	1138	5015	18166	56276
A_{35}	0	0	1	18	157	948	4444	16862	53368
A_{36}	0	0	3	31	211	1138	4969	18166	56128

*Identifies Chiral Representation

†Identifies Alternating Representation

Table 15: EN SON TABLO

$[\lambda]$	23 9	22 10	21 11	20 12	19 13	18 14	17 15	16 16
A_1	9013	19963	38073	65664	98804	133576	158658	169112
A_2*	6300	14972	30730	54528	84854	115772	139549	148312
$A_3\dagger$	9013	19591	38073	64985	98804	132622	158658	168028
A_4	6300	14955	30730	54502	84854	115733	139549	148272
A_5	26577	62443	127170	224457	348060	473805	570371	605924
A_6	31935	72346	141756	246631	375831	509313	608445	647402
A_7	26577	62656	127170	224857	348060	474370	570371	606564
A_8	31935	71835	141756	245691	375831	507976	608445	645892
A_9	35457	82216	165022	289831	446538	607012	728648	774616
A_{10}	38137	87161	172314	300905	460423	624750	747682	795338
A_{11}	35457	82075	165022	289569	446538	606644	728648	774200
A_{12}	38137	86673	172314	299996	460423	623459	747682	793876
A_{13}	40948	91573	179829	310939	474635	640973	767103	814338
A_{14}	32877	77754	157900	279619	432914	590482	709920	755258
A_{15}	40948	91426	179829	310676	474635	640598	767103	813920
A_{16}	32877	77628	157900	279385	432914	590142	709920	754876
A_{17}	43199	99880	200138	350931	540233	733809	880619	935962
A_{18}	43199	99934	200138	351041	540233	733952	880619	936136
A_{19}	68334	159792	322922	569118	879452	1197022	1438568	1529340
A_{20}	69776	162501	327308	575734	888293	1208086	1450990	1542436
A_{21}	79085	178556	352143	611502	935058	1265251	1514785	1609132
A_{22}	75134	171312	341894	595902	916064	1240734	1489064	1580692
A_{23}	68334	159703	322922	568954	879452	1196786	1438568	1529076
A_{24}	69776	162590	327308	575898	888293	1208322	1450990	1542700
A_{25}	79085	178099	352143	610672	935058	1264057	1514785	1607796
A_{26}	75134	171769	341894	596732	916064	1241928	1489064	1582028
A_{27}	73594	169021	337336	590062	906961	1230818	1476330	1568876
A_{28}	73594	168748	337336	589565	906961	1230103	1476330	1568076
A_{29}	105233	244539	492330	865233	1334831	1814626	2179638	2316518
A_{30}	113271	258295	514208	896465	1376487	1865012	2236746	2375486
A_{31}	105233	244665	492330	865467	1334831	1814966	2179638	2316900
A_{32}	113271	258442	514208	896728	1376487	1865387	2236746	2375904
A_{33}	143370	330976	664644	1164802	1795254	2437474	2927320	3109712
A_{34}	148728	340879	679230	1186958	1823025	2472982	2965394	3151168
A_{35}	143370	331338	664644	1165463	1795254	2438425	2927320	3110776
A_{36}	148728	340517	679230	1186297	1823025	2472031	2965394	3150104

Identifies Chiral Representation
†Identifies Alternating Representation

References

[1] R. Carbó-Dorca, *Boolean hypercubes and the structure of vector spaces*, J. Math. Sciences and Model. **1**(1) (2018), 1-14.
[2] R. Carbó-Dorca, *N-dimensional Boolean hypercubes and the goldbach conjecture*, J. Math. Chem. **54**(6) (2016), 1213-1220. https://doi.org/10.1007/s10910-016-0628-5
[3] R. Carbó-Dorca, *DNA, unnatural base pairs and hypercubes*, J. Math. Chem. **56**(5) (2018), 1353-1356. https://doi.org/10.1007/s10910-018-0866-9
[4] R. Carbó-Dorca, *About Erdös discrepancy conjecture*, J. Math. Chem. **54**(3) (2016), 657-660. https://doi.org/10.1007/s10910-015-0585-4
[5] R. Carbó-Dorca, *Boolean hypercubes as time representation holders*, J. Math. Chem. **56**(5) (2018), 1349-1352. https://doi.org/10.1007/s10910-018-0865-x
[6] A. A. Gowen, C. P. O'Donnell, P. J. Cullen, S. E. J. Bell, *Recent applications of chemical imaging to pharmaceutical process monitoring and quality control*, European Journal of Pharmaceutics and Biopharmaceutics **69**(1) (2008), 10-22.
[7] P. G. Mezey, *Similarity analysis in two and three dimensions using lattice animals and ploycubes*, J. Math. Chem. **11**(1) (1992), 27-45.
[8] A. Frolov, E. Jako, P. G. Mezey, *Logical models for molecular shapes and their families*, J. Math. Chem. **30**(4) (2001), 389-409.
[9] P. G. Mezey, *Some dimension problems in molecular databases*, J. Math. Chem. **45**(1) (2009), 1-6.
[10] P. G. Mezey, *Shape similarity measures for molecular bodies: A three-dimensional topological approach in quantitative shape-activity relations*, J. Chem. Inf. Comput. Sci. **32**(6) (1992), 650-656.
[11] K. Balasubramanian, *Combinatorial multinomial generators for colorings of 4D-hypercubes and their applications*, J. Math. Chem. **56**(9) (2018), 2707-2723.
[12] W. K. Clifford, *Mathematical papers*, Macmillan and Company, London, 1882.
[13] W. K. Clifford, *On the types of compound statement involving four classes*, Memoirs of the Literary and Philosophical Society of Manchester **16** (1877), 88-101.
[14] G. Pólya, R. C. Read, *Combinatorial enumeration of groups, graphs and chemical compounds*, Springer, New York, 1987.
[15] G. Pólya, *Kombinatorische anzahlbestimmugen für gruppen, graphen und chemische verbindugen*, Acta. Math. **68**(1) (1937), 145-254.
[16] J. H. Redfield, *The theory of group-reduced distributions*, American Journal of Mathematics **49**(3) (1927), 433-455.
[17] G. Pólya, *Sur les types des propositions composées*, The Journal of Symbolic Logic **5**(3) (1940), 98-103.
[18] M. A. Harrison, R. G. High, *On the cycle index of a product of permutation groups*, Journal of Combinatorial Theory **4**(3) (1968), 277-299.
[19] D. C. Banks, S. A. Linton, P. K. Stockmeyer, *Counting cases in substitope algorithms*, IEEE Transactions on Visualization and Computer Graphics **10**(4) (2004), 371-384.
[20] D. C. Banks, P. K. Stockmeyer, *DeBruijn counting for visualization algorithms*, T. Móller, B. Hamann, R. D. Russell (editors), *Mathematical foundations of scientific visualization, computer graphics and massive data exploration*, Springer, Berlin, 2009, pp. 69-88.

[21] W. Y. C. Chen, *Induced cycle structures of the hyperoctahedral group*, SIAM J. Discrete Math. **6**(3) (1993), 353-362.
[22] G. M. Ziegler, *Lectures on polytopes (graduate texts in mathematics; 152)*, Springer-Verlag, 1994.
[23] P. W. H. Lemmens, *Pólya theory of hypercubes*, Geometriae Dedicata **64**(2) (1997), 145-155.
[24] P. Bhaniramka, R. Wenger, R. Crawfis, *Isosurfacing in higher dimensions*, Proceedings of IEEE Visualization 2000, (2000), 267-273.
[25] O. Aichholzer, *Extremal properties of 0/1-polytopes of dimension 5*, G. Kalai, G. M. Ziegler (editors), *Polytopes - combinatorics and computation*, Birkhäuser, Basel, 2000, pp. 111-130.
[26] R. Perez-Aguila, *Enumerating the configurations in the n-dimensional polytopes through Pólya's counting and a concise representation*, 3rd International Conference on Electrical and Electronics Engineering, (2006), 1-4.
[27] M. Liu, K. E. Bassler, *Finite size effects and symmetry breaking in the evolution of networks of competing Boolean nodes*, Journal of Physics A: Mathematical and Theoretical **44**(4) (2010), 045101.
[28] R. Perez-Aguila, *Towards a new approach for volume datasets based on orthogonal polytopes in four-dimensional color space*, Engineering Letters **18**(4) (2010), 326-340.
[29] W. Y. C. Chen, P. L. Guo, *Equivalence classes of full-dimensional 0/1-polytopes with many vertices*, (2011), arXiv:1101.0410v1 [math.CO].
[30] N. G. de Bruijn, *Enumeration of tree-shaped molecules*, W. T. Tutte (editor), *Recent progress in combinatorics: proceedings of the 3rd Waterloo conference on combinatorics*, Academic Press, New York, 1969, pp. 59-68.
[31] F. Harary, E. M. Palmer, *Graphical enumeration*, Academic Press, New York, 1973.
[32] I. G. Macdonald, E. M. Palmer, *Symmetric functions and Hall polynomials*, Clarendon Press, Oxford, 1979.
[33] A. T. Balaban, *Enumeration of isomers*, D.Bonchev, D. H. Rouvray (editors), *Chemical graph theory: introduction and fundamentals*, Abacus Press/Gordon and Breach Science Publishers, New York, 1991, pp. 177-234.
[34] C. J. O. Reichhardt, K. E. Bassler, *Canalization and symmetry in Boolean models for genetic regulatory networks*, Journal of Physics A: Mathematical and Theoretical **40**(16) (2007), 4339.
[35] K. Balasubramanian, *Combinatorial enumeration of ragas (scales of integer sequences) of Indian music*, Journal of Integer Sequences **5** (2002), Article 02.2.6.
[36] K. Balasubramanian, *Applications of combinatorics and graph theory to spectroscopy and quantum chemistry*, Chem. Rev. **85**(6) (1985), 599-618.
[37] K. Balasubramanian, *The symmetry groups of nonrigid molecules as generalized wreath-products and their representations*, J. Chem. Phys. **72**(1) (1980), 665-677.
[38] K. Balasubramanian, *Relativistic double group spinor representations of nonrigid molecules*, J. Chem. Phys. **120**(12) (2004), 5524-5535.
[39] K. Balasubramanian, *Generalization of de Bruijn's extension of Pólya's theorem to all characters*, J. Math. Chem. **14**(1) (1993), 113-120.
[40] K. Balasubramanian, *Generalization of the Harary-Palmer power group theorem to all irreducible representations of object and color groups-color combinatorial group theory*, J. Math. Chem. **52**(2) (2014), 703-728.
[41] R. Wallace, *Spontaneous symmetry breaking in a non-rigid molecule approach to intrinsically disordered proteins*, Molecular BioSystems **8**(1) (2012), 374-377.
[42] R. Wallace, *Tools for the future: hidden symmetries*, *Computational Psychiatry*, Springer, Cham, 2017, pp. 153-165.
[43] M. R. Darafsheh, Y. Farjami, A. R. Ashrafi, *Computing the full non-rigid group of tetranitrocubane and octanitrocubane using wreath product*, MATCH Commun. Math. Comput. Chem. **54**(1) (2005),53-74.
[44] R. Foote, G. Mirchandani, D. Rockmore, *Two-dimensional wreath product group-based image processing*, Journal of Symbolic Computation **37**(2) (2004), 187-207.
[45] K. Balasubramanian, *A generalized wreath product method for the enumeration of stereo and position isomers of polysubstituted organic compounds*, Theoret. Chim. Acta **51**(1) (1979), 37-54.
[46] K. Balasubramanian, *Symmetry simplifications of space types in configuration interaction induced by orbital degeneracy*, International Journal of Quantum Chemistry **20**(6) (1981), 1255-1271.
[47] K. Balasubramanian, *Enumeration of the isomers of the gallium arsenide clusters (Ga_mAs_n)*, Chemical Physics Letters **150**(1-2) (1988), 71-77.
[48] K. Balasubramanian, *Nuclear-spin statistics of C_{60}, $C_{60}H_{60}$ and $C_{60}D_{60}$*, Chemical Physics Letters **183**(3-4) (1991), 292-296.
[49] K. Balasubramanian, *Group theoretical analysis of vibrational modes and rovibronic levels of extended aromatic $C_{48}N_{12}$ azafullerene*, Chemical Physics Letters **391**(1-3) (2004), 64-68.
[50] K. Balasubramanian, *Group theory and nuclear spin statistics of weakly-bound $(H_2O)_n$, $(NH_3)_n$, $(CH_4)_n$, and $NH^+{}_4(NH_3)_n$*, J. Chem. Phys. **95**(11) (1991), 8273-8286.
[51] K. Balasubramanian, *Generators of the character tables of generalized wreath product groups*, Theoretica Chimica Acta **78**(1) (1990), 31-43.
[52] X. Liu, K. Balasubramanian, *Computer generation of character tables of generalized wreath product groups*, Journal of Computational Chemistry **11**(5) (1990), 589-602.
[53] K. Balasubramanian, *Multinomial combinatorial group representations of the octahedral and cubic symmetries*, Journal of Mathematical Chemistry **35**(4) (2004), 345-365.
[54] K. Balasubramanian, *Enumeration of internal rotation reactions and their reaction graphs*, Theoretica Chimica Acta **53**(2) (1979), 129-146.
[55] K. Balasubramanian, *A method for nuclear-spin statistics in molecular spectroscopy*, J. Chem. Phys. **74**(12) (1981), 6824-6829.
[56] K. Balasubramanian, *Operator and algebraic methods for NMR spectroscopy. II. NMR projection operators and spin functions*, J. Chem. Phys. **78**(11) (1983), 6369-6376.
[57] K. Balasubramanian, M. Randić, *The characteristic polynomials of structures with pending bonds*, Theoretica Chimica Acta **61**(4) (1982), 307-323.
[58] S. C. Basak, D. Mills, M. M. Mumtaz, K. Balasubramanian, *Use of topological indices in predicting aryl hydrocarbon receptor binding potency of dibenzofurans: A hierarchical QSAR approach*, Indian Journal of Chemistry-Section A **42A** (2003), 1385-1391.
[59] T. Ruen, *Free Public Domain Work*, available to anyone to use for any purpose at https://commons.wikimedia.org/wiki/File:5-cube_t024.svg
[60] N. G. de Bruijn, *Color Patterns that are invariant under permutation of colors*, Journal of Combinatorial Theory **2**(4) (1967), 418-421.
[61] K. Balasubramanian, *Computational multinomial combinatorics for colorings of 5D-hypercubes for all irreducible representations and applications*, J. Math. Chem. (2018), https://doi.org/10.1007/s10910-018-0978-2
[62] J. M. Price, M. W. Crofton, Y. T. Lee, *Vibrational spectroscopy of the ammoniated ammonium ions $NH_4+(NH_3)_n(n=1-10)$*, Journal of Physical Chemistry **95**(6) (1991), 2182-2195.
[63] K. Balasubramanian, *Enumeration of stable stereo and position isomers of polysubstitued alcohols*, ANNALS of the New York Academy of Sciences **319**(1) (1979), 33-36.
[64] K. Balasubramanian, *Nonrigid group theory, tunneling splittings, and nuclear spin statistics of water pentamer: $(H_2O)_5$*, The Journal of Physical Chemistry A **108**(26) (2004), 5527-5536.
[65] H. S. M. Coxeter, *Regular polytopes*, Dover Publications, New York, 1973.
[66] J. W. Kennedy, M. Gordon, *Graph contraction and a generalized Möbius inversion*, Annals of the New York Academy of Sciences **319**(1) (1979), 331-348.
[67] V. Krishnamurthy, *Combinatorics: theory and applications*, Ellis Harwood, New York, 1986.
[68] K. Balasubramanian, *Generating functions for the nuclear spin statistics of nonrigid molecules*, J. Chem. Phys. **75**(9) (1981), 4572-4585.
[69] K. Balasubramanian, *Operator and algebraic methods for NMR spectroscopy. I. Generation of NMR spin species*, J. Chem. Phys. **78**(11) (1983), 6358-6368.

Journal of Mathematical Sciences and Modelling, 1 (3) (2018) 181-191
Research Article

Journal of Mathematical Sciences and Modelling

Journal Homepage: www.dergipark.gov.tr/jmsm
ISSN 2636-8692

The Form of the Solutions of System of Rational Difference Equation

E. M. Elsayed[a,b*] and Marwa M. Alzubaidi[a,c]

[a]*King Abdulaziz University, Faculty of Science, Mathematics Department, P.O. Box 80203, Jeddah 21589,Saudi Arabia*
[b]*Department of Mathematics, Faculty of Science, Mansoura University,Mansoura35516, Egypt.*
[c]*Mathematics Department , The University College of Duba, University of Tabuk, Tabuk, Saudi Arabia.*
[*]*Corresponding author*

Article Info

Keywords: *Difference Equation, System difference equations, Periodicity*
2010 AMS: *39A10*
Received: *26 May 2018*
Accepted: *3 November 2018*
Available online: *30 December 2018*

Abstract

In this article, we study the form of the solutions of the system of difference equations $x_{n+1} = ((y_{n-8})/(1+y_{n-2}x_{n-5}y_{n-8}))$, $y_{n+1} = ((x_{n-8})/(1x_{n-2}y_{n-5}x_{n-8}))$, with the initial conditions are real numbers. Also, we give the numerical examples of some of difference equations and got some related graphs and figures using by Matlab.

1. Introduction

Our aim in this studying to get the techniques of solutions of the system of rational difference equations

$$x_{n+1} = \frac{y_{n-8}}{1+y_{n-2}x_{n-5}y_{n-8}}, \qquad y_{n+1} = \frac{x_{n-8}}{\pm 1 \pm x_{n-2}y_{n-5}x_{n-8}},$$

with real number‘s initial conditions $x_{-8}, x_{-7}, x_{-6}, x_{-5}, x_{-4}, x_{-3}, x_{-2}, x_{-1}, x_0, y_{-8}, y_{-7}, y_{-6}, y_{-5}, y_{-4}, y_{-3}, y_{-2}, y_{-1}, y_0$.
Lately, difference equations appear as discrete analogues of discovered evolution because most analysis of time evolving variables are discrete. Also, there has been an increasing interest in the study of qualitative analysis of system of rational difference equations. Discrete systems can be described as operators acting on functions with countable domains. These functions are also called discrete functions or sequences. Although difference equations looks simple in form, but it is highly difficult to understand thoroughly the behaviors of their solutions, see [1]-[44] and the references cited therein. There are many papers with related to the difference equations system for example, Ahmed and Elsayed [1] has got the expressions of solutions of some rational difference equations systems

$$x_{n+1} = \frac{x_{n-1}y_{n-2}}{y_n(-1 \pm x_{n-1}y_{n-2})}, \qquad y_{n+1} = \frac{y_{n-1}x_{n-2}}{x_n(\pm 1 \pm y_{n-1}x_{n-2})}.$$

Din investigated the boundedness character, the local asymptotic stability of equilibrium points and global of the unique positive equilibrium point of a discrete perdator-pery model given by

$$x_{n+1} = \frac{\alpha x_n - \beta x_n y_n}{1+\gamma x_n}, \qquad y_{n+1} = \frac{\delta x_n y_n}{x_n + \eta y_n}.$$

El-Dessoky [2] obtained the solutions and periodicity for some systems of third-order rational difference equations

$$x_{n+1} = \frac{y_{n-1}y_{n-2}}{x_n(\pm 1 \pm y_{n-1}y_{n-2})}, \qquad y_{n+1} = \frac{x_{n-1}x_{n-2}}{y_n(\pm 1 \pm x_{n-1}x_{n-2})}.$$

Email addresses and ORCID numbers: **emmelsayed@yahoo.com, 0000-0003-0894-8472 (E. M. Elsayed), mmialzubaidi@hotmail.com, 0000-0002-3314-5244 (E. M. Elsayed)**

In [3], El-Dessoky and Elsayed studied the solution and periodic nature of some systems of rational difference equations

$$x_{n+1}=\frac{x_n y_{n-1}}{y_{n-1}\pm y_n},\qquad y_{n+1}=\frac{y_n x_{n-1}}{x_{n-1}\pm x_n}.$$

El-Dessoky et al. [4] obtained the rational system of difference equations

$$x_{n+1}=\frac{x_{n-3}y_{n-4}}{y_n\left(\pm 1\pm x_{n-3}y_{n-4}\right)},\quad y_{n+1}=\frac{y_{n-3}x_{n-4}}{x_n\left(\pm 1\pm y_{n-3}x_{n-4}\right)}.$$

Elsayed and Ibrahim [5] solved solutions for some systems of nonlinear rational difference equations

$$x_{n+1}=\frac{x_{n-2}y_{n-1}}{y_n(\pm 1\pm x_{n-2}y_{n-1})},\qquad y_{n+1}=\frac{y_{n-2}x_{n-1}}{x_n(\pm 1\pm y_{n-2}x_{n-1})}.$$

Elsayed and Alghamdi [6] solved the form of the solution of nonlinear difference equation systems

$$x_{n+1}=\frac{x_{n-7}}{1+x_{n-7}y_{n-3}},\quad y_{n+1}=\frac{y_{n-7}}{\pm 1\pm y_{n-7}x_{n-3}}.$$

Haddad et al [7] obtained solution form of a higher-order system of difference equations and dynamical behavior of its special case

$$x_{n+1}=\frac{x^{p}_{n-k+1}y_n}{ay^{p}_{n-k}+by_n},\quad y_{n+1}=\frac{y^{p}_{n-k+1}x_n}{\alpha x^{p}_{n-k}+\beta x_n}.$$

In [8] Kurbanli studied the behavior of solutions of the following systems of difference equations

$$x_{n+1}=\frac{x_{n-1}}{y_n x_{n-1}-1},\quad y_{n+1}=\frac{y_{n-1}}{x_n y_{n-1}-1}.$$

Kurbanli et al. [9, 10] obtained the solutions of following problems

$$\begin{aligned} x_{n+1}&=\tfrac{x_{n-1}+y_n}{y_n x_{n-1}-1},\quad y_{n+1}=\tfrac{y_{n-1}+x_n}{x_n y_{n-1}-1}.\\ x_{n+1}&=\tfrac{x_{n-1}}{y_n x_{n-1}+1},\quad y_{n+1}=\tfrac{y_{n-1}}{x_n y_{n-1}+1}.\end{aligned}$$

Mansour et al. [11] investigated the solutions and periodicity of some system of difference equations

$$x_{n+1}=\frac{x_{n-5}}{-1+x_{n-5}y_{n-2}},\quad y_{n+1}=\frac{y_{n-5}}{\pm 1\pm y_{n-5}x_{n-2}}.$$

Touafek and Elsayed [12] gave the solutions of following systems of difference equations

$$x_{n+1}=\frac{x_{n-3}}{\pm 1\pm x_{n-3}y_{n-1}},\quad y_{n+1}=\frac{y_{n-3}}{\pm 1\pm y_{n-3}x_{n-1}}.$$

Definition 1.1. *A sequence $\{x_n\}_{n=-k}^{\infty}$ is said to be periodic with period p if $x_{n+p}=x_n$ for all $n\geq -k$.*

2. The main results

2.1. The first system: $x_{n+1}=\frac{y_{n-8}}{1+y_{n-2}x_{n-5}y_{n-8}}, y_{n+1}=\frac{x_{n-8}}{1+x_{n-2}y_{n-5}x_{n-8}}$

In this part, we study the solutions of the system of difference equations

$$x_{n+1}=\frac{y_{n-8}}{1+y_{n-2}x_{n-5}y_{n-8}},y_{n+1}=\frac{x_{n-8}}{1+x_{n-2}y_{n-5}x_{n-8}},$$

with a real number‘s initial conditions.

Theorem 2.1. *Suppose that $x_{-8}=a$, $x_{-7}=b$, $x_{-6}=c$, $x_{-5}=d$, $x_{-4}=e$, $x_{-3}=f$, $x_{-2}=g$, $x_{-1}=h$, $x_0=k$, $y_{-8}=l$, $y_{-7}=m$, $y_{-6}=p$, $y_{-5}=q$, $y_{-4}=r$, $y_{-3}=s$, $y_{-2}=t$, $y_{-1}=u$, $y_0=v$ are arbitrary real numbers and let $\{x_n,y_n\}$ be solutions of the system 2.1. Then all solutions of 2.1 are given by*

$$
\begin{aligned}
x_{18n-8} &= a\prod_{i=0}^{n-1}\frac{(1+(6i)agq)(1+(6i+3)agq)}{(1+(6i+1)agq)(1+(6i+4)agq)},\\
x_{18n-7} &= b\prod_{i=0}^{n-1}\frac{(1+6ibhr)(1+(6i+3)bhr)}{(1+(6i+1)bhr)(1+(6i+4)bhr)},\\
x_{18n-6} &= c\prod_{i=0}^{n-1}\frac{(1+6icks)(1+(6i+3)cks)}{(1+(6i+1)cks)(1+(6i+4)cks)},\\
x_{18n-5} &= d\prod_{i=0}^{n-1}\frac{(1+(6i+1)dlt)(1+(6i+4)dlt)}{(1+(6i+2)dlt)(1+(6i+5)dlt)},\\
x_{18n-4} &= e\prod_{i=0}^{n-1}\frac{(1+(6i+1)emu)(1+(6i+4)emu)}{(1+(6i+2)emu)(1+(6i+5)emu)},\\
x_{18n-3} &= f\prod_{i=0}^{n-1}\frac{(1+(6i+1)fpv)(1+(6i+4)fpv)}{(1+(6i+2)fpv)(1+(6i+5)fpv)},\\
x_{18n-2} &= g\prod_{i=0}^{n-1}\frac{(1+(6i+2)agq)(1+(6i+5)agq)}{(1+(6i+3)agq)(1+(6i+6)agq)},\\
x_{18n-1} &= h\prod_{i=0}^{n-1}\frac{(1+(6i+2)bhr)(1+(6i+5)bhr)}{(1+(6i+3)bhr)(1+(6i+6)bhr)},\\
x_{18n} &= k\prod_{i=0}^{n-1}\frac{(1+(6i+2)cks)(1+(6i+5)cks)}{(1+(6i+3)cks)(1+(6i+6)cks)},\\
x_{18n+1} &= \frac{l}{1+dlt}\prod_{i=0}^{n-1}\frac{(1+(6i+3)dlt)(1+(6i+6)dlt)}{(1+(6i+4)dlt)(1+(6i+7)dlt)},\\
x_{18n+2} &= \frac{m}{1+emu}\prod_{i=0}^{n-1}\frac{(1+(6i+3)emu)(1+(6i+6)emu)}{(1+(6i+4)emu)(1+(6i+7)emu)},\\
x_{18n+3} &= \frac{p}{1+fpv}\prod_{i=0}^{n-1}\frac{(1+(6i+3)fpv)(1+(6i+6)fpv)}{(1+(6i+4)fpv)(1+(6i+7)fpv)},\\
x_{18n+4} &= \frac{q(1+agq)}{(1+2agq)}\prod_{i=0}^{n-1}\frac{(1+(6i+4)agq)(1+(6i+7)agq)}{(1+(6i+5)agq)(1+(6i+8)agq)},\\
x_{18n+5} &= \frac{r(1+bhr)}{(1+2bhr)}\prod_{i=0}^{n-1}\frac{(1+(6i+4)bhr)(1+(6i+7)bhr)}{(1+(6i+5)bhr)(1+(6i+8)bhr)},\\
x_{18n+6} &= \frac{s(1+cks)}{(1+2cks)}\prod_{i=0}^{n-1}\frac{(1+(6i+4)cks)(1+(6i+7)cks)}{(1+(6i+5)cks)(1+(6i+8)cks)},\\
x_{18n+7} &= \frac{t(1+2dlt)}{(1+3dlt)}\prod_{i=0}^{n-1}\frac{(1+(6i+5)dlt)(1+(6i+8)dlt)}{(1+(6i+6)dlt)(1+(6i+9)dlt)},\\
x_{18n+8} &= \frac{u(1+2emu)}{(1+3emu)}\prod_{i=0}^{n-1}\frac{(1+(6i+5)emu)(1+(6i+8)emu)}{(1+(6i+6)emu)(1+(6i+9)emu)},\\
x_{18n+9} &= \frac{v(1+2fpv)}{(1+3fpv)}\prod_{i=0}^{n-1}\frac{(1+(6i+5)fpv)(1+(6i+8)fpv)}{(1+(6i+6)fpv)(1+(6i+9)fpv)},\\
y_{18n-8} &= l\prod_{i=0}^{n-1}\frac{(1+6idlt)(1+(6i+3)dlt)}{(1+(6i+1)dlt)(1+(6i+4)dlt)},\\
y_{18n-7} &= m\prod_{i=0}^{n-1}\frac{(1+6iemu)(1+(6i+3)emu)}{(1+(6i+1)emu)(1+(6i+4)emu)},\\
y_{18n-6} &= p\prod_{i=0}^{n-1}\frac{(1+6fpv)(1+(6i+3)fpv)}{(1+(6i+1)fpv)(1+(6i+4)fpv)},\\
y_{18n-5} &= q\prod_{i=0}^{n-1}\frac{(1+(6i+1)agq)(1+(6i+4)agq)}{(1+(6i+2)agq)(1+(6i+5)agq)},\\
y_{18n-4} &= r\prod_{i=0}^{n-1}\frac{(1+(6i+1)bhr)(1+(6i+4)bhr)}{(1+(6i+2)bhr)(1+(6i+5)bhr)},
\end{aligned}
$$

$$y_{18n-3} = s\prod_{i=0}^{n-1}\frac{(1+(6i+1)cks)(1+(6i+4)cks)}{(1+(6i+2)cks)(1+(6i+5)cks)},$$

$$y_{18n-2} = t\prod_{i=0}^{n-1}\frac{(1+(6i+2)dlt)(1+(6i+5)dlt)}{(1+(6i+3)dlt)(1+(6i+6)dlt)},$$

$$y_{18n-1} = u\prod_{i=0}^{n-1}\frac{(1+(6i+2)emu)(1+(6i+5)emu)}{(1+(6i+3)emu)(1+(6i+6)emu)},$$

$$y_{18n} = v\prod_{i=0}^{n-1}\frac{(1+(6i+2)fpv)(1+(6i+5)fpv)}{(1+(6i+3)fpv)(1+(6i+6)fpv)},$$

$$y_{18n+1} = \frac{a}{1+agq}\prod_{i=0}^{n-1}\frac{(1+(6i+3)agq)(1+(6i+6)agq)}{(1+(6i+4)agq)(1+(6i+7)agq)},$$

$$y_{18n+2} = \frac{b}{1+bhr}\prod_{i=0}^{n-1}\frac{(1+(6i+3)bhr)(1+(6i+6)bhr)}{(1+(6i+4)bhr)(1+(6i+7)bhr)},$$

$$y_{18n+3} = \frac{c}{1+cks}\prod_{i=0}^{n-1}\frac{(1+(6i+3)cks)(1+(6i+6)cks)}{(1+(6i+4)cks)(1+(6i+7)cks)},$$

$$y_{18n+4} = \frac{d(1+dlt)}{(1+2dlt)}\prod_{i=0}^{n-1}\frac{(1+(6i+4)dlt)(1+(6i+7)dlt)}{(1+(6i+5)dlt)(1+(6i+8)dlt)},$$

$$y_{18n+5} = \frac{e(1+emu)}{(1+2emu)}\prod_{i=0}^{n-1}\frac{(1+(6i+4)emu)(1+(6i+7)emu)}{(1+(6i+5)emu)(1+(6i+8)emu)},$$

$$y_{18n+6} = \frac{f(1+fpv)}{(1+2fpv)}\prod_{i=0}^{n-1}\frac{(1+(6i+4)fpv)(1+(6i+7)fpv)}{(1+(6i+5)fpv)(1+(6i+8)fpv)},$$

$$y_{18n+7} = \frac{g(1+2agq)}{(1+3agq)}\prod_{i=0}^{n-1}\frac{(1+(6i+5)agq)(1+(6i+8)agq)}{(1+(6i+6)agq)(1+(6i+9)agq)},$$

$$y_{18n+8} = \frac{h(1+2bhr)}{(1+3bhr)}\prod_{i=0}^{n-1}\frac{(1+(6i+5)bhr)(1+(6i+8)bhr)}{(1+(6i+6)bhr)(1+(6i+9)bhr)},$$

$$y_{18n+9} = \frac{k(1+2cks)}{(1+3cks)}\prod_{i=0}^{n-1}\frac{(1+(6i+5)cks)(1+(6i+8)cks)}{(1+(6i+6)cks)(1+(6i+9)cks)}.$$

Proof. For $n=0$, the result holds. Now, assume that $n>0$ and that our assumption holds for $n-1$. That is,

$$x_{18n-17} = \frac{l}{1+dlt}\prod_{i=0}^{n-2}\frac{(1+(6i+3)dlt)(1+(6i+6)dlt)}{(1+(6i+4)dlt)(1+(6i+7)dlt)},$$

$$x_{18n-16} = \frac{m}{1+emu}\prod_{i=0}^{n-2}\frac{(1+(6i+3)emu)(1+(6i+6)emu)}{(1+(6i+4)emu)(1+(6i+7)emu)},$$

$$x_{18n-15} = \frac{p}{1+fpv}\prod_{i=0}^{n-2}\frac{(1+(6i+3)fpv)(1+(6i+6)fpv)}{(1+(6i+4)fpv)(1+(6i+7)fpv)},$$

$$x_{18n-14} = \frac{q(1+agq)}{(1+2agq)}\prod_{i=0}^{n-2}\frac{(1+(6i+4)agq)(1+(6i+7)agq)}{(1+(6i+5)agq)(1+(6i+8)agq)},$$

$$x_{18n-13} = \frac{r(1+bhr)}{(1+2bhr)}\prod_{i=0}^{n-2}\frac{(1+(6i+4)bhr)(1+(6i+7)bhr)}{(1+(6i+5)bhr)(1+(6i+8)bhr)},$$

$$x_{18n-12} = \frac{s(1+cks)}{(1+2cks)}\prod_{i=0}^{n-2}\frac{(1+(6i+4)cks)(1+(6i+7)cks)}{(1+(6i+5)cks)(1+(6i+8)cks)},$$

$$x_{18n-11} = \frac{t(1+2dlt)}{(1+3dlt)}\prod_{i=0}^{n-2}\frac{(1+(6i+5)dlt)(1+(6i+8)dlt)}{(1+(6i+6)dlt)(1+(6i+9)dlt)},$$

$$x_{18n-10} = \frac{u(1+2emu)}{(1+3emu)}\prod_{i=0}^{n-2}\frac{(1+(6i+5)emu)(1+(6i+8)emu)}{(1+(6i+6)emu)(1+(6i+9)emu)},$$

$$x_{18n-9} = \frac{v(1+2fpv)}{(1+3fpv)}\prod_{i=0}^{n-2}\frac{(1+(6i+5)fpv)(1+(6i+8)fpv)}{(1+(6i+6)fpv)(1+(6i+9)fpv)}$$

$$
\begin{aligned}
y_{18n-17} &= \frac{a}{1+agq}\prod_{i=0}^{n-2}\frac{(1+(6i+3)agq)(1+(6i+6)agq)}{(1+(6i+4)agq)(1+(6i+7)agq)},\\
y_{18n-16} &= \frac{b}{1+bhr}\prod_{i=0}^{n-2}\frac{(1+(6i+3)bhr)(1+(6i+6)bhr)}{(1+(6i+4)bhr)(1+(6i+7)bhr)},\\
y_{18n-15} &= \frac{c}{1+cks}\prod_{i=0}^{n-2}\frac{(1+(6i+3)cks)(1+(6i+6)cks)}{(1+(6i+4)cks)(1+(6i+7)cks)},\\
y_{18n-14} &= \frac{d(1+dlt)}{(1+2dlt)}\prod_{i=0}^{n-2}\frac{(1+(6i+4)dlt)(1+(6i+7)dlt)}{(1+(6i+5)dlt)(1+(6i+8)dlt)},\\
y_{18n-13} &= \frac{e(1+emu)}{(1+2emu)}\prod_{i=0}^{n-2}\frac{(1+(6i+4)emu)(1+(6i+7)emu)}{(1+(6i+5)emu)(1+(6i+8)emu)},\\
y_{18n-12} &= \frac{f(1+fpv)}{(1+2fpv)}\prod_{i=0}^{n-2}\frac{(1+(6i+4)fpv)(1+(6i+7)fpv)}{(1+(6i+5)fpv)(1+(6i+8)fpv)},\\
y_{18n-11} &= \frac{g(1+2agq)}{(1+3agq)}\prod_{i=0}^{n-2}\frac{(1+(6i+5)agq)(1+(6i+8)agq)}{(1+(6i+6)agq)(1+(6i+9)agq)},\\
y_{18n-10} &= \frac{h(1+2bhr)}{(1+3bhr)}\prod_{i=0}^{n-2}\frac{(1+(6i+5)bhr)(1+(6i+8)bhr)}{(1+(6i+6)bhr)(1+(6i+9)bhr)},\\
y_{18n-9} &= \frac{k(1+2cks)}{(1+3cks)}\prod_{i=0}^{n-2}\frac{(1+(6i+5)cks)(1+(6i+8)cks)}{(1+(6i+6)cks)(1+(6i+9)cks)}.
\end{aligned}
$$

Now, it follows from system 2.1 that

$$x_{18n-8} = \frac{y_{18n-17}}{1+y_{18n-11}x_{18n-14}y_{18n-17}}$$

$$
= \frac{\frac{a}{1+agq}\prod_{i=0}^{n-2}\frac{(1+(6i+3)agq)(1+(6i+6)agq)}{(1+(6i+4)agq)(1+(6i+7)agq)}}{1+\begin{pmatrix} \frac{g(1+2agq)}{(1+3agq)}\prod_{i=0}^{n-2}\frac{(1+(6i+5)agq)(1+(6i+8)agq)}{(1+(6i+6)agq)(1+(6i+9)agq)}\prod_{i=0}^{n-2}\frac{(1+(6i+4)agq)(1+(6i+7)agq)}{(1+(6i+5)agq)(1+(6i+8)agq)} \\ \frac{a}{1+agq}\prod_{i=0}^{n-2}\frac{(1+(6i+3)agq)(1+(6i+6)agq)}{(1+(6i+4)agq)(1+(6i+7)agq)} \end{pmatrix}}
$$

$$
\begin{aligned}
&= \frac{\frac{a}{1+agq}\prod_{i=0}^{n-2}\frac{(1+(6i+3)agq)(1+(6i+6)agq)}{(1+(6i+4)agq)(1+(6i+7)agq)}}{1+\frac{agq}{(1+3agq)}\prod_{i=0}^{n-2}\frac{(1+(6i+3)agq)(1+(6i+6)agq)}{(1+(6i+6)agq)(1+(6i+9)agq)}} = \frac{\frac{a}{1+agq}\prod_{i=0}^{n-2}\frac{(1+(6i+3)agq)(1+(6i+6)agq)}{(1+(6i+4)agq)(1+(6i+7)agq)}}{1+\frac{agq(1+3agq)}{(1+3agq)(1+(6n-3)agq}}\\
&= \frac{\frac{a}{1+agq}\prod_{i=0}^{n-2}\frac{(1+(6i+3)agq)(1+(6i+6)agq)}{(1+(6i+4)agq)(1+(6i+7)agq)}}{\frac{(1+(6n-2)agq}{(1+(6n-3)agq}}\\
&= \frac{a}{1+agq}\prod_{i=0}^{n-2}\frac{(1+(6i+3)agq)(1+(6i+6)agq)}{(1+(6i+4)agq)(1+(6i+7)agq)}\,\frac{(1+(6n-3)agq}{(1+(6n-2)agq}.
\end{aligned}
$$

Hence, we have

$$x_{18n-8} = a\prod_{i=0}^{n-1}\frac{(1+6iagq)\,(1+(6i+3)agq)}{(1+(6i+1)agq)\,(1+(6i+4)agq)},$$

and

$$y_{18n-8} = \frac{x_{18n-17}}{1+x_{18n-11}y_{18n-14}x_{18n-17}}$$

$$
= \frac{\frac{l}{1+dlt}\prod_{i=0}^{n-2}\frac{(1+(6i+3)dlt)(1+(6i+6)dlt)}{(1+(6i+4)dlt)(1+(6i+7)dlt)}}{1+\begin{pmatrix} \frac{t(1+2dlt)}{(1+3dlt)}\prod_{i=0}^{n-2}\frac{(1+(6i+5)dlt)(1+(6i+8)dlt)}{(1+(6i+6)dlt)(1+(6i+9)dlt)}\,\frac{l}{1+dlt}\prod_{i=0}^{n-2}\frac{(1+(6i+3)dlt)(1+(6i+6)dlt)}{(1+(6i+4)dlt)(1+(6i+7)dlt)} \\ \frac{d(1+dlt)}{(1+2dlt)}\prod_{i=0}^{n-2}\frac{(1+(6i+4)dlt)(1+(6i+7)dlt)}{(1+(6i+5)dlt)(1+(6i+8)dlt)} \end{pmatrix}}
$$

$$
\begin{aligned}
&= \frac{\frac{l}{1+dlt}\prod_{i=0}^{n-2}\frac{(1+(6i+3)dlt)(1+(6i+6)dlt)}{(1+(6i+4)dlt)(1+(6i+7)dlt)}}{1+\frac{dlt}{(1+3dlt)}\prod_{i=0}^{n-2}\frac{(1+(6i+3)dlt)(1+(6i+6)dlt)}{(1+(6i+6)dlt)(1+(6i+9)dlt)}} == \frac{\frac{l}{1+dlt}\prod_{i=0}^{n-2}\frac{(1+(6i+3)dlt)(1+(6i+6)dlt)}{(1+(6i+4)dlt)(1+(6i+7)dlt)}}{1+\frac{dlt(1+3dlt)}{(1+3dlt)(1+(6n-3)dlt}}\\
&= \frac{\frac{l}{1+dlt}\prod_{i=0}^{n-2}\frac{(1+(6i+3)dlt)(1+(6i+6)dlt)}{(1+(6i+4)dlt)(1+(6i+7)dlt)}}{\frac{(1+(6n-2)dlt}{(1+(6n-3)dlt}}\\
&= \frac{l}{1+dlt}\prod_{i=0}^{n-2}\frac{(1+(6i+3)dlt)(1+(6i+6)dlt)}{(1+(6i+4)dlt)(1+(6i+7)dlt)}\,\frac{(1+(6n-3)dlt}{(1+(6n-2)dlt}.
\end{aligned}
$$

Therefore, we have

$$y_{18n-8} = l\prod_{i=0}^{n-1}\frac{(1+6idlt)(1+(6i+3)dlt)}{(1+(6i+1)dlt)(1+(6i+4)dlt)}.$$

Similarly, we can prove the other relations. □

Lemma 2.2. *If x_i, y_i, since $i = -8, -7, -6, ..., -1, 0$ are arbitrary real numbers and let $\{x_i, y_i\}$ be solutions of system 2.1, then the following statements are true*

(i) *If* $x_{-8} = a = 0$ *then we get*

$x_{18n-8} = y_{18n+1} = 0,\ x_{18n-2} = y_{18n+7} = g,\ x_{18n+4} = y_{18n-5} = q.$

(ii) *If* $x_{-7} = b = 0$ *then we obtain*

$x_{18n-7} = y_{18n+2} = 0,\ x_{18n-1} = y_{18n+8} = h,\ x_{18n+5} = y_{18n-4} = r.$

(iii) *If* $x_{-6} = c = 0$ *then*

$x_{18n-6} = y_{18n+3} = 0,\ x_{18n} = y_{18n+9} = k,\ x_{18n+6} = y_{18n-3} = s.$

(iv) *If* $x_{-5} = d = 0$ *then*

$x_{18n-5} = y_{18n+4} = 0,\ x_{18n+1} = y_{18n-8} = l,\ x_{18n+7} = y_{18n-2} = t.$

(v) *If* $x_{-4} = e = 0$ *then*

$x_{18n-4} = y_{18n+5} = 0,\ x_{18n+2} = y_{18n-7} = m,\ x_{18n+8} = y_{18n-1} = u.$

(vi) *If* $x_{-3} = f = 0$ *then we see that*

$x_{18n-3} = y_{18n+6} = 0,\ x_{18n+3} = y_{18n-6} = p,\ x_{18n+9} = y_{18n} = v.$

(vii) *If* $x_{-2} = g = 0$ *then we have*

$x_{18n-2} = y_{18n+7} = 0,\ x_{18n+4} = y_{18n-5} = q,\ x_{18n-8} = y_{18n+1} = a.$

$(viii)$ *If* $x_{-1} = h = 0$ *then*

$x_{18n-1} = y_{18n+8} = 0,\ x_{18n+5} = y_{18n-4} = r,\ x_{18n-7} = y_{18n+2} = b.$

(ix) *If* $x_0 = k = 0$ *then we get*

$x_{18n} = y_{18n+9} = 0,\ x_{18n+6} = y_{18n-3} = s,\ x_{18n-6} = y_{18n+3} = c.$

(x) *If* $y_{-8} = l = 0$ *then*

$y_{18n-8} = x_{18n+1} = 0,\ y_{18n-2} = x_{18n+7} = t,\ y_{18n+4} = x_{18n-5} = d.$

(xi) *If* $y_{-7} = m = 0$ *then we get*

$y_{18n-7} = x_{18n+2} = 0,\ y_{18n-1} = x_{18n+8} = u,\ y_{18n+5} = x_{18n-4} = e.$

(xii) *If* $y_{-6} = p = 0$ *then we have*

$y_{18n-6} = x_{18n+3} = 0,\ y_{18n} = x_{18n+9} = v,\ y_{18n+6} = x_{18n-3} = f.$

$(xiii)$ *If* $y_{-5} = q = 0$ *then*

$y_{18n-5} = x_{18n+4} = 0,\ y_{18n+1} = x_{18n-8} = a,\ y_{18n+7} = x_{18n-2} = g.$

(xiv) *If* $y_{-4} = r = 0$ *then we see*

$y_{18n-4} = x_{18n+5} = 0,\ y_{18n+2} = x_{18n-7} = b,\ y_{18n+8} = x_{18n-1} = h.$

(xv) *If* $y_{-3} = s = 0$ *then*

$y_{18n-3} = x_{18n+6} = 0,\ y_{18n+3} = x_{18n-6} = c,\ y_{18n+9} = x_{18n} = k.$

(xvi) *If* $y_{-2} = t = 0$ *then*

$y_{18n-2} = x_{18n+7} = 0,\ y_{18n+4} = x_{18n-5} = d,\ y_{18n-8} = x_{18n+1} = l.$

$(xvii)$ *If* $y_{-1} = u = 0$ *then we get*

$y_{18n-1} = x_{18n+8} = 0,\ y_{18n+5} = x_{18n-4} = e,\ y_{18n-7} = x_{18n+2} = m.$

$(xviii)$ *If* $y_0 = v = 0$ *then we obtain*

$y_{18n} = x_{18n+9} = 0,\ y_{18n+6} = x_{18n-3} = f,\ y_{18n-6} = x_{18n+3} = p.$

Proof. The proof follows from the form of the solutions of system 2.1. □

Lemma 2.3. *Let $\{x_n, y_n\}$ be a positive solution of System 2.1, then $\{x_n\}, \{y_n\}$ are bounded and converges to zero.*

Proof. It follows from System 2.1 that

$$x_{n+1} = \frac{y_{n-8}}{1+y_{n-2}x_{n-5}y_{n-8}} \le y_{n-8}, \quad y_{n+1} = \frac{x_{n-8}}{1+x_{n-2}y_{n-5}x_{n-8}} \le x_{n-8}.$$

Then we have

$$x_{n+10} = \frac{y_{n+1}}{1+y_{n+7}x_{n+4}y_{n+1}} \le y_{n+1} \le x_{n-8},\ y_{n+10} = \frac{x_{n+1}}{1+x_{n+7}y_{n+4}x_{n+1}} \le x_{n+1} \le y_{n-8}.$$

Then the subsequences $\{x_{18n-8}\}_{n=0}^{\infty}$, $\{x_{18n-7}\}_{n=0}^{\infty}$, ..., $\{x_{18n+9}\}_{n=0}^{\infty}$ are decreasing and so are bounded from above by $M = \max\{x_{-8}, x_{-7}, ..., x_8, x_9\}$. Also, the subsequences $\{y_{18n-8}\}_{n=0}^{\infty}$, $\{y_{18n-7}\}_{n=0}^{\infty}$,..., $\{y_{18n+9}\}_{n=0}^{\infty}$ are decreasing and so are bounded from above by $L = \max\{y_{-8}, y_{-7}, ..., y_8, y_9\}$. □

2.2. The second system: $x_{n+1}=\frac{y_{n-8}}{1+y_{n-2}x_{n-5}y_{n-8}}, y_{n+1}=\frac{x_{n-8}}{1-x_{n-2}y_{n-5}x_{n-8}}$

In this subsection, we get the solutions of the following system of the difference equations

$$x_{n+1}=\frac{y_{n-8}}{1+y_{n-2}x_{n-5}y_{n-8}}, y_{n+1}=\frac{x_{n-8}}{1-x_{n-2}y_{n-5}x_{n-8}}, \tag{2.1}$$

where the initial conditions are arbitrary real numbers with $y_{-2}x_{-5}y_{-8},\ y_{-1}x_{-4}y_{-7},\ y_0x_{-3}y_{-6}\neq -1$ and $x_{-2}y_{-5}x_{-8},\ x_{-1}y_{-4}x_{-7},\ x_0y_{-3}x_{-6}\neq 1$.

Theorem 2.4. *System 2.1 has a periodic solution of period eighteen. Moreover $\{x_n,y_n\}_{n=-8}^{\infty}$ takes the form*

$$\begin{aligned}\{x_n\} &= \left\{\begin{array}{c} a,b,c,d,e,f,g,h,k,\frac{l}{1+dlt},\frac{m}{1+emu},\frac{p}{1+fpv},q-agq^2,\\ r-bhr^2,s-cks^2,\frac{t}{1+dlt},\frac{u}{1+emu},\frac{v}{1+fpv},a,b,c,\ldots\end{array}\right\},\\ \{y_n\} &= \left\{\begin{array}{c} l,m,p,q,r,s,t,u,v,\frac{a}{1-agq},\frac{b}{1-bhr},\frac{c}{1-cks},d(1+dlt),\\ e(1+emu),f(1+fpv),\frac{g}{1-agq},\frac{h}{1-bhr},\frac{k}{1-cks},l,m,p,\ldots\end{array}\right\}.\end{aligned}$$

or

$$\begin{aligned} x_{18n-8} &= a,\ x_{18n-7}=b,\ x_{18n-6}=c,\ x_{18n-5}=d,\ x_{18n-4}=e,\ x_{18n-3}=f,\\ x_{18n-2} &= g,\ x_{18n-1}=h,\ x_{18n}=k,\ x_{18n+1}=\frac{l}{1+dlt},\ x_{18n+2}=\frac{m}{1+emu},\\ x_{18n+3} &= \frac{p}{1+fpv},\ x_{18n+4}=q-agq^2,\ x_{18n+5}=r-bhr^2,\\ x_{18n+6} &= s-cks^2,\ x_{18n+7}=\frac{t}{1+dlt},\ x_{18n+8}=\frac{u}{1+emu},\ x_{18n+9}=\frac{v}{1+fpv},\end{aligned}$$

and

$$\begin{aligned} y_{18n-8} &= l,\ y_{18n-7}=m,\ y_{18n-6}=p,\ y_{18n-5}=q,\ y_{18n-4}=r,\ y_{18n-3}=s,\\ y_{18n-2} &= t,\ y_{18n-1}=u,\ y_{18n}=v,\ y_{18n+1}=\frac{a}{1-agq},\ y_{18n+2}=\frac{b}{1-bhr},\\ y_{18n+3} &= \frac{c}{1-cks}, y_{18n+4}=d(1+dlt),\ y_{18n+5}=e(1+emu),\\ y_{18n+6} &= f(1+fpv),\ y_{18n+7}=\frac{g}{1-agq},\ y_{18n+8}=\frac{h}{1-bhr}, y_{18n+9}=\frac{k}{1-cks}.\end{aligned}$$

Proof. For $n=0$, the result holds. Now, assume that $n>0$ and that our assumption holds for $n-1$. That is,

$$\begin{aligned} x_{18n-17} &= \frac{l}{1+dlt},\ x_{18n-16}=\frac{m}{1+emu},\ x_{18n-15}=\frac{p}{1+fpv},\\ x_{18n-14} &= q-agq^2,\ x_{18n-13}=r-bhr^2,\ x_{18n-12}=s-cks^2,\\ x_{18n-11} &= \frac{t}{1+dlt},\ x_{18n-10}=\frac{u}{1+emu},\ x_{18n-9}=\frac{v}{1+fpv},\end{aligned}$$

and

$$\begin{aligned} y_{18n-17} &= \frac{a}{1-agq},\ y_{18n-16}=\frac{b}{1-bhr},\ y_{18n-15}=\frac{c}{1-cks},\\ y_{18n-14} &= d(1+dlt),\ y_{18n-13}=e(1+emu),\ y_{18n-12}=f(1+fpv),\\ y_{18n-11} &= \frac{g}{1-agq},\ y_{18n-10}=\frac{h}{1-bhr}, y_{18n-9}=\frac{k}{1-cks}.\end{aligned}$$

Now, it follows from system 2.1 that

$$\begin{aligned} x_{18n-8} &= \frac{y_{18n-17}}{1+y_{18n-11}x_{18n-14}y_{18n-17}}=\frac{\frac{a}{1-agq}}{1+\frac{g}{1-agq}(q-agq^2)\frac{a}{1-agq}}\\ &= \frac{\frac{a}{1-agq}}{1+\frac{agq}{1-agq}}=\frac{a}{1-agq+agq}=a,\end{aligned}$$

also,

$$\begin{aligned} y_{18n-8} &= \frac{x_{18n-17}}{1-x_{18n-11}y_{18n-14}x_{18n-17}}=\frac{\frac{l}{1+dlt}}{1-\frac{t}{1+dlt}d(1+dlt)\frac{l}{1+dlt}}\\ &= \frac{\frac{l}{1+dlt}}{1-\frac{dlt}{1+dlt}}=l.\end{aligned}$$

The other relations can be proved by similar way. □

The following cases can be proved similarly.

2.3. The third system: $x_{n+1} = \frac{y_{n-8}}{1+y_{n-2}x_{n-5}y_{n-8}}, y_{n+1} = \frac{x_{n-8}}{-1+x_{n-2}y_{n-5}x_{n-8}}$

In this part, we obtain the form of the solutions of the following system of the difference equations

$$x_{n+1} = \frac{y_{n-8}}{1+y_{n-2}x_{n-5}y_{n-8}}, y_{n+1} = \frac{x_{n-8}}{-1+x_{n-2}y_{n-5}x_{n-8}}, \tag{2.2}$$

where the initial conditions are arbitrary real numbers with $y_{-2}x_{-5}y_{-8}, y_{-1}x_{-4}y_{-7}, y_0x_{-3}y_{-6} \neq -1$ and $x_{-2}y_{-5}x_{-8}, x_{-1}y_{-4}x_{-7}, x_0y_{-3}x_{-6} \neq 1$.

Theorem 2.5. *System 2.2 has a periodic solution of period (36) which takes the form*

$$\{x_n\} = \left\{ \begin{array}{c} a,b,c,d,e,f,g,h,k, \frac{l}{1+dlt}, \frac{m}{1+emu}, \frac{p}{1+fpv}, \frac{q(-1+agq)}{-1+2agq}, \\ \frac{r(-1+bhr)}{-1+2bhr}, \frac{s(-1+cks)}{-1+2cks}, \frac{t}{1-dlt}, \frac{u}{1-emu}, \frac{v}{1-fpv}, \\ -a,-b,-c,-d,-e,-f,-g,-h,-k, \frac{-l}{1+dlt}, \frac{-m}{1+emu}, \frac{-p}{1+fpv}, \\ \frac{-q(-1+agq)}{-1+2agq}, \frac{-r(-1+bhr)}{-1+2bhr}, \frac{-s(-1+cks)}{-1+2cks}, \frac{t}{-1+dlt}, \\ \frac{u}{-1+emu}, \frac{v}{-1+fpv}, a,b,c,d,\ldots \end{array} \right\},$$

$$\{y_n\} = \left\{ \begin{array}{c} l,m,p,q,r,s,t,u,v, \frac{a}{-1+agq}, \frac{b}{-1+bhr}, \frac{c}{-1+cks}, \\ -d(1+dlt), -e(1+emu), -f(1+fpv), \frac{g-2ag^2q}{-1+agq}, \\ \frac{h-2bh^2r}{-1+bhr}, \frac{k-2ck^2s}{-1+cks}, \frac{l(-1+dlt)}{1+dlt}, \frac{m(-1+emu)}{1+emu}, \frac{p(-1+fpv)}{1+fpv}, \frac{q}{-1+2agq}, \\ \frac{r}{-1+2bhr}, \frac{s}{-1+2cks}, \frac{t(1+dlt)}{-1+dlt}, \frac{u(1+emu)}{-1+emu}, \frac{v(1+fpv)}{-1+fpv}, \frac{a(-1+2agq)}{-1+agq}, \\ \frac{b(-1+2bhr)}{-1+bhr}, \frac{c(-1+2cks)}{-1+cks}, d-d^2lt, e-e^2mu, f-f^2pv, \\ \frac{g}{1-agq}, \frac{h}{1-bhr}, \frac{k}{1-cks}, l,m,p,\ldots \end{array} \right\}.$$

2.4. The fourth system: $x_{n+1} = \frac{y_{n-8}}{1+y_{n-2}x_{n-5}y_{n-8}}, y_{n+1} = \frac{x_{n-8}}{-1-x_{n-2}y_{n-5}x_{n-8}}$

In this case, we solve the form of the solutions of the following system of the difference equations

$$x_{n+1} = \frac{y_{n-8}}{1+y_{n-2}x_{n-5}y_{n-8}}, y_{n+1} = \frac{x_{n-8}}{-1-x_{n-2}y_{n-5}x_{n-8}}, \tag{2.3}$$

where the initial conditions are arbitrary real numbers with $y_{-2}x_{-5}y_{-8}$, $y_{-1}x_{-4}y_{-7}, y_0x_{-3}y_{-6} \neq -1$ and $x_{-2}y_{-5}x_{-8}, x_{-1}y_{-4}x_{-7}, x_0y_{-3}x_{-6} \neq -1$.

Theorem 2.6. *Every solutions of system 2.3 are periodic with period (36). Moreover $\{x_n, y_n\}_{n=-8}^{\infty}$ takes the form*

$$\{x_n\} = \left\{ \begin{array}{c} a,b,c,d,e,f,g,h,k, \frac{l}{1+dlt}, \frac{m}{1+emu}, \frac{p}{1+fpv}, q(1+agq), \\ r(1+bhr), s(1+cks), \frac{t(1+2dlt)}{1+dlt}, \frac{u(1+2emu)}{1+emu}, \frac{v(1+2fpv)}{1+fpv}, \\ \frac{a(-1+agq)}{1+agq}, \frac{b(-1+bhr)}{1+bhr}, \frac{c(-1+cks)}{1+cks}, \frac{-d}{1+2dlt}, \frac{-e}{1+2emu}, \\ \frac{-f}{1+2fpv}, \frac{g(1+agq)}{-1+agq}, \frac{h(1+bhr)}{-1+bhr}, \frac{k(1+cks)}{-1+cks}, \frac{-l(1+2dlt)}{1+dlt}, \\ \frac{-m(1+2emu)}{1+emu}, \frac{-p(1+2fpv)}{1+fpv}, q(-1+agq), r(-1+bhr), \\ s(-1+cks), \frac{-t}{1+dlt}, \frac{-u}{1+emu}, \frac{-v}{1+fpv}, a,b,c,\ldots \end{array} \right\},$$

$$\{y_n\} = \left\{ \begin{array}{c} l,m,p,q,r,s,t,u,v, \frac{-a}{1+agq}, \frac{-b}{1+bhr}, \frac{-c}{1+cks}, \\ \frac{-d(1+dlt)}{1+2dlt}, \frac{-e(1+emu)}{1+2emu}, \frac{-f(1+fpv)}{1+2fpv}, \frac{g}{-1+agq}, \frac{h}{-1+bhr}, \\ \frac{k}{-1+cks}, -l,-m,-p,-q-r,-s,-t,-u,-v, \\ \frac{a}{1+agq}, \frac{b}{1+bhr}, \frac{c}{1+cks}, \frac{d(1+dlt)}{1+2dlt}, \frac{e(1+emu)}{1+2emu)}, \frac{f(1+fpv)}{1+2f[v)}, \\ \frac{g}{1-agq}, \frac{h}{1-bhr}, \frac{k}{1-cks}, l,m,p,\ldots \end{array} \right\}.$$

3. Numerical examples

Here we consider some numerical examples to illustrate the behavior of the solutions of the systems which we studied.

Example 3.1. *Consider the System 2.1 with the initial conditions* $x_{-8} = 15$, $x_{-7} = -6.2$, $x_{-6} = -0.26$, $x_{-5} = -13$, $x_{-4} = 12$, $x_{-3} = 6$, $x_{-2} = 9$, $x_{-1} = -2$, $x_0 = -6$, $y_{-8} = 7$, $y_{-7} = 8$, $y_{-6} = -0.3$, $y_{-5} = 11$, $y_{-4} = 14$, $y_{-3} = 2.5$, $y_{-2} = 16$, $y_{-1} = -9$, $y_0 = -0.3$. *See Figure 3.1 and see Figure 3.2 when we put* $x_{-8} = 15$, $x_{-7} = 6.2$, $x_{-6} = 0.26$, $x_{-5} = 13$, $x_{-4} = 2$, $x_{-3} = 16$, $x_{-2} = 9$, $x_{-1} = 2$, $x_0 = 6$, $y_{-8} = 7$, $y_{-7} = 18$, $y_{-6} = 0.3$, $y_{-5} = 11$, $y_{-4} = 34$, $y_{-3} = 2.5$, $y_{-2} = 26$, $y_{-1} = 9$, $y_0 = 0.3$.

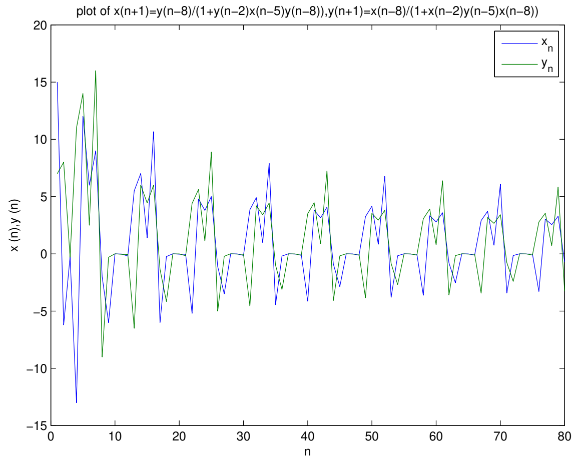

Figure 3.1

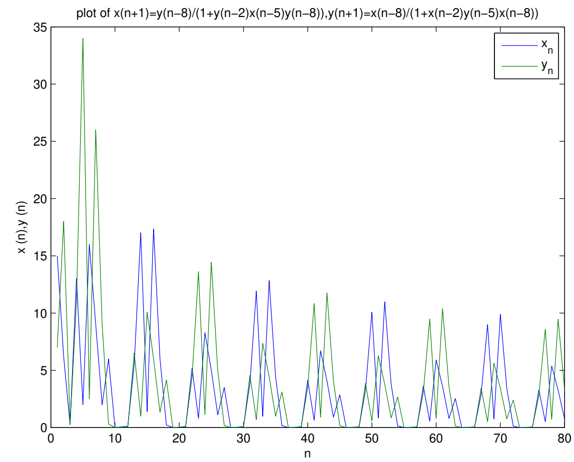

Figure 3.2

Example 3.2. *See Figure 3.3, when we take System 2.1 and put* $x_{-8} = -1.5$, $x_{-7} = 6.2$, $x_{-6} = 0.6$, $x_{-5} = 1.3$, $x_{-4} = 1.2$, $x_{-3} = 0.6$, $x_{-2} = 0.9$, $x_{-1} = 0.2$, $x_0 = 0.6$, $y_{-8} = 0.7$, $y_{-7} = -1.8$, $y_{-6} = 0.3$, $y_{-5} = 1.1$, $y_{-4} = 1.4$, $y_{-3} = 2.5$, $y_{-2} = 1.6$, $y_{-1} = 0.9$, $y_0 = 0.3$.

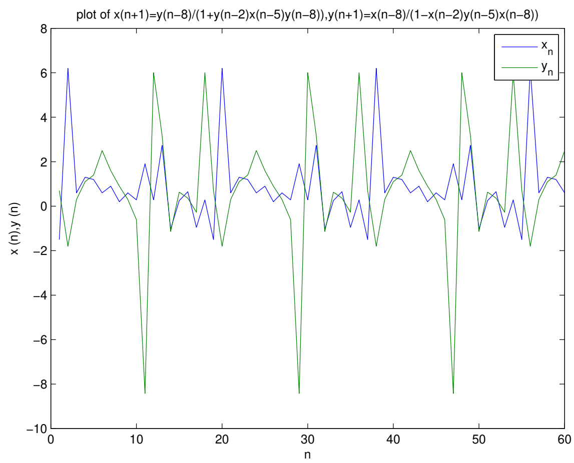

Figure 3.3

Example 3.3. *Figure 3.4 below describe the periodic solutions of System 2.2 when* $x_{-8} = -1.5$, $x_{-7} = -6.2$, $x_{-6} = 0.6$, $x_{-5} = 1.3$, $x_{-4} = 1.2$, $x_{-3} = -0.6$, $x_{-2} = 0.9$, $x_{-1} = 0.2$, $x_0 = 0.6$, $y_{-8} = 0.7$, $y_{-7} = -1.8$, $y_{-6} = 0.3$, $y_{-5} = 1.1$, $y_{-4} = 1.4$, $y_{-3} = 2.5$, $y_{-2} = 1.6$, $y_{-1} = 0.9$, $y_0 = 0.3$.

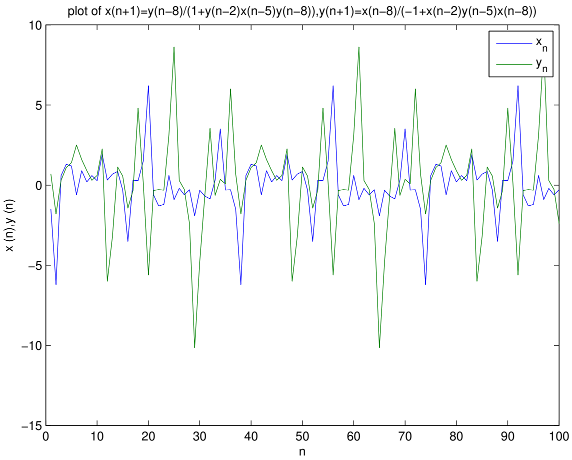

Figure 3.4

Example 3.4. *Consider the System 2.3 when* $x_{-8}=-1.5$, $x_{-7}=-6.2$, $x_{-6}=0.6$, $x_{-5}=1.3$, $x_{-4}=-1.2$, $x_{-3}=-0.6$, $x_{-2}=0.9$, $x_{-1}=0.2$, $x_0=0.6$, $y_{-8}=0.7$, $y_{-7}=-1.8$, $y_{-6}=0.3$, $y_{-5}=1.1$, $y_{-4}=-1.4$, $y_{-3}=-2.5$, $y_{-2}=1.6$, $y_{-1}=0.9$, $y_0=0.3$. *See Figure 3.5.*

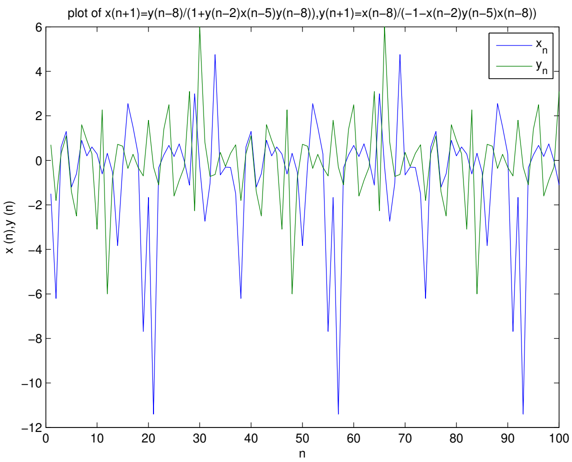

Figure 3.5

References

[1] A. M. Ahmed, E. M. Elsayed, *The expressions of solutions and the periodicity of some rational difference equations system*, J. Appl. Math. Inform. **34**(1-2) (2016), 35–48.
[2] M. M. El-Dessoky, *The form of solutions and periodicity for some systems of third-order rational difference equations*, Math. Meth. Appl. Sci., **39** (2016), 1076–1092.
[3] M. M. El-Dessoky, E. M. Elsayed, *On the solutions and periodic nature of some systems of rational difference equations*, J. Comput. Anal. Appl., **18**(2) (2015), 206–218.
[4] M. M. El-Dessoky, A. Khaliq, A. Asiri, *On some rational system of difference equations*, J. Nonlinear Sci. Appl., **11** (2018), 49–72.
[5] E. M. Elsayed, T. F. Ibrahim, *Periodicity and solutions for some systems of nonlinear rational difference equations,* Hacettepe Journal of Mathematics and Statistics, **44** (6) (2015), 1361–1390.
[6] E. M. Elsayed, A. Alghamdi, *The form of the solutions of nonlinear difference equations systems*, J. Nonlinear Sci. Appl., **9** (2016), 3179–3196.
[7] N. Haddad , N. Touafek, J. F. T. Rabago, *Solution form of a higher-order system of difference equations and dynamical behavior of its special case*, Math. Methods Appl. Sci., **40** (2017), 3599–3607.
[8] A. S. Kurbanli, *On the behavior of solutions of the system of rational difference equations* $x_{n+1}=x_{n-1}/(y_nx_{n-1}-1)$, $y_{n+1}=y_{n-1}/(x_ny_{n-1}-1)$, World Appl. Sci. J., **10**(11) (2010), 1344-1350.
[9] A. S. Kurbanli, C. Çinar, D. Şimşek, *On the periodicity of solutions of the system of rational difference equations* $x_{n+1}=x_{n-1}+y_n/(y_nx_{n-1}-1)$, $y_{n+1}=y_{n-1}+x_n/(x_ny_{n-1}-1)$, Appl. Math., **2** (2011), 410-413.
[10] A. S. Kurbanli, C. Çinar, I. Yalçinkaya, *On the behavior of positive solutions of the system of rational difference equations* $x_{n+1}=x_{n-1}/(y_nx_{n-1}+1)$, $y_{n+1}=y_{n-1}/(x_ny_{n-1}+1)$, Math. Comput. Modelling, **53** (2011), 1261–1267.
[11] M. Mansour, M. M. El-Dessoky, E. M. Elsayed, *The form of the solutions and periodicity of some systems of difference equations*, Discrete Dyn. Nat. Soc., **2012** (2012), Article ID 406821, 1-17.
[12] N. Touafek and E. M. Elsayed, *On the solutions of systems of rational difference equations*, Math. Comput. Modelling, **55** (2012), 1987-1997.
[13] S. A. Abramov, D. E. Khmelnov, *Denominators of rational solutions of linear difference systems of an arbitrary order,* Program. Comput. Softw., **38** (2) (2012), 84–91.
[14] R. Abu-Saris, C. Cinar, I. Yalcinkaya, *On the Asymptotic Stability of* $x_{n+1}=a+x_nx_{n-k}/x_n+x_{n-k}$, Comput. Math. Appl., **56**(5) (2008), 1172-1175.
[15] N. Battaloglu, C. Cinar, I. Yalcinkaya, *The dynamics of the difference equation* $x_{n+1}=(\alpha x_{n-m})/(\beta+\gamma x^p_{n-(k+1)})$, , Ars Combin., **97** (2010), 281–288.
[16] O. H. Criner, W. E. Taylor, J. L. Williams, *On the solutions of a system of nonlinear difference equations*, Int. J. Difference Equ., **10**(2) (2015), 161–166.

[17] I. Dekkar, N. Touafek, Y. Yazlik, *Global stability of a third-order nonlinear system of difference equations with period-two coefficients*, Rev. R. Acad. Cienc. Exactas Fís. Nat. Ser. A Mat., **111**(2) (2017), 325–347.
[18] Q. Din, *Qualitative nature of a discrete predator-prey system,* Contem. Methods Math. Phys. Grav., **1** (2015), 27-42.
[19] E. M. Elabbasy, H. El-Metwally, E. M. Elsayed, *Some properties and expressions of solutions for a class of nonlinear difference equation*, Util. Math., **87** (2012), 93–110.
[20] E. M. Elabbasy, S. M. Eleissawy, *Periodicty and stability of solutions of rational difference systems*, Appl. Comput. Math., **1**(4) (2012), 1-6.
[21] E. M. Elabbasy, A. A. Elsadany, S. Ibrahim, *Behavior and periodic solutions of a two-dimensional systems of rational difference equations*, J. Interpolat. Approx. Sci. Comput., **2016**(2) (2016), 87-104.
[22] M. M. El-Dessoky, *Solution for rational systems of difference equations of order three*, Mathematics, **4**(3) (2016), 1-12.
[23] M. M. El-Dessoky, E. M. Elsayed, E. O. Alzahrani, *The form of solutions and periodic nature for some rational difference equations systems,* J. Nonlinear Sci. Appl., **9** (2016), 5629-5647.
[24] E. M. Elsayed, *Dynamics of recursive sequence of order two*, Kyungpook Math. J., **50**(4) (2010), 483-497.
[25] E. M. Elsayed, *Solution and attractivity for a rational recursive sequence*, Discrete Dyn. Nat. Soc., **2011** (2011), Article ID 982309, 17 pages.
[26] E. M. Elsayed, *On the dynamics of a higher-order rational recursive sequence*, Commun. Math. Anal., **12**(1) (2012), 117–133.
[27] E. M. Elsayed, M. M. El-Dessoky, A. Alotaibi, *On the solutions of a general system of difference equations*, Discrete Dyn. Nat. Soc., **2012** (2012), Article ID 892571, 12 pages.
[28] M. Gumus, O. Ocalan, *The qualitative analysis of a rational system of difference equations*, J. Fract. Calc. Appl., **9**(2) (2018), 113-126.
[29] N. Haddad, N. Touafek, E. M. Elsayed, *A note on a system of difference equations*, Analele Stiintifice ale universitatii al i cuza din iasi serie noua matematica, **LXIII**(3) (2017), 599-606.
[30] N. Haddad, N. Touafek, J. T. Rabago, *Well-defined solutions of a system of difference equations*, J. Appl. Math. Comput., **56** (1-2) (2018), 439–458.
[31] Y. Halim, N. Touafek, Y. Yazlik, *Dynamic behavior of a second-order nonlinear rational difference equation*, Turkish J. Math., **39** (2015), 1004-1018.
[32] Y. Halim, *A system of difference equations with solutions associated to Fibonacci numbers,* Int. J. Difference Equ., **11**(1) (2016), 65–77.
[33] G. Hu, *Global behavior of a system of two nonlinear difference equation*, World J. Res. Rev., **2**(6) (2016), 36-38.
[34] W. Ji, D. Zhang, L. Wang, *Dynamics and behaviors of a third-order system of difference equation*, Math. Sci., **7**(34) (2013), 1-6.
[35] A. Khaliq, E. M. Elsayed, *The dynamics and solution of some difference equations*, J. Nonlinear Sci. Appl., **9** (2016), 1052-1063.
[36] A. S. Kurbanli, *On the behavior of solutions of the system of rational difference equations* $x_{n+1}=x_{n-1}/(y_nx_{n-1}-1)$, $y_{n+1}=y_{n-1}/(x_ny_{n-1}-1)$, $z_{n+1}=1/y_nz_n$, Adv. Difference Equ., **2011** (2011), 40.
[37] A. S. Kurbanli, C. Çinar, M. E. Erdogan, *On the behavior of solutions of the system of rational difference equations* $x_{n+1}=x_{n-1}/(y_nx_{n-1}-1)$, $y_{n+1}=y_{n-1}/(x_ny_{n-1}-1),\ z_{n+1}=x_n/(y_nz_{n-1})$, Appl. Math., **2** (2011), 1031-1038.
[38] A. S. Kurbanli, I. Yalcinkaya, A. Gelisken, *On the behavior of the Solutions of the system of rational difference equations* $x_{n+1}=x_{n-1}/(y_nx_{n-1}-1)$, $y_{n+1}=y_{n-1}/(x_ny_{n-1}-1)$, $z_{n+1}=x_nz_{n-1}/y_n$, Int. J. Phys. Sci., **8**(2) (2013), 51-56.
[39] D. Simsek, B. Demir,C. Cinar, *On the solutions of the system of difference equations* $x_{n+1}=\max\left\{\frac{1}{x_n},\frac{y_n}{x_n}\right\}$, $y_{n+1}=\max\left\{\frac{1}{y_n},\frac{x_n}{y_n}\right\}$, Discrete Dyn. Nat. Soc., **2009** (2009), Article ID 325296, 11 pages.
[40] J. L. Williams, *On a class of nonlinear max-type difference equations*, Cogent Math., **3** (2016), 1269597, 1-11.
[41] I. Yalcinkaya, C. Cinar, *On the solutions of a systems of difference equations*, Int. J. Math. Stat., **9** (S11) (2011), 62–67.
[42] Y. Yazlik, D. T. Tollu, N. Taskara, *On the solutions of difference equation systems with Padovan numbers*, Appl. Math., **4** (2013), 15-20.
[43] Y. Yazlik, D. T. Tollu, N. Taskara, *On the solutions of a max-type difference equation system*, Math. Meth. Appl. Sci., **38** (2015), 4388–4410.
[44] Q. Zhang, J. Liu, Z. Luo, *Dynamical behavior of a system of third-order rational difference equation*, Discrete Dyn. Nat. Soc., **2015** (2015), Article ID 530453, 6 pages.

Journal of Mathematical Sciences and Modelling, 1 (3) (2018) 192-201
Research Article

Journal of Mathematical Sciences and Modelling

Journal Homepage: www.dergipark.gov.tr/jmsm
ISSN 2636-8692

An Efficient Operational Matrix Method for Solving a Class of Two-Dimensional Singular Volterra Integral Equations

Somayeh Nemati[a*]

[a]*Department of Mathematics, Faculty of Mathematical Sciences, University of Mazandaran, Babolsar, Iran*
[*]*Corresponding author*

Article Info

Keywords: *Modification of hat functions, Operational matrix, Riemann-Liouville integral operator, Two-dimensional singular Volterra integral equations*
2010 AMS: *45E10, 26A33, 65N35*
Received: *12 May 2018*
Accepted: *3 November 2018*
Available online: *30 December 2018*

Abstract

In this paper, we consider a spectral method to solve a class of two-dimensional singular Volterra integral equations using some basic concepts of fractional calculus. This method uses a modification of hat functions for finding a numerical solution of the considered equation. Some properties of the modification of hat functions are presented. The main contribution of this work is to introduce the fractional order operational matrix of integration for the considered basis functions. Making use of the Riemann-Liouville fractional integral operator helps us to reduce the main problem to a system of linear algebraic equations which can be solved easily. After that, error analysis of the method is discussed. Finally, numerical examples are included to confirm the accuracy and applicability of the suggested method.

1. Introduction

Singular integral equations consist a class of integral equations in which the kernel is singular within the range of integration, or one or both limits of integration are infinite [1]. There are some analytical and numerical methods to solve one-dimensional singular integral equations with different kinds of singularity. Ioakimidis [2] has used quadrature methods for obtaining a numerical solution for singular integral equations with singular kernels. In [3], a numerical method has been proposed for the numerical solution of singular integral equations of the Cauchy type via replacing the integral equation by integral relations at a discrete set of points. Gauss-Chebyshev formulae has been used to find the numerical solution of singular integral equations of the Cauchy type in [4]. Monegato and Scuderi in [5] introduced high order methods for the second kind Fredholm integral equations with weakly singular kernels. For more methods on these equations, the interested reader can refer to [6]-[13].
The main aim of this paper is to introduce an application of fractional calculus in solving a class of two-dimensional Volterra integral equations as

$$u(x,t) = f(x,t) + \int_0^t \int_0^x (x-y)^{-\alpha}(t-z)^{-\beta} u(y,z)dydz, \quad (x,t) \in D, \tag{1.1}$$

where $u(x,t)$ is the unknown function on $D := [0,l] \times [0,T]$, $f(x,t)$ is a given known function and $0 < \alpha, \beta < 1$. This equation, is a singular integral equation with weakly singular convolution kernel. In recent decades fractional calculus provided a wonderful tool for the explanation of many mathematical models in science and engineering [14, 15]. A general outlook of fractional calculus and its basic theories can be found in [16]-[24].
In this work, we propose a numerical method to solve Eq. (1.1) using the modification of hat functions (MHFs). The MHFs have been employed to obtain numerical solutions of two-dimensional linear Fredholm integral equations [25], nonlinear Stratonovich Volterra integral equations [26], Volterra-Fredholm integral equations [27] and systems of linear Stratonovich Volterra integral equations [28]. The operational matrix technique is used to reduce the main problem to a system of algebraic equations. It should be noted that any other well-known basis functions that their operational matrix of fractional integration are known such as Legendre polynomials [29], Chebyshev polynomials [30], Haar wavelet functions [31] and hat functions [32] could be employed in our new approach to solve Eq. (1.1).
This paper is organized as follows: Some preliminaries in fractional calculus and properties of the MHFs are given in Section 2. Section 3 is committed to introducing the operational matrix of fractional integration of the MHFs. In Section 4, a numerical method is given to solve Eq.

Email addresses: **s.nemati@umz.ac.ir, 0000-0003-1724-6296 (S. Nemati)**

(1.1). Error analysis of the method is discussed in Section 5. Numerical examples are given in Section 6 to demonstrate the accuracy and applicability of the method. Concluding remarks are presented in Section 7.

2. Basic concepts

In this section, we give some definitions which will be used further in this paper.

There are different definitions for fractional integral in literature (see [19]). Here, we consider the Riemann-Liouville fractional integral operator I_x^α to reach our aim.

Definition 2.1. *The Riemann-Liouville integral operator I_x^α of order $\alpha > 0$ is given by [17]*

$$I_x^\alpha f(x) = \frac{1}{\Gamma(\alpha)} \int_0^x (x-y)^{\alpha-1} f(y) dy,$$

where $\Gamma(\alpha)$ is the gamma function; as

$$\Gamma(\alpha) = \int_0^\infty t^{\alpha-1} e^{-t} dt.$$

Definition 2.2. *Let $a = (a_1, a_2) \in (0,\infty)\times(0,\infty)$, $\theta = (0,0)$ and $u \in L^1(D)$. The left-sided mixed Riemann-Liouville integral of order a of u is defined by [33]*

$$I_\theta^a u(x,t) = \frac{1}{\Gamma(a_1)\Gamma(a_2)} \int_0^t \int_0^x (x-y)^{a_1-1}(t-z)^{a_2-1} u(y,z) dy dz.$$

Hat functions are defined on the interval $[0,1]$ and are linear piecewise continuous functions with shape hats [32]. Here we consider the MHFs which are quadratic piecewise continuous functions with shape hats and replace the domain of the definition to $[0,l]$.

Definition 2.3. *A set of $(n+1)$-MHFs consists of $n+1$ functions which are defined on the interval $[0,l]$ as follows [25]:*

$$\psi_{0,l}(x) = \begin{cases} \frac{1}{2h^2}(x-h)(x-2h), & 0 \le x \le 2h, \\ 0, & \text{otherwise}, \end{cases}$$

when i is odd and $1 \le i \le n-1$:

$$\psi_{i,l}(x) = \begin{cases} \frac{-1}{h^2}(x-(i-1)h)(x-(i+1)h), & (i-1)h \le x \le (i+1)h, \\ 0, & \text{otherwise}, \end{cases}$$

when i is even and $2 \le i \le n-2$:

$$\psi_{i,l}(x) = \begin{cases} \frac{1}{2h^2}(x-(i-1)h)(x-(i-2)h), & (i-2)h \le x \le ih, \\ \frac{1}{2h^2}(x-(i+1)h)(x-(i+2)h), & ih \le x \le (i+2)h, \\ 0, & \text{otherwise}, \end{cases}$$

and

$$\psi_{n,l}(x) = \begin{cases} \frac{1}{2h^2}(x-(l-h))(x-(l-2h)), & l-2h \le x \le l, \\ 0, & \text{otherwise}. \end{cases}$$

where $h = \frac{l}{n}$ and $n \ge 2$ is an even integer number. These functions are linearly independent functions in $L^2[0,l]$.

Using Definition 2.3, the MHFs satisfy the following properties:

$$\psi_{i,l}(jh) = \begin{cases} 1, & i = j, \\ 0, & i \ne j, \end{cases} \tag{2.1}$$

$$\sum_{i=0}^n \psi_{i,l}(x) = 1,$$

$$\psi_{i,l}(x)\psi_{j,l}(x) = \begin{cases} 0, & \text{if } i \text{ is even and } |i-j| \ge 3, \\ 0, & \text{if } i \text{ is odd and } |i-j| \ge 2. \end{cases}$$

An arbitrary function $f(x) \in L^2[0,l]$ may be approximated in terms of the MHFs as

$$f(x) \simeq f_n(x) = \sum_{i=0}^n f_i \psi_{i,l}(x) = F^T \psi_l(x) = \psi_l^T(x) F,$$

where

$$\psi_l(x) = [\psi_{0,l}(x), \psi_{1,l}(x), \ldots, \psi_{n,l}(x)]^T, \tag{2.2}$$

and

$$F = [f_0, f_1, \ldots, f_n]^T,$$

in which $f_i = f(ih)$.

Definition 2.4. *A $(n+1)\times(m+1)$-set of two-dimensional modification of hat functions (2DMHFs) includes $(n+1)\times(m+1)$ functions which are defined on D as*

$$\phi_{i,j}(x,t) = \psi_{i,l}(x)\psi_{j,T}(t).$$

A function $u(x,t)$ in $L^2(D)$ can be approximated in terms of the 2DMHFs as

$$u(x,t) \simeq \sum_{i=0}^{n}\sum_{j=0}^{m} u_{i,j}\phi_{i,j}(x,t) = U^T\phi(x,t),$$

where

$$\phi(x,t) = \psi_l(x) \otimes \psi_T(t), \tag{2.3}$$

in which $\otimes$ denotes the Kronecker product and

$$U = \left[u_{0,0}, u_{0,1}, \ldots, u_{0,m}, \ldots, u_{n,0}, u_{n,1}, \ldots, u_{n,m}\right]^T,$$

such that $u_{i,j} = u(ih_1, jh_2)$ with $h_1 = \frac{l}{n}$ and $h_2 = \frac{T}{m}$.

From (2.1), it is seen that

$$\phi_{i,j}(ph_1, qh_2) = \begin{cases} 1, & p=i \quad \& \quad q=j, \\ 0, & \text{otherwise}. \end{cases} \tag{2.4}$$

3. Operational matrix of fractional integration

In this section, the fractional order operational matrix of integration of the MHFs is introduced.

Theorem 3.1. *Let $\psi(x)$ be the MHFs vector given by (2.2) and $\alpha > 0$, then*

$$I_x^{\alpha}\psi_l(x) \simeq P_l^{(\alpha)}\psi_l(x),$$

where $P_l^{(\alpha)}$ is the $(n+1)\times(n+1)$ operational matrix of fractional integration of order α in the Riemann-Liouville sense and is defined as follows

$$P_l^{(\alpha)} = \frac{h^{\alpha}}{2\Gamma(\alpha+3)}\begin{bmatrix} 0 & \beta_1 & \beta_2 & \beta_3 & \beta_4 & \ldots & \beta_{n-1} & \beta_n \\ 0 & \eta_0 & \eta_1 & \eta_2 & \eta_3 & \ldots & \eta_{n-2} & \eta_{n-1} \\ 0 & \xi_{-1} & \xi_0 & \xi_1 & \xi_2 & \ldots & \xi_{n-3} & \xi_{n-2} \\ 0 & 0 & 0 & \eta_0 & \eta_1 & \ldots & \eta_{n-4} & \eta_{n-3} \\ 0 & 0 & 0 & \xi_{-1} & \xi_0 & \ldots & \xi_{n-5} & \xi_{n-4} \\ \vdots & \vdots & \vdots & \vdots & \vdots & & \vdots & \vdots \\ 0 & 0 & 0 & 0 & 0 & \ldots & \eta_0 & \eta_1 \\ 0 & 0 & 0 & 0 & 0 & \ldots & \xi_{-1} & \xi_0 \end{bmatrix},$$

where

$$\begin{aligned}
&\beta_1 = \alpha(3+2\alpha), \\
&\beta_k = k^{\alpha+1}(2k-6-3\alpha) + 2k^{\alpha}(1+\alpha)(2+\alpha) - (k-2)^{\alpha+1}(2k-2+\alpha), \qquad k = 2,3,\ldots,n, \\
&\eta_0 = 4(1+\alpha), \\
&\eta_k = 4[(k-1)^{\alpha+1}(k+1+\alpha) - (k+1)^{\alpha+1}(k-1-\alpha)], \qquad k = 1,2,\ldots,n-1, \\
&\xi_{-1} = -\alpha, \\
&\xi_0 = 2^{\alpha+1}(2-\alpha), \\
&\xi_1 = 3^{\alpha+1}(4-\alpha) - 6(2+\alpha), \\
&\xi_k = (k+2)^{\alpha+1}(2k+2-\alpha) - 6k^{\alpha+1}(2+\alpha) - (k-2)^{\alpha+1}(2k-2+\alpha), \qquad k = 2,3,\ldots,n-2.
\end{aligned}$$

Proof. For proof see [34], Theorem 3.1.

4. Numerical method

In this section, a numerical method is proposed to solve Eq. (1.1) using the properties of the MHFs. To this aim, we need the following theorem.

Theorem 4.1. *Let $\phi(x,t)$ be the 2DMHFs vector defined by (2.3) and $0<\alpha,\beta<1$, then*

$$\int_0^t\int_0^x (x-y)^{-\alpha}(t-z)^{-\beta}\phi(y,z)dydz \simeq \chi_{\alpha,\beta}Q^{(\alpha,\beta)}\phi(x,t), \tag{4.1}$$

where

$$\chi_{\alpha,\beta}=\Gamma(1-\alpha)\Gamma(1-\beta), \tag{4.2}$$

and

$$Q^{(\alpha,\beta)}=P_l^{(1-\alpha)}\otimes P_T^{(1-\beta)}. \tag{4.3}$$

Proof. By considering the Riemann-Liouville integral operator in Definition 2.2 and after some manipulation, we obtain

$$\begin{aligned}
\int_0^t\int_0^x (x-y)^{-\alpha}(t-z)^{-\beta}\phi(y,z)dydz &= \frac{\Gamma(1-\alpha)\Gamma(1-\beta)}{\Gamma(1-\alpha)\Gamma(1-\beta)}\times\int_0^t\int_0^x (x-y)^{(1-\alpha)-1}(t-z)^{(1-\beta)-1}\psi_l(y)\otimes\psi_T(z)dydz\\
&=\Gamma(1-\alpha)\Gamma(1-\beta)\left(\frac{1}{\Gamma(1-\alpha)}\int_0^x (x-y)^{(1-\alpha)-1}\psi_l(y)dy\right)\\
&\quad\otimes\left(\frac{1}{\Gamma(1-\beta)}\int_0^t (t-z)^{(1-\beta)-1}\psi_T(z)dz\right)\\
&=\Gamma(1-\alpha)\Gamma(1-\beta)\left(I_x^{1-\alpha}\psi_l(x)\right)\otimes\left(I_t^{1-\beta}\psi_T(t)\right)\\
&\simeq\Gamma(1-\alpha)\Gamma(1-\beta)\left(P_l^{(1-\alpha)}\psi_l(x)\right)\otimes\left(P_T^{(1-\beta)}\psi_T(t)\right)\\
&=\Gamma(1-\alpha)\Gamma(1-\beta)\left(P_l^{(1-\alpha)}\otimes P_T^{(1-\beta)}\right)(\psi_L(x)\otimes\psi_T(t))\\
&=\Gamma(1-\alpha)\Gamma(1-\beta)\left(P_l^{(1-\alpha)}\otimes P_T^{(1-\beta)}\right)\phi(x,t).
\end{aligned} \tag{4.4}$$

Therefore, taking into account Eqs. (4.2)–(4.4) the proof is completed.□

Now, by employing Theorem 4.1 we suggest our numerical method for solving Eq. (1.1). To do this, we expand the functions $u(x,t)$ and $f(x,t)$ in terms of the 2DMHFs by the way mentioned in Section 2, respectively, as follows

$$u(x,t)\simeq U^T\phi(x,t), \tag{4.5}$$

$$f(x,t)\simeq F^T\phi(x,t), \tag{4.6}$$

where U is the unknown vector. Substituting Eqs. (4.5) and (4.6) into Eq. (1.1), we have

$$U^T\phi(x,t)=F^T\phi(x,t)+\int_0^t\int_0^x (x-y)^{-\alpha}(t-z)^{-\beta}U^T\phi(y,z)dydz. \tag{4.7}$$

Utilizing Eq. (4.1) in (4.7) gives

$$U^T\phi(x,t)=F^T\phi(x,t)+\chi_{\alpha,\beta}U^TQ^{(\alpha,\beta)}\phi(x,t).$$

Finally, we obtain the following system

$$U^T-F^T-\chi_{\alpha,\beta}U^TQ^{(\alpha,\beta)}=0,$$

that can be rewritten in a matrix form equation as

$$(I-\chi_{\alpha,\beta}Q^{(\alpha,\beta)^T})U=F, \tag{4.8}$$

where I is the identity matrix of order $(n+1)(m+1)\times(n+1)(m+1)$.

In our implementation, we have used the Mathematica function *Solve* for solving the final system in (4.8).

5. Error analysis

The purpose of this section is to introduce an error estimate for the numerical solution of Eq. (1.1) obtained by the presented method. For convenience, suppose that $l = T = 1$ and $h := \frac{1}{n}$. Then we get the following results.

Theorem 5.1. *Assume that $u(x,t) \in C^3(D)$, and*

$$u_n(x,t) = \sum_{i=0}^{n} \sum_{j=0}^{n} u(ih, jh)\phi_{i,j}(x,t)$$

is the approximation of $u(x,t)$ by the 2DMHFs. Then, we have

$$|u(x,t) - u_n(x,t)| = O(h^3). \tag{5.1}$$

Proof. Suppose that $D_{i,j} = [x_i, x_{i+2}] \times [t_j, t_{j+2}]$, $i, j = 0, 1, \ldots, n-2$, therefore we have $D = \bigcup D_{i,j}$. From Eq. (2.4) it is seen that $u_n(x,t)$ is a quadratic polynomial which interpolates $u(x,t)$ at $(x,t) = (ph, qh)$, $p = i, i+1, i+2$, $q = j, j+1, j+2$ on $D_{i,j}$. So for the interpolation error on $D_{i,j}$ we have [35]

$$\begin{aligned} u(x,t) - u_n(x,t) =& \frac{1}{6} \frac{\partial^3 u(\xi,t)}{\partial x^3} \prod_{p=i}^{i+2} (x - ph) + \frac{1}{6} \frac{\partial^3 u(x,\eta)}{\partial t^3} \prod_{q=j}^{j+2} (t - qh) \\ & - \frac{1}{36} \frac{\partial^6 u(\xi',\eta')}{\partial x^3 \partial t^3} \prod_{p=i}^{i+2} (x - ph) \prod_{q=j}^{j+2} (t - qh), \end{aligned}$$

where $\xi, \xi' \in [x_i, x_{i+2}]$ and $\eta, \eta' \in [t_j, t_{j+2}]$. Therefore

$$\begin{aligned} |u(x,t) - u_n(x,t)| \leq & \frac{1}{6} \max_{(x,t) \in D_{i,j}} \left| \frac{\partial^3 u(\xi,t)}{\partial x^3} \right| \left| \prod_{p=i}^{i+2} (x - ph) \right| \\ & + \frac{1}{6} \max_{(x,t) \in D_{i,j}} \left| \frac{\partial^3 u(x,\eta)}{\partial t^3} \right| \left| \prod_{q=j}^{j+2} (t - qh) \right| \\ & + \frac{1}{36} \max_{(x,t) \in D_{i,j}} \left| \frac{\partial^6 u(\xi',\eta')}{\partial x^3 \partial t^3} \right| \left| \prod_{p=i}^{i+2} (x - ph) \right| \left| \prod_{q=j}^{j+2} (t - qh) \right|. \end{aligned} \tag{5.2}$$

There are real numbers M_1, M_2 and M_3, such that

$$\max_{(x,t) \in D_{i,j}} \left| \frac{\partial^3 u(\xi,t)}{\partial x^3} \right| \leq M_1, \tag{5.3}$$

$$\max_{(x,t) \in D_{i,j}} \left| \frac{\partial^3 u(x,\eta)}{\partial t^3} \right| \leq M_2, \tag{5.4}$$

$$\max_{(x,t) \in D_{i,j}} \left| \frac{\partial^6 u(\xi',\eta')}{\partial x^3 \partial t^3} \right| \leq M_3. \tag{5.5}$$

On the other hand, we know that

$$\left| \prod_{p=i}^{i+2} (x - ph) \right| \leq \frac{2\sqrt{3}}{9} h^3, \tag{5.6}$$

$$\left| \prod_{q=j}^{j+2} (t - qh) \right| \leq \frac{2\sqrt{3}}{9} h^3. \tag{5.7}$$

Using (5.3)–(5.7) in (5.2) gives

$$|u(x,t) - u_n(x,t)| \leq \frac{\sqrt{3}M_1}{27} h^3 + \frac{\sqrt{3}M_2}{27} h^3 + \frac{M_3}{243} h^6,$$

which completes the proof.□

Theorem 5.2. *Let $u(x,t) \in C^3(D)$ be the exact solution of Eq. (1.1) and $u_n(x,t)$ be its approximation obtained by the proposed method in the previous section, then*

$$|u(x,t) - u_n(x,t)| = O(h^3).$$

Proof. Using Definition 2.2 and (4.2) we rewrite Eq. (1.1) as

$$u(x,t) = f(x,t) + \chi_{\alpha,\beta} I_\theta^a u(x,t), \tag{5.8}$$

where $a_1 = 1-\alpha$ and $a_2 = 1-\beta$. Similarly, by neglecting the error of the operational matrix, it is seen from (4.7) that

$$u_n(x,t) = f_n(x,t) + \chi_{\alpha,\beta} I_\theta^a u_n(x,t). \tag{5.9}$$

Subtracting (5.9) from (5.8) yields

$$|u(x,t) - u_n(x,t)| \le |f(x,t) - f_n(x,t)| + \chi_{\alpha,\beta} |I_\theta^a(u) - I_\theta^a(u_n)|. \tag{5.10}$$

By employing (5.1), we obtain the following estimates

$$|f(x,t) - f_n(x,t)| = O(h^3), \tag{5.11}$$

$$|I_\theta^a(u) - I_\theta^a(u_n)| = O(h^3). \tag{5.12}$$

Therefore, using (5.10)–(5.12), the proof is completed.□

6. Numerical examples

In this section, four examples are included to show the applicability, efficiency and accuracy of the proposed method. In all the examples, we consider $l = T = 1$, $n = m$ and $h = \frac{1}{n}$. In order to demonstrate the error of the method we introduce the notations

$$e_n = \max_{\substack{1\le i\le n\\ 1\le j\le n}} |u(ih,jh) - u_n(ih,jh)|,$$

$$\varepsilon_n = \log_2\left(\frac{e_n}{e_{2n}}\right),$$

where $u(x,t)$ is the exact solution and $u_n(x,t)$ is the computed solution obtained by the present method. The computations were performed on a personal computer using a 2.60 GHz processor and the codes were written in Mathematica 11.

Example 6.1. *As the first example, consider Eq. (1.1) with $\alpha = \beta = \frac{1}{2}$ and the function $f(x,t)$ is such that the exact solution of the problem is $u(x,t) = \sin(xt)$.*

We have solved the considered equation in this example with different values of n and reported the numerical results in Table 1, Table 2 and Fig. 6.1. The numerical results confirm that the convergence order of the proposed method is $O(h^3)$.

Table 1: The absolute error at $x = 0.5$ and some selected values of t with $n = 2,4,8,16$ for Example 6.1.

t	$n=2$	$n=4$	$n=8$	$n=16$
0.1	$2.8061E-02$	$1.6256E-04$	$1.2950E-05$	$1.7363E-06$
0.2	$5.4755E-02$	$1.2044E-04$	$1.2440E-05$	$5.7903E-07$
0.3	$8.0205E-02$	$1.7403E-06$	$1.8686E-05$	$1.3683E-06$
0.4	$1.0453E-01$	$8.0012E-05$	$1.9832E-06$	$2.1673E-06$
0.5	$1.2786E-01$	$8.6827E-06$	$9.2267E-07$	$1.1182E-08$
0.6	$1.5032E-01$	$1.4418E-04$	$1.5849E-05$	$1.4427E-06$
0.7	$1.7203E-01$	$1.6602E-04$	$3.5720E-06$	$6.4436E-08$
0.8	$1.9310E-01$	$1.9260E-04$	$3.2879E-05$	$2.2763E-06$
0.9	$2.1364E-01$	$3.4021E-04$	$2.8298E-05$	$3.9246E-06$

Table 2: Numerical results for Example 6.1.

n	4	8	16	32
e_n	$4.2610E-03$	$3.5930E-03$	$2.6193E-05$	$2.1096E-06$
ε_n	3.57	3.78	3.63	—

Example 6.2. *Consider Eq. (1.1) with $\alpha = \frac{2}{3}$, $\beta = \frac{1}{3}$ and*

$$f(x,t) = x^6\left(t^{\frac{4}{3}} + t^3\right) - \frac{729}{6086080} x^{\frac{19}{3}} t^2 \left(6561 t^{\frac{5}{3}} + 1760\sqrt{3}\pi\right),$$

which has the exact solution $u(x,t) = x^6\left(t^{\frac{4}{3}} + t^3\right)$.

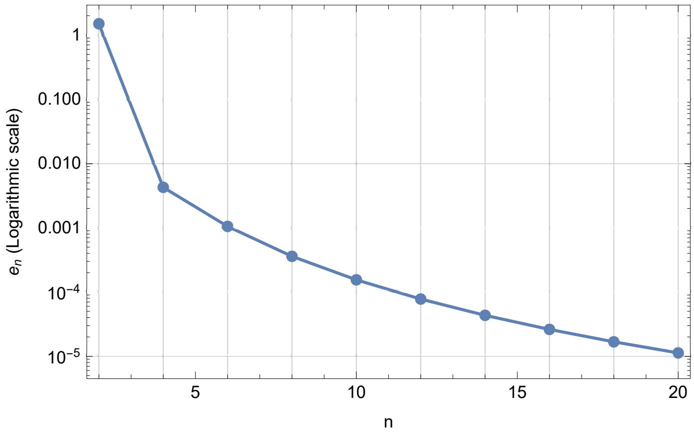

Figure 6.1: e_n on logarithmic scale for Example 6.1.

Table 3: The absolute error at $x = 0.5$ and some selected values of t with $n = 2, 4, 8, 16$ for Example 6.2.

t	$n=2$	$n=4$	$n=8$	$n=16$
0.1	$4.5191E-03$	$5.8186E-05$	$2.2606E-05$	$4.1468E-06$
0.2	$1.4798E-02$	$1.4233E-04$	$1.6604E-05$	$3.7513E-06$
0.3	$3.0914E-02$	$3.2751E-04$	$3.4959E-05$	$5.9114E-06$
0.4	$5.2822E-02$	$5.7154E-04$	$7.5115E-05$	$9.1917E-06$
0.5	$8.0458E-02$	$8.0863E-04$	$1.0657E-04$	$1.5264E-05$
0.6	$1.1374E-01$	$1.3920E-03$	$1.3247E-04$	$2.1537E-05$
0.7	$1.5260E-01$	$1.7557E-03$	$1.6985E-04$	$2.5701E-05$
0.8	$1.9695E-01$	$1.8155E-03$	$1.5472E-04$	$2.7789E-05$
0.9	$2.4669E-01$	$1.4851E-03$	$1.1840E-04$	$2.7401E-05$

Table 4: Numerical results for Example 6.2.

n	4	8	16	32
e_n	$2.1663E-01$	$2.4800E-02$	$2.0087E-03$	$1.9377E-04$
ε_n	3.12	3.63	3.37	—

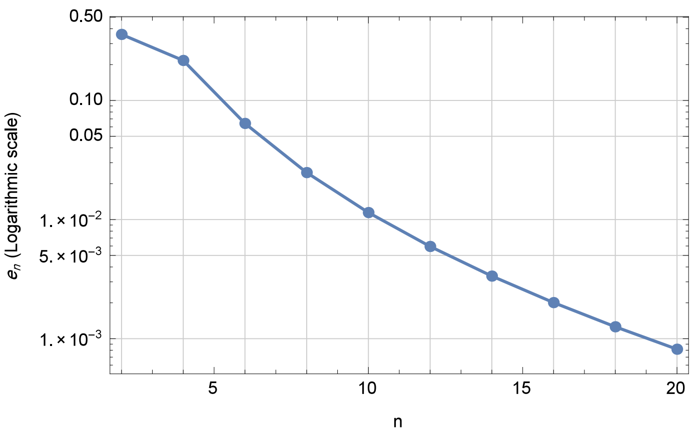

Figure 6.2: e_n on logarithmic scale for Example 6.2.

The presented method has been applied to this equation with different values of n. The numerical results for this example are seen in Table 3, Table 4 and Fig. 6.2. Table 3 shows the absolute error at some selected grid points with different n. The values of ε_n in Table 4 confirm that the error is $O(h^3)$ and Fig. 6.2 displays the convergence of the method.

Example 6.3. *Consider Eq. (1.1) with* $\alpha = \frac{1}{2}$, $\beta = \frac{1}{3}$ *and*

$$f(x,t) = x^2 t^4 - \frac{972}{1925} x^{\frac{5}{2}} t^{\frac{14}{3}}.$$

Table 5: The absolute error at $x = 0.5$ and some selected values of t with $n = 2, 4, 8, 16$ for Example 6.3.

t	$n = 2$	$n = 4$	$n = 8$	$n = 16$
0.1	$1.9964E-02$	$1.5950E-03$	$6.0907E-05$	$6.5053E-06$
0.2	$2.9903E-02$	$1.1848E-03$	$1.0031E-04$	$7.2572E-06$
0.3	$3.0716E-02$	$3.3073E-03$	$2.9834E-04$	$1.7434E-05$
0.4	$2.3903E-02$	$1.4516E-03$	$9.4651E-05$	$4.2587E-05$
0.5	$1.1564E-02$	$7.7908E-05$	$1.1807E-05$	$1.3121E-06$
0.6	$3.6003E-03$	$5.2420E-03$	$3.1794E-04$	$5.0484E-05$
0.7	$1.8291E-02$	$3.7167E-03$	$4.2978E-04$	$2.5486E-05$
0.8	$2.8607E-02$	$7.5402E-04$	$7.2285E-04$	$4.6354E-05$
0.9	$3.0050E-02$	$3.6701E-03$	$2.0164E-04$	$9.3176E-05$

Here, the exact solution is $u(x,t) = x^2t^4$. The numerical results for this example can be observed in Table 5, Table 6 and Fig. 6.3.

Table 6: Numerical results for Example 6.3.

n	4	8	16	32
e_n	$1.1627E-02$	$9.8060E-04$	$7.6913E-05$	$5.8282E-06$
ε_n	3.57	3.67	3.72	—

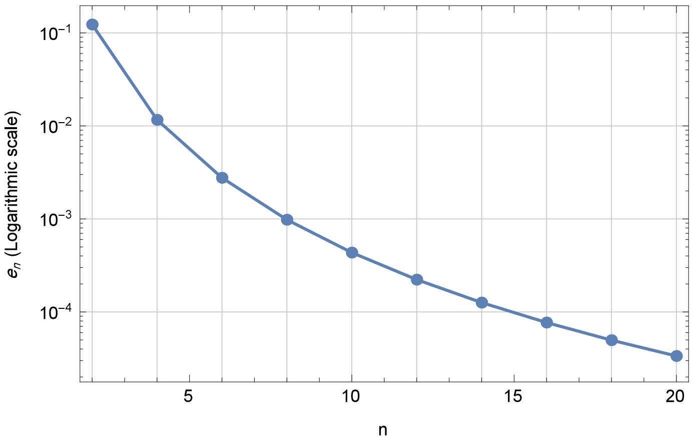

Figure 6.3: e_n on logarithmic scale for Example 6.3.

Example 6.4. *In Eq. (1.1), consider $\alpha = \beta = \frac{1}{2}$ and*

$$f(x,t) = -\frac{4}{105}t^{\frac{1}{2}}x^{\frac{1}{2}}\left(56t^2 + 48x^3 + 105\right) + t^2 + x^3 + 1,$$

which its exact solution is $u(x,t) = x^3 + t^2 + 1$.

The numerical results foe Example 6.4 are displayed in Table 7, Table 8 and Fig. 6.4.

Table 7: The absolute error at $t = 0.5$ and some selected values of x with $n = 4, 8, 16, 32$ for Example 6.4.

x	$n = 4$	$n = 8$	$n = 16$	$n = 32$
0.1	$1.3321E-02$	$1.1337E-03$	$5.7134E-05$	$1.6212E-06$
0.2	$1.5102E-02$	$9.5963E-05$	$1.9323E-05$	$1.5189E-05$
0.3	$1.1342E-02$	$1.5772E-03$	$1.2592E-04$	$7.2678E-06$
0.4	$8.0404E-03$	$8.8473E-04$	$1.6926E-04$	$1.3029E-05$
0.5	$1.1197E-02$	$8.0388E-04$	$5.5802E-05$	$3.8313E-06$
0.6	$2.6582E-02$	$2.1404E-03$	$2.0027E-05$	$4.2261E-06$
0.7	$3.0561E-02$	$1.0987E-03$	$1.0930E-04$	$2.2050E-05$
0.8	$2.9134E-02$	$2.9554E-03$	$2.3026E-04$	$6.9424E-07$
0.9	$2.8302E-02$	$2.4703E-03$	$2.8957E-04$	$2.2221E-05$

Table 8: Numerical results for Example 6.4.

n	4	8	16	32
e_n	$2.8859E-01$	$2.1523E-02$	$1.5844E-03$	$1.1787E-04$
ε_n	3.75	3.76	3.75	—

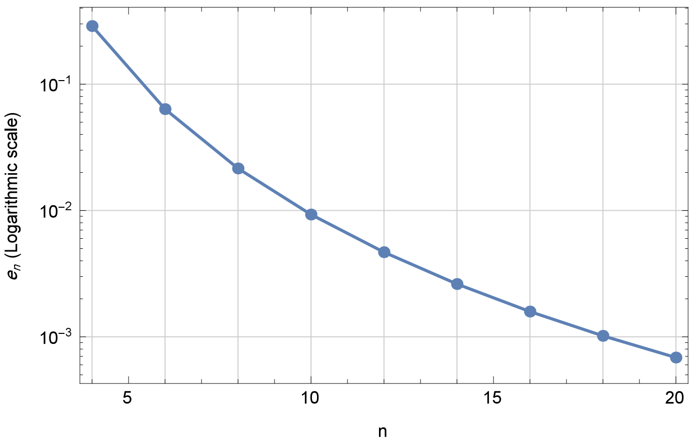

Figure 6.4: e_n on logarithmic scale for Example 6.4.

Table 9 reports the computing time (in seconds) for solving the final system in Eq. (4.8) with different values of n for Examples 6.1–6.4.

Table 9: The computing time (in seconds) for Examples 6.1–6.4.

n	2	4	8	16	32
Example 6.1	0.000	0.015	0.032	0.188	1.875
Example 6.2	0.000	0.000	0.031	0.141	1.875
Example 6.3	0.000	0.000	0.016	0.141	1.984
Example 6.4	0.000	0.000	0.000	0.078	1.407

7. Conclusion

In this paper, the MHFs have been used to solve the two-dimensional Volterra integral equations with weakly singular kernels. The operational matrix of fractional integration was obtained which helped us to reduce the main problem to a system of algebraic equations. The error analysis verified that the convergence order is $O(h^3)$ and also the numerical results in Section 6 (Tables 2, 4, 6 and 8) confirmed this convergence order. Compared to the other piecewise functions such as block-pulse functions ($O(h)$), Haar wavelet functions ($O(h^2)$) and hat functions ($O(h^2)$), the MHFs have higher order of convergence. The fractional order operational matrix of integration of the MHFs has a large number of zeros and it makes the proposed method computationally attractive. Table 9 shows the high performance of the method even when we have a large system of equations with 1089 unknown parameters (for $n = 32$).

References

[1] R. Estrada, R.P. Kanwal, *Singular Integral Equations*, Birkhäuser Basel, 2000.
[2] N.I. Ioakimidis, *On the quadrature methods for the numerical solution of singular integral equations*, J. Comput. Appl. Math., **8** (1982), 81–86.
[3] A. Gerasoulis, R.P. Srivastav, *A method for the numerical solution of singular integral equations with a principal value integral*, Int. J. Eng. Sci., **19** (1981), 1293–1298.
[4] R. P. Srivastav, *Numerical solution of sigular integral equations using Gauss-type formulae II: quadrature and collocation on Chebyshev nodes*, IMA J. Numer. Anal., **3** (1983), 305–318.
[5] G. Monegato, L. Scuderi, *High order methods for weakly singular integral equations with nonsmooth input functions*, Math. Comput., **67** (1998), 1493–1515.
[6] G. C. Sih (Ed.), *Methods of analysis and solutions of crack problems*, Chapter 7, 368-425, Springer Netherlands, 1973.
[7] B. N. Mandal, A. Chakrabarti, *Applied Singular Integral Equations*, CRC Press, 2011.
[8] P.K. Kythe, P. Puri, *Computational Methods for Linear Integral Equations*, Birkhäuser Basel, 2002.
[9] M.L. Dow, D. Elliott, *The numerical solution of singular integral equations over* $(-1,1)$, SIAM J. Numer. Anal., **16** (1979), 115–134.
[10] D. Berthold, P. Junghanns, *New error bounds for the quadrature method for the solution of Cauchy singular integral equations*, SIAM J. Numer. Anal., **30** (1993), 1351–1372.
[11] R. P. Srivastav, F. Zhang, *Solving Cauchy singular integral equations by using general quadrature-collocation nodes*, Comput. Math. Appl., **21** (1991), 59–71.
[12] V. V. Zozulya, P. I. Gonzalez-Chi, *Weakly singular, singular and hypersingular integrals in 3-D elasticity and fracture mechanics*, J. Chin. Inst. Eng., **22** (1999), 763–775.
[13] P. Assari, H. Adibi, M. Dehghan, *The numerical solution of weakly singular integral equations based on the meshless product integration (MPI) method with error analysis*, Appl. Numer. Math., **81** (2014), 76–93.

[14] R. Metzler, J. Klafter, *The restaurant at the end of the random walk: recent developments in the description of anomalous transport by fractional dynamics*, J. Phys. A, **37** (2004), 161–208.
[15] R. Bagley, P. Torvik, *A theoretical basis for the application of fractional calculus to viscoelasticity*, J. Rheol., **27** (1983), 201–210.
[16] S.G. Samko, A.A. Kilbas, O.I. Marichev, *Fractional Integrals and Derivatives: Theory and Applications*, Gordon and Breach, Yverdon, 1993.
[17] I. Podlubny, *Fractional Differential Equations*, Academic Press, San Diego, CA, 1999.
[18] R. Hilfer (Ed.), *Applications of Fractional Calculus in Physics*, World Scientific, Singapore, 2000.
[19] A. Loverro, *Fractional Calculus: History, Definitions and Applications for Engineer*, USA: Department of Aerospace and Mechanical Engineering, University of Notre Dame, 2004.
[20] F. Mainardi, *Fractional Calculus and Waves in Linear Viscoelasticity*, Imperial College Press, London, 2010.
[21] K. Diethelm, *The Analysis of Fractional Differential Equations*, Springer-Verlag, Berlin, 2010.
[22] R. Herrmann, *Fractional Calculus: An Introduction for Physicists*, World Scientific, Singapore, 2011.
[23] D. Baleanu, K. Diethelm, E. Scalas, J. J. Trujillo, *Fractional Calculus: Models and Numerical Methods*, World Scientific, Singapore, 2012.
[24] H. Jafari, S. A. Yousefi, M. A. Firoozjaee, S. Momani, C. M. Khalique, *Application of Legendre wavelets for solving fractional differential equations*, Comput. Math. Appl., **62** (2011), 1038–1045.
[25] F. Mirzaee, E. Hadadiyan, *Numerical solution of linear Fredholm integral equations via two-dimensional modification of hat functions*, Appl. Math. Comput., **250** (2015), 805–816.
[26] F. Mirzaee, E. Hadadiyan, *Approximation solution of nonlinear Stratonovich Volterra integral equations by applying modification of hat functions*, J. Comput. Appl. Math., **302** (2016), 272–284.
[27] F. Mirzaee, E. Hadadiyan, *Numerical solution of Volterra-Fredholm integral equations via modification of hat functions*, Appl. Math. Comput., **280** (2016), 110–123.
[28] F. Mirzaee, E. Hadadiyan, *Solving system of linear Stratonovich Volterra integral equations via modification of hat functions*, Appl. Math. Comput., **293** (2017), 254–264.
[29] A. Lotfi, M. Dehghan, S.A. Yousefi, *A numerical technique for solving fractional optimal control problems*, Comput. Math. Appl., **62** (2011), 1055–1067.
[30] A. H. Bhrawy, A. S. Alofi, *The operational matrix of fractional integration for shifted Chebyshev polynomials*, Appl. Math. Lett., **26** (2013), 25–31.
[31] Y. Li, W. Zhao, *Haar wavelet operational matrix of fractional order integration and its applications in solving the fractional order differential equations*, Appl. Math. Comput., **216** (2010), 2276–2285.
[32] M. P. Tripathi, V. K. Baranwal, R. K. Pandey, O. P. Singh, *A new numerical algorithm to solve fractional differential equations based on operational matrix of generalized hat functions*, Commun. Nonlinear Sci. Numer. Simulat., **18** (2013), 1327–1340.
[33] A. N. Vityuk, A. V. Golushkov, *Existence of solutions of systems of partial differential equations of fractional order*, Nonlinear Oscil., **7** (2004), 318–325.
[34] S. Nemati, P. M. Lima, *Numerical solution of nonlinear fractional integro-differential equations with weakly singular kernels via a modification of hat functions*, Appl. Math. Comput., **327** (2018), 79–92.
[35] S. Nemati, P. M. Lima, Y. Ordokhani, *Numerical solution of a class of two-dimensional nonlinear Volterra integral equations using Legendre polynomials*, J. Comput. Appl. Math., **242** (2013), 53–69.

Journal of Mathematical Sciences and Modelling, 1 (3) (2018) 202-205
Research Article

Journal of Mathematical Sciences and Modelling

Journal Homepage: www.dergipark.gov.tr/jmsm
ISSN 2636-8692

Finite Difference Solution to the Space-Time Fractional Partial Differential-Difference Toda Lattice Equation

Refet Polat[a*]

[a]*Department of Mathematics, Yaşar University, Bornova, İzmir - Turkey*
[*]*Corresponding author*

Article Info

Keywords: *Finite differences method, Space-time fractional differential-difference equations, Toda lattice equation*
2010 AMS: *35R30, 47A52, 35L20*
Received: *14 September 2018*
Accepted: *13 November 2018*
Available online: *30 December 2018*

Abstract

This paper deals with the numerical solution of space-time fractional partial differential-difference Toda lattice equation $\frac{\partial^{2\alpha}u_n}{\partial x^\alpha \partial t^\alpha} = (1+\frac{\partial^\alpha u_n}{\partial t^\alpha})(u_{n-1}-2u_n+u_{n+1})$, $\alpha \in (0,1)$. The finite differences method (FD-method) is used for numerical solution of this problem. According to the method, we approximate the unknown values u_n of the desired function by finite differences approximation. As an application we demonstrate the capabilities of this method for identification of various values of order of fractional derivative α. Numerical results show that the proposed version of FD-method allows to obtain all data from the initial and boundary conditions with enough high accuracy.

1. Introduction

In this paper, we shall consider the space-time fractional (2+1)-dimensional Toda lattice equation described in equation (1) and (2) below. The importance of Toda lattice is, together with the Korteweg –de Vires equation, one of the most classical and significant completely integrable systems. Several methods have been developed to reveal its philosophical mathematical structure [1]. The (2+1)-dimensional Toda lattice hierarchy has been proposed as an extension of the KP hierarchy. This comprises the (2+1)-dimensional Toda lattice equation as the modest nontrivial differential-difference equation. The Toda lattice equation and the sine-Gordon equation are derived by imposing suitable reductions on the (2+1)-dimensional Toda lattice equation [2]. These type of equations, usually, describe the evolution of certain phenomena over the course of time [3].

This paper studies the space-time fractional differential-difference Toda lattice equation (denote $I=(a,b)$),

$$\frac{\partial^{2\alpha}u^n}{\partial x^\alpha \partial t^\alpha} = (1+\frac{\partial^\alpha u^n}{\partial t^\alpha})(u^{n-1}-2u^n+u^{n+1}), \quad (x,t)\in I\times(0,T] \tag{1.1}$$

from the initial and homogeneous Dirichlet boundary condition

$$\begin{cases} u(x,0)=\phi(x),\ x\in I, \\ u(a,t)=u(b,t)=0,\ t\in(0,T], \end{cases}$$

where the mixed derivative $\frac{\partial^{2\alpha}u^n}{\partial x^\alpha \partial t^\alpha}$ denotes the space-time derivative with fractional order 2α of the function $u=u(x,t)$ at $t=t_n$. The derivative $\frac{\partial^\alpha u^n}{\partial t^\alpha}$ also denotes time derivative with fractional order $\alpha\in(0,1)$. We consider the most frequently used the Riemann–Liouville and the Caputo derivative for fractional derivatives in (1.1). Riemann-Liouville fractional derivative with fractional order α of the function $u=u(x,t)$ is defined by [4, 5], i.e.,

$$\left[\frac{\partial^\alpha u(x,t)}{\partial t^\alpha}\right]_{RL} = \frac{1}{\Gamma(1-\alpha)}\frac{\partial}{\partial t}\int_0^t \frac{u(x,\tau)}{(t-\tau)^\alpha}d\tau, \quad t>0. \tag{1.2}$$

where $\Gamma(x)$ is the Euler's Gamma Function. Another definition of fractional derivative is Caputo derivative. Caputo fractional derivative with fractional order α of the function $u=u(x,t)$ is defined by [4, 5] as follows:

$$\left[\frac{\partial^\alpha u(x,t)}{\partial t^\alpha}\right]_{C} = \frac{1}{\Gamma(1-\alpha)}\int_0^t \frac{1}{(t-\tau)^\alpha}\frac{\partial u(x,\tau)}{\partial t}d\tau, \quad t>0. \tag{1.3}$$

Email addresses: **refet.polat@yasar.edu.tr, 0000-0001-9761-8787 (R. Polat)**

From (1.2) and (1.3), it is clear that definitions of Riemann–Liouville derivative and Caputo derivative are not equivalent. But, there is a fact that, almost all the numerical methods for the Riemann–Liouville derivative can be theoretically extended to the Caputo derivative if the function $u(x,t)$ satisfies suitable smooth conditions. Following equality shows the relation between the Riemann–Liouville and Caputo derivatives for $0<\alpha<1$:

$$\left[\frac{\partial^{\alpha}u(x,t)}{\partial t^{\alpha}}\right]_{RL}=\left[\frac{\partial^{\alpha}u(x,t)}{\partial t^{\alpha}}\right]_{C}+\frac{t^{-\alpha}u(x,0)}{\Gamma(1-\alpha)},\quad t>0. \tag{1.4}$$

Hence, a natural way to discretize the Caputo derivative in the equation (1.1) is to use the Grünwald–Letnikov approximation [6].

2. Numerical implementation

One method of the solutions of fractional equations based on numerical methods and solutions are determined by implementing the numerical methods on original (physical) domain. These methods are adapted for fractional integrals (Riemann-Liouville integrals etc.) and derivatives (Caputo derivatives and the Riesz Derivatives etc.) based on polynomial interpolation, Gauss interpolation or linear multistep methods.
For the numerical solution to the considered problem above we construct a uniform grid of mesh points t_n with $t_n=n\Delta t,\ n=0,1,\ldots,N_t$ and $\Delta t=T/N_t$. One can define the space step size $\Delta x=(b-a)/N_x$. The space grid point x_k is given by $x_k=a+k\Delta x,\ k=0,1,\ldots,N_x$. We denote the exact solution $u(x,t)$ at (x_k,t_n) by $u_k^n=u(x_k,t_n)$ and approximate solution by U_k^n at the same grid point (x_k,t_n).

Toda Lattice Equation for Riemann-Liouville derivative in time: For the numerical solution to the considered problem (1.1), we consider Riemann-Liouville time-fractional derivative:

$$\left[\frac{\partial^{2\alpha}u^n}{\partial x^{\alpha}\partial t^{\alpha}}\right]_{RL}=\left(1+\left[\frac{\partial^{\alpha}u^n}{\partial t^{\alpha}}\right]_{RL}\right)(u^{n-1}-2u^n+u^{n+1}),\quad (x,t)\in I\times(0,T] \tag{2.1}$$

We can discretize the Riemann-Liouville fractional derivative of $u(x,t)$ at $t=t_n$ by the Grünwald–Letnikov formula as follows:

$$\left[\frac{\partial^{\alpha}u(x_k,t^n)}{\partial t^{\alpha}}\right]_{RL}=\frac{1}{\Delta t^{\alpha}}\sum_{j=0}^{n}w_j^{\alpha}u_k^{n-j}+O(\Delta t^{p}),\ t>0$$

where w_j^{α} are the coefficients of the generating function, that is $w_0^{\alpha}=1,\ w_j^{\alpha}=(1-(\alpha+1)/j)w_{j-1}^{\alpha},\ j\geq 1$ and $p=1$ [4, 5]. Then the finite difference approximation of (2.1) is given as follows:

$$\frac{1}{\Delta t^{\alpha}}\sum_{j=0}^{n}w_j^{\alpha}(\delta_x^{\alpha}U_k^{n-j})=\left(1+\frac{1}{\Delta t^{\alpha}}\sum_{j=0}^{n}w_j^{\alpha}U_k^{n-j}\right)(U_k^{n-1}-2U_k^n+U_k^{n+1}),\ n\geq 1, \tag{2.2}$$

where $\delta_x^{\alpha}U_k^{n-j}$ is the approximation of the Riemann-Liouville space-fractional derivative $\frac{\partial^{\alpha}u^n}{\partial x^{\alpha}}$ and defined by the Grünwald–Letnikov formula similarly:

$$\delta_x^{\alpha}U_k^n=\frac{1}{\Delta x^{\alpha}}\sum_{i=0}^{k}w_i^{\alpha}U_{k-i}^n.$$

So (2.2) gives the approximate solution for all points $(x_k,t_n),\ k=\overline{1,N_x-1},\ n=\overline{1,N_t-1}$ as follows:

$$\begin{cases}\frac{1}{\Delta t^{\alpha}}\frac{1}{\Delta x^{\alpha}}\sum_{j=0}^{n}\sum_{i=0}^{k}w_j^{\alpha}w_i^{\alpha}U_{k-i}^{n-j}=\left(1+\frac{1}{\Delta t^{\alpha}}\sum_{j=0}^{n}w_j^{\alpha}U_k^{n-j}\right)(U_k^{n-1}-2U_k^n+U_k^{n+1}),\ n\geq 0,\\ U_k^0=\phi(x_k),\ k=\overline{0,N_x},\quad U_0^n=U_{N_x}^n=0,\ n=\overline{1,N_t}.\end{cases}$$

Example 1. We consider here $\phi(x)=10x(10-x),\ 0\leq x\leq 10$ as initial data and $\alpha=0.75$ as fractional order of derivative. In this example the time step size is $\Delta t=0.001$, number of time nodes is $N_t=41$ and the space step size is $\Delta x=0.5$, number of space nodes is $N_x=21$. The left Figure 2.1 shows numerical solution $U(x,t)$ for $x\in[0,10],\ t\in(0,T],\ T=0.04$. The right Figure 2.1 shows final time profile of numerical solution at $T=0.04$.

Toda Lattice Equation for Caputo derivative in time: For the numerical solution to the considered problem (1.1), we consider Caputo time-fractional derivative:

$$\left[\frac{\partial^{2\alpha}u^n}{\partial x^{\alpha}\partial t^{\alpha}}\right]_{C}=\left(1+\left[\frac{\partial^{\alpha}u^n}{\partial t^{\alpha}}\right]_{C}\right)(u^{n-1}-2u^n+u^{n+1}),\quad (x,t)\in I\times(0,T]. \tag{2.3}$$

We can discretize the Caputo fractional derivative of $u(x,t)$ at $t=t_n$ by the *L1-method* defined as follows:

$$\left[\frac{\partial^{\alpha}u(x_k,t^n)}{\partial t^{\alpha}}\right]_{C}=\frac{1}{\Delta t^{\alpha}}\sum_{j=0}^{n-1}b_{n-j-1}^{\alpha}(u_k^{j+1}-u_k^{j})+O(\Delta t^{p}),\ t>0$$

where b_{n-j-1}^{α} are the coefficients, that is $b_j^{\alpha}=\frac{1}{\Gamma(2-\alpha)}[(j+1)^{1-\alpha}-(j)^{1-\alpha}]$ and $p=1$ [4, 5]. Then the finite difference approximation of (2.3) is given as follows:

$$\frac{1}{\Delta t^{\alpha}}\sum_{j=0}^{n-1}b_{n-j-1}^{\alpha}[\delta_x^{\alpha}(U_k^{j+1}-U_k^{j})]=\left(1+\frac{1}{\Delta t^{\alpha}}\sum_{j=0}^{n-1}b_{n-j-1}^{\alpha}[\delta_x^{\alpha}(U_k^{j+1}-U_k^{j})]\right)(U_k^{n-1}-2U_k^n+U_k^{n+1}),\ n\geq 1, \tag{2.4}$$

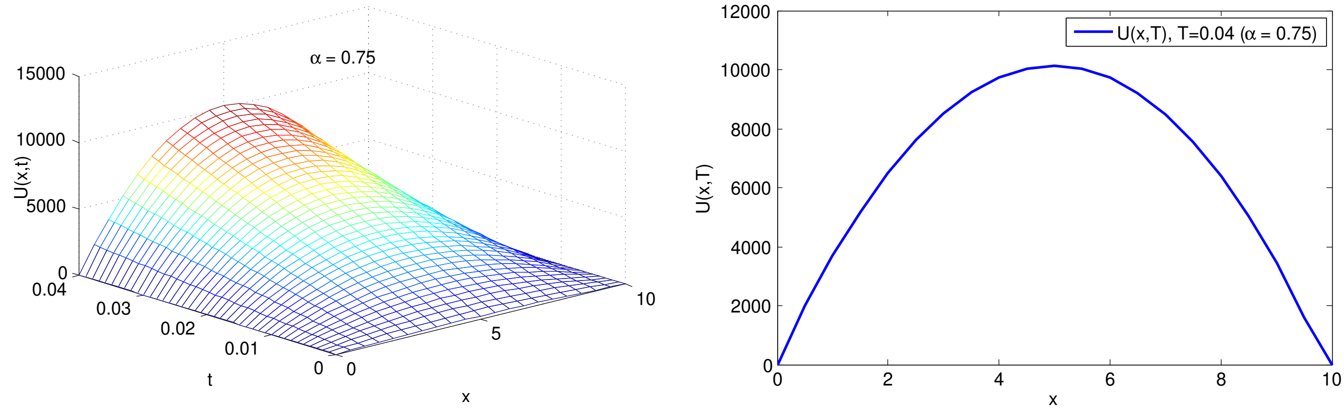

Figure 2.1: Numerical solutions for Riemann-Liouville fractional derivative ($\alpha = 0.75$)

where $\delta_x^\alpha U_k^n$ is the approximation of the Riemann-Liouville space-fractional derivative $\frac{\partial^\alpha u^n}{\partial x^\alpha}$ and defined by the Grünwald–Letnikov formula similarly. So (2.4) gives the approximate solution for all points (x_k, t_n), $k = \overline{1, N_x - 1}$, $n = \overline{1, N_t - 1}$ as follows:

$$\begin{cases} \frac{1}{\Delta t^\alpha} \frac{1}{\Delta x^\alpha} \sum_{j=0}^{n-1} \sum_{i=0}^{k} b_{n-j-1}^\alpha w_i^\alpha (U_{k-i}^{j+1} - U_{k-i}^{j}) = \left(1 + \frac{1}{\Delta t^\alpha} \sum_{j=0}^{n-1} b_{n-j-1}^\alpha (U_k^{j+1} - U_k^j)\right)(U_k^{n-1} - 2U_k^n + U_k^{n+1}),\ n \geq 1 (U_{k-i}^{j+1} - U_{k-i}^{j}), \\ U_k^0 = \phi(x_k),\ k = \overline{0, N_x}, \quad U_0^n = U_{N_x}^n = 0,\ n = \overline{1, N_t}. \end{cases} \tag{2.5}$$

Example 2. We consider same data in Example 1 to compare the numerical solutions corresponding to the two type of fractional derivatives. Thus, $\phi(x) = 10x(10 - x)$, $0 \leq x \leq 10$ is initial data and $\alpha = 0.75$ is fractional order of derivative. The time step size is $\Delta t = 0.001$, number of time nodes is $N_t = 41$ and the space step size is $\Delta x = 0.5$, number of space nodes is $N_x = 21$. The left Figure 2.2 shows numerical solution $U(x,t)$ for $x \in [0, 10]$, $t \in (0, T]$, $T = 0.04$. The right Figure 2.2 shows final time profile of numerical solution at $T = 0.04$. Figure 2.3 shows a slight differences difference on the solutions with Riemann–Liouville fractional derivative and Caputo fractional derivatives for ($\alpha = 0.75$). This slight difference, may be interpreted as, that is, due to the second term on r.h.s of equation (1.4) which states the relation between the Riemann–Liouville and Caputo derivatives for $0 < \alpha < 1$.

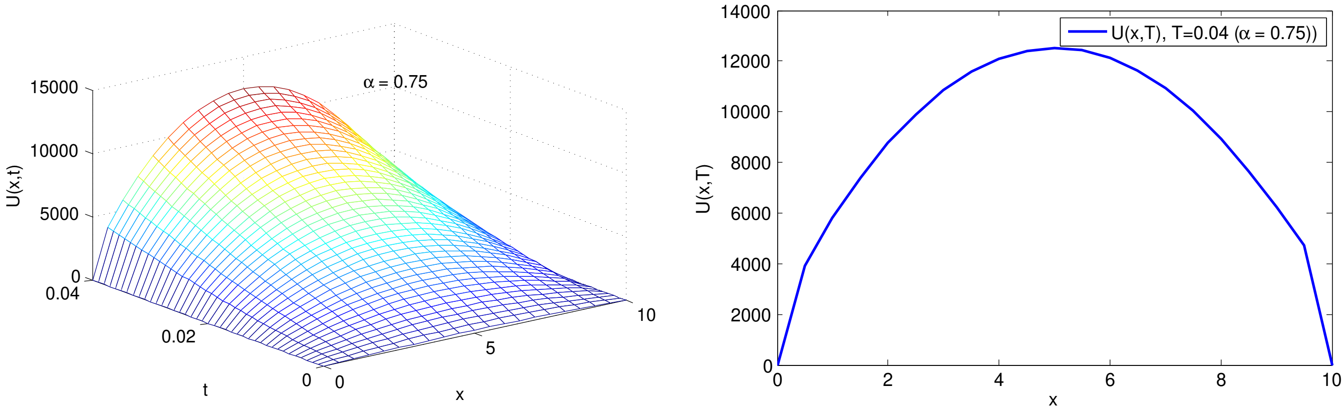

Figure 2.2: Numerical solutions for Caputo fractional derivative ($\alpha = 0.75$)

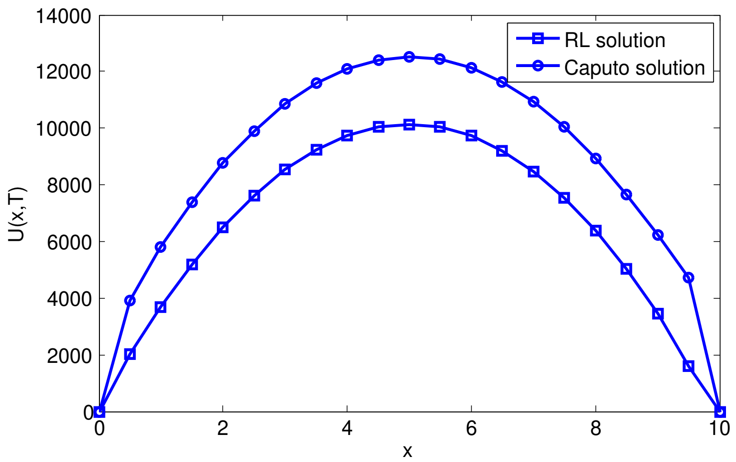

Figure 2.3: Numerical solutions for both Riemann-Liouville and Caputo fractional derivative ($\alpha = 0.75$)

3. Conclusion

In this study the space-time fractional partial differential-difference Toda lattice equation is considered. We use the finite differences method for numerical solution of the problem and present computational results for the case of two type of time fractional derivative (Riemann Liouville and Caputo) with fractional order $\alpha = 0.75$. Numerical experiments show that any of the fractional (Riemann–Liouville and Caputo) derivatives may be used for any physical problem without any reluctance and the choice of the fractional derivative is negligible at least the problem considered in this study.

Acknowledgement

The author thanks to Prof. Dr. Turgut Ozis for the recommendation of the problem and helpful and constructive discussions. The author also thanks the referee for carefully reading the paper and the valuable suggestions that improved the paper.

References

[1] M. Toda, *Theory of Nonlinear Lattices*, Springer-Verlag, New-York, 1989.
[2] K. Kajiwara,J. Satsuma, *The conserved quantities and symmetries of the two-dimensional Toda lattice hierarchy*, J. Math. Phys., **32** (1991), 506—514.
[3] J. J. Mohan, G. V. S. R. Deekshitulu, *Fractional order difference equations*, Int. J. Differ. Equ., **2012**(2012), Article ID 780619, 11 pages, https://doi.org/10.1155/2012/780619.
[4] M. Cui, *Compact finite difference method for the fractional diffusion equation* J. Comput. Phys., **228** (2009), 7792–7804.
[5] I. Podlubny, *Fractional Differential Equations*, Academic Press, San Diego, 1999.
[6] C. Li, F. Zeng, *Numerical Methods for Fractional Calculus* CRC Press, Boca Raton, 2015.

Journal of Mathematical Sciences and Modelling, 1 (3) (2018) 206-210
Research Article

Journal of Mathematical Sciences and Modelling

Journal Homepage: www.dergipark.gov.tr/jmsm
ISSN: 2636-8692

Introduction to Timelike Uniform B-splineCurves in Minkowski-3 Space

Hatice Kuşak Samancı[a*]

[a]*Department of Mathematics, Faculty of Science and Arts, Bitlis Eren University, Bitlis, Turkey*
[*]*Corresponding author*

Article Info

Keywords: *B-spline curve, Minkowski 3-space, Timelike curve*
2010 AMS: *53A04, 51B20*
Received: *18 May 2018*
Accepted: *18 July 2018*
Available online: *30 December 2018*

Abstract

The intention of this article is to study on timelike uniform B-spline curves in Minkowski-3 space. In our paper, we take the control points of uniform B-spline curves as a timelike point in Minkowski-3 space. Then we calculate some geometric elements for this new curve in Minkowski-3 space.

1. Introduction

B-spline curves were described by Schoenberg who was worked on B-spline curves for statistical data collection in [1]. The B-spline curves was constructed for computing a convolution of some probability distributions. Moreover, de Boor and Hollig considered a different approach to B-spline curves in [2]. Recently, in Computer Aided Geometric Design (CAGD), B-spline curves have been commonly used for designing an automobile, a boat, an aircraft, [3] and [4]. There are many studies on the B-spline curves, see some of them in [2], [5], [6]. Although degree d of a Bezier curve has $d+1$ control points, degree d of a B-spline curves can have any number of control points supplied a sufficient number of knots are defined in [7] and [8]. In addition, the control points of the Bezier curves provide a global change on the curve, while the control points of the B-spline curves provide a local change on the curve. For this reason, B-spline curves can be given additional freedom by increasing the number of control points in order to define complex curve shapes without increasing the degree of the curve, [9]. Minkowski space was introduced by H. Minkowski. In our paper, we try to investigate some geometric properties of the B-spline curves in Minkowski 3-space. We present the curvature and torsion of the B-spline curves in Minkowski 3-space.

2. Preliminaries

In this section the B-spline curves are defined and some preliminaries are given. Then some basics of Minkowski space is given.

Definition 2.1. *Let $t_0, t_1, ..., t_m$ be knot vectors of the B-spline basis function of degree d. The B-spline basis function denoted $N_{i,d}(t)$ is defined by*

$$N_{i,0}(t) = \begin{cases} 1, & if\ t \in [t_i, t_{i+1}) \\ 0, & otherwise \end{cases} \tag{2.1}$$

$$N_{i,d}(t) = \frac{t-t_i}{t_{i+d}-t_i} N_{i,d-1}(t) + \frac{t_{i+d+1}-t}{t_{i+d+1}-t_{i+1}} N_{i+1,d-1}(t) \tag{2.2}$$

for $i = 0, ..., n$ and $d \geq 1$.

Email address and ORCID number: **hkusak@beu.edu.tr, 0000-0001-6685-236X (H. Kuşak Samancı)**

Definition 2.2. *If the B-spline curve of degree d with control points $b_0,...,b_n$ and knots $t_0,t_1,...,t_m$ is defined on the interval $[a,b]=[t_d,t_{m-d}]$, then the curve can be written in the form*

$$B(t)=\sum_{i=0}^{n} b_i N_{i,d}(t).$$

When the B-spline curves are in the rational form, they are often called integral B-spline curves. Moreover, if the knots are equally spaced, then a B-spline curve is called uniform.

On the other hand, Minkowski 3-space $\mathbb{R}_1^3$ is a vector space $\mathbb{R}^3$ provide with the Lorentzian inner product g given by

$$\mathrm{g}(v,\lambda)=v_1\lambda_1+v_2\lambda_2-v_3\lambda_3,$$

where $v=(v_1,v_2,v_3)$ and $\lambda=(\lambda_1,\lambda_2,\lambda_3)\in\mathbb{R}_1^3$. A vector in Minkowski 3-space $\lambda=(\lambda_1,\lambda_2,\lambda_3)\in\mathbb{R}_1^3$ is called spacelike if $\mathrm{g}(\lambda,\lambda)>0$ or $\lambda=0$; timelike if $\mathrm{g}(\lambda,\lambda)<0$; lightlike if $\mathrm{g}(\lambda,\lambda)=0$ and $\lambda\neq 0$. The vectors v and λ are ortogonal if and only if $\mathrm{g}(v,\lambda)=0$. The norm of a vector v on Minkowski space $\mathbb{R}_1^3$ is defined by $\|v\|_{\mathbb{L}}=\sqrt{|\mathrm{g}(v,v)|}$. If the vector is timelike, then the form will be $\|v\|_{\mathbb{L}}=\sqrt{-\mathrm{g}(v,v)}$. Let (c) be curve in $\mathbb{R}_1^3$. We say that (c) is timelike curve (resp. spacelike, lightlike) at t if the tangent vector $(c)'(t)$ is a timelike (resp. spacelike, lightlike) vector. The vector fields of the moving Serret-Frenet from along the curve (c) are denoted by $\{\mathbf{T},\mathbf{N},\mathbf{B}\}$ where $\mathbf{T}$, $\mathbf{N}$ and $\mathbf{B}$ are called with the tangent, the principal normal and the binormal vector of the curve (c), respectively. If the curve (c) is time-like curve, then $\mathbf{T}$ is timelike vector, $\mathbf{N}$ and $\mathbf{B}$ are spacelike vectors which satisfy $\mathbf{T}\wedge_{\mathbb{L}}\mathbf{N}=-\mathbf{B}$, $\mathbf{N}\wedge_{\mathbb{L}}\mathbf{B}=\mathbf{T}$, $\mathbf{B}\wedge_{\mathbb{L}}\mathbf{T}=-\mathbf{N}$. The derivative of Serret-Frenet frame equations for a timelike curve is

$$\begin{aligned}\mathbf{T}'&=\kappa\mathbf{N}\\ \mathbf{N}'&=\kappa\mathbf{T}+\tau\mathbf{B}\\ \mathbf{B}'&=-\tau\mathbf{N}.\end{aligned}$$

3. Main result

Definition 3.1. *Let $X=\{b_0,b_1,...,b_n\}$ be a timelike points set in $\mathbb{R}_1^3$. The*

$$TCH\{X\}=\left\{\lambda_0 b_0+...+\lambda_n b_n \,|\, \sum_{i=0}^{n}\lambda_i=1,\lambda_i\geq 0\right\}$$

set formed by these X points are called timelike convex hull of a timelike uniform B-spline curve.

Definition 3.2. *If the control points $b_0,...,b_n\in TCH\{X\}$ are timelike and the knots $t_0,t_1,...,t_m$ on the interval $[a,b]=[t_d,t_{m-d}]$ are equally spaced, then the timelike uniform B-spline curve of degree d in Minkowski 3-space is defined by*

$$B(t)=\sum_{i=0}^{n} b_i N_{i,d}(t),$$

where $N_{i,d}(t)$ are the basis functions.

Example: Lets consider the timelike uniform B-spline curve $B(t)$ of degree $d=2$ defined on the knots $t_0=0,t_1=1,t_2=2,t_3=3,t_4=4,t_5=5,t_6=6,t_7=7$ and with control points $b_0(2,3),b_1(-1,7),b_2(2,5),b_3(4,5),b_4(1,3)$. The basis graphic and the curve shape are in the following figures.

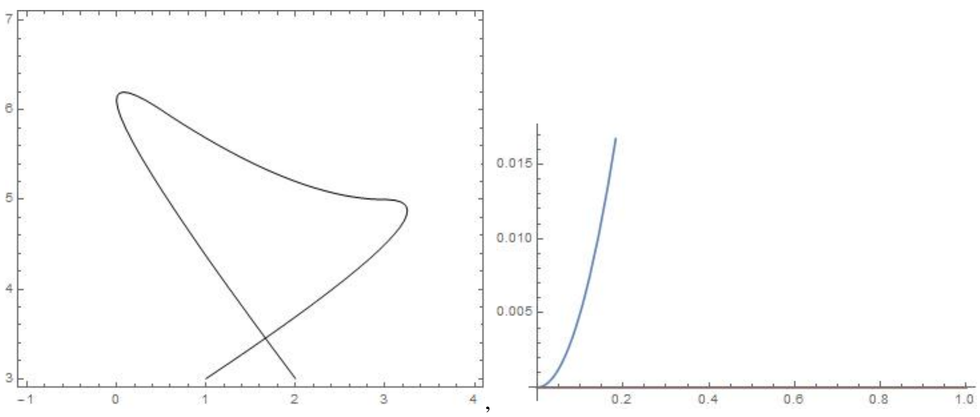

Figure 3.1: a) Basis function graphic b) A timelike uniform B-spline curve

Theorem 3.3. *Let $B(t)$ be a timelike uniform B-spline curve of degree d with the knot vector $t_0,...,t_m$ in Minkowski 3-space. If $t\in[t_r,t_{r+1})$ $(d\leq r\leq m-d-1)$ then $B(t)=\sum_{i=r-d}^{r} b_i N_{i,d}(t)$. Therefore to compute $B(t)$ its sufficient to compute $N_{r-d,d}(t),...,N_{r,d}(t)$. This shows us that the B-spline curve is achieved by the local control. If $t\in[t_r,t_{r+1})$ $(d\leq r\leq m-d-1)$ then $B(t)\in TCH\{b_{r-d},...,b_r\}$. This means that B-spline curve has an convex hull. If p_i is the multiplicity of the breakpoint $t=u_i$ then $B(t)$ is C^{d-p_i} (or greater) at*

$t = u_i$ and C^∞ elsewhere. Thus, it is seen that the B-spline curve is satisfied the continuity property. Let T be an affine transformation. If $T(\sum_{i=0}^{n} b_i N_{i,d}(t)) = \sum_{i=0}^{n} T(b_i) N_{i,d}(t)$, the B-spline curve is invariant under affine transformations.

Theorem 3.4. *Let $B(t)$ be a timelike uniform B-spline curve of degree d with the knot vector $t_0,...,t_m$ in Minkowski 3-space. The second and third derivative of the control points b_i are calculated by*

$$\begin{aligned} b_i^{(2)} &= (d-1).m_i.\Delta b_i^{(1)} \\ b_i^{(3)} &= (d-1)(d-2).p_i.(n_i.\Delta b_{i+1}^{(1)} - m_i \Delta b_i^{(1)}) \end{aligned}$$

where m_i, n_i, p_i are some constants of t_i.

Proof. Using the Eq.(2.1) and Eq.(2.2) the control points can be written as

$$\begin{aligned} b_i^{(2)} &= (d-1)\frac{b_{i+1}^{(1)} - b_i^{(1)}}{t_{i+d+1} - t_{i+2}} \\ &= (d-1).m_i.\Delta b_i^{(1)}, \\ b_i^{(3)} &= \frac{(d-2)}{t_{i+d+1} - t_{i+3}}\left(b_{i+1}^{(2)} - b_i^{(2)}\right) \\ &= \frac{(d-2)}{t_{i+d+1} - t_{i+3}}\left((d-1).n_i.(b_{i+2}^{(2)} - b_{i+1}^{(1)}) - (d-1).m_i.(b_{i+1}^{(1)} - b_i^{(1)})\right) \\ &= \frac{(d-1)(d-2)}{t_{i+d+1} - t_{i+3}}\left(.n_i.(b_{i+2}^{(2)} - b_{i+1}^{(1)}) - m_i.(b_{i+1}^{(1)} - b_i^{(1)})\right) \\ &= (d-1)(d-2).p_i.(n_i.\Delta b_{i+1}^{(1)} - m_i \Delta b_i^{(1)}) \end{aligned}$$

where $m_i = \frac{1}{t_{i+d+1} - t_{i+2}}$, $n_i = \frac{1}{t_{i+d+2} - t_{i+3}}$ and $p_i = \frac{1}{t_{i+d+1} - t_{i+3}}$. □

Theorem 3.5. *Let $B(t)$ be a timelike uniform B-spline curve of degree d with the knot vector $t_0,...,t_m$ in Minkowski 3-space. The derivatives of B-spline curve is computed by*

$$\begin{aligned} B^{(1)}(t) &= \sum_{i=0}^{n-1} b_i{}^{(1)} N^{(1)}{}_{i,d-1}(t) \\ B^{(2)}(t) &= (d-1)\sum_{i=0}^{n-2} m_i.\Delta b_i^{(1)}.N_{i,d-2}^{(2)} \\ B^{(3)}(t) &= (d-1)(d-2)\sum_{i=0}^{n-3} p_i.\left(n_i.\Delta b_{i+1}^{(1)} - m_i \Delta b_i^{(1)}\right).N_{i,d-3}^{(3)}. \end{aligned}$$

Proof. Substituting the above results in Eq.(2.2), the proof is obvious. □

Theorem 3.6. *Let $B(t)$ be an arbitrary timelike uniform B-spline curve and $\{T,N,B\}|_{t=0}$ be the Serret-Frenet frame of $B(t)$, where T is timelike, N and B are spacelike. Then the following conditions are satisfied*

$$\begin{gathered} g(T,T) = -1, g(N,N) = 1, g(B,B) = 1 \\ g(T,N) = 0, g(T,B) = 0, g(N,B) = 0. \end{gathered}$$

The Serret-Frenet frame of the timelike uniform B-spline curve $B(t)$ is obtained by

$$\begin{aligned} T &= \frac{\sum_{i=0}^{n-1} b_i{}^{(1)} N^{(1)}{}_{i,d-1}(t)}{\left\|\sum_{i=0}^{n-1} b_i{}^{(1)} N^{(1)}{}_{i,d-1}(t)\right\|} \\ B &= \frac{\sum_{i=0}^{n-1} b_i{}^{(1)} N_{i,d-1}^{(1)}(t) \wedge \sum_{i=0}^{n-2} m_i.\Delta b_i^{(1)}.N_{i,d-2}^{(2)}}{\left\|\sum_{i=0}^{n-1} b_i{}^{(1)} N_{i,d-1}^{(1)}(t) \wedge \sum_{i=0}^{n-2} m_i.\Delta b_i^{(1)}.N_{i,d-2}^{(2)}\right\|} \\ N &= -\frac{\begin{array}{c} -g\left(\sum_{i=0}^{n-1} b_i{}^{(1)} N_{i,d-1}^{(1)}(t), \sum_{i=0}^{n-1} b_i{}^{(1)} N^{(1)}{}_{i,d-1}(t)\right)\left(\sum_{i=0}^{n-2} m_i.\Delta b_i^{(1)}.N_{i,d-2}^{(2)}\right) \\ +g\left(\sum_{i=0}^{n-2} m_i.\Delta b_i^{(1)}.N_{i,d-2}^{(2)}, \sum_{i=0}^{n-1} b_i{}^{(1)} N_{i,d-1}^{(1)}(t)\right)\left(\sum_{i=0}^{n-1} b_i{}^{(1)} N_{i,d-1}^{(1)}(t)\right) \end{array}}{\left\|\sum_{i=0}^{n-1} b_i{}^{(1)} N_{i,d-1}^{(1)}(t) \wedge \sum_{i=0}^{n-2} m_i.\Delta b_i^{(1)}.N_{i,d-2}^{(2)}\right\| \left\|\sum_{i=0}^{n-1} b_i{}^{(1)} N^{(1)}{}_{i,d-1}(t)\right\|} \end{aligned}$$

Proof. Let consider the B-spline curve $B(t)$ is non unit speed curve in Minkowski 3-space. Using the scalar and vector product in Minkowski 3-space, the tangent vector of the timelike uniform B-spline curve $B(t)$ is calculated as

$$\begin{aligned} T &= \frac{B^{(1)}(t)}{\left\|B^{(1)}(t)\right\|} \\ &= \frac{\sum\limits_{i=0}^{n-1} b_i{}^{(1)} N^{(1)}{}_{i,d-1}(t)}{\left\|\sum\limits_{i=0}^{n-1} b_i{}^{(1)} N^{(1)}{}_{i,d-1}(t)\right\|}, \end{aligned}$$

and the binormal vector of the timelike B-spline curve is

$$\begin{aligned} B &= \frac{B^{(1)}(t)\wedge B^{(2)}(t)}{\left\|B^{(1)}(t)\wedge B^{(2)}(t)\right\|} \\ &= \frac{\sum\limits_{i=0}^{n-1} b_i{}^{(1)} N^{(1)}_{i,d-1}(t)\wedge (d-1)\sum\limits_{i=0}^{n-2} m_i.\Delta b_i^{(1)}.N^{(2)}_{i,d-2}}{\left\|\sum\limits_{i=0}^{n-1} b_i{}^{(1)} N^{(1)}_{i,d-1}(t)\wedge (d-1)\sum\limits_{i=0}^{n-2} m_i.\Delta b_i^{(1)}.N^{(2)}_{i,d-2}\right\|} \\ &= \frac{\sum\limits_{i=0}^{n-1} b_i{}^{(1)} N^{(1)}_{i,d-1}(t)\wedge \sum\limits_{i=0}^{n-2} m_i.\Delta b_i^{(1)}.N^{(2)}_{i,d-2}}{\left\|\sum\limits_{i=0}^{n-1} b_i{}^{(1)} N^{(1)}_{i,d-1}(t)\wedge \sum\limits_{i=0}^{n-2} m_i.\Delta b_i^{(1)}.N^{(2)}_{i,d-2}\right\|}. \end{aligned}$$

The principal normal can be obtained as

$$\begin{aligned} N &= -B\wedge T \\ &= -\frac{\sum\limits_{i=0}^{n-1} b_i{}^{(1)} N^{(1)}_{i,d-1}(t)\wedge \sum\limits_{i=0}^{n-2} m_i.\Delta b_i^{(1)}.N^{(2)}_{i,d-2}}{\left\|\sum\limits_{i=0}^{n-1} b_i{}^{(1)} N^{(1)}_{i,d-1}(t)\wedge \sum\limits_{i=0}^{n-2} m_i.\Delta b_i^{(1)}.N^{(2)}_{i,d-2}\right\|}\wedge\frac{\sum\limits_{i=0}^{n-1} b_i{}^{(1)} N^{(1)}{}_{i,d-1}(t)}{\left\|\sum\limits_{i=0}^{n-1} b_i{}^{(1)} N^{(1)}{}_{i,d-1}(t)\right\|} \\ &= -\frac{\left(\sum\limits_{i=0}^{n-1} b_i{}^{(1)} N^{(1)}_{i,d-1}(t)\wedge \sum\limits_{i=0}^{n-2} m_i.\Delta b_i^{(1)}.N^{(2)}_{i,d-2}\right)\wedge\sum\limits_{i=0}^{n-1} b_i{}^{(1)} N^{(1)}{}_{i,d-1}(t)}{\left\|\sum\limits_{i=0}^{n-1} b_i{}^{(1)} N^{(1)}_{i,d-1}(t)\wedge \sum\limits_{i=0}^{n-2} m_i.\Delta b_i^{(1)}.N^{(2)}_{i,d-2}\right\|\left\|\sum\limits_{i=0}^{n-1} b_i{}^{(1)} N^{(1)}{}_{i,d-1}(t)\right\|} \\ &= -\frac{\begin{array}{l}-g\left(\sum\limits_{i=0}^{n-1} b_i{}^{(1)} N^{(1)}_{i,d-1}(t),\sum\limits_{i=0}^{n-1} b_i{}^{(1)} N^{(1)}{}_{i,d-1}(t)\right)\left(\sum\limits_{i=0}^{n-2} m_i.\Delta b_i^{(1)}.N^{(2)}_{i,d-2}\right)\\ +g\left(\sum\limits_{i=0}^{n-2} m_i.\Delta b_i^{(1)}.N^{(2)}_{i,d-2},\sum\limits_{i=0}^{n-1} b_i{}^{(1)} N^{(1)}_{i,d-1}(t)\right)\sum\limits_{i=0}^{n-1} b_i{}^{(1)} N^{(1)}_{i,d-1}(t)\end{array}}{\left\|\sum\limits_{i=0}^{n-1} b_i{}^{(1)} N^{(1)}_{i,d-1}(t)\wedge \sum\limits_{i=0}^{n-2} m_i.\Delta b_i^{(1)}.N^{(2)}_{i,d-2}\right\|\left\|\sum\limits_{i=0}^{n-1} b_i{}^{(1)} N^{(1)}{}_{i,d-1}(t)\right\|}. \end{aligned}$$

□

Theorem 3.7. *If the B-spline curve of degree d with control points $b_0,...,b_n$ and knots $t_0,t_1,...,t_m$ is defined on the interval $[a,b]=[t_d,t_{m-d}]$, the curvature of timelike uniform B-spline curve $B(t)$ is found as*

$$\kappa = |d-1|\frac{\left\|\sum\limits_{i=0}^{n-1} b_i{}^{(1)} N^{(1)}_{i,d-1}(t)\wedge \sum\limits_{i=0}^{n-2} m_i.\Delta b_i^{(1)}.N^{(2)}_{i,d-2}\right\|}{\left\|\sum\limits_{i=0}^{n-1} b_i{}^{(1)} N^{(1)}_{i,d-1}(t)\right\|^3}$$

Proof. From the definition of curvature of the non-unit speed curve, we have

$$\begin{aligned} \kappa &= \frac{\left\|B^{(1)}(t)\wedge B^{(2)}(t)\right\|}{\left\|B^{(1)}(t)\right\|^3} \\ &= \frac{\left\|\sum\limits_{i=0}^{n-1} b_i{}^{(1)} N^{(1)}_{i,d-1}(t)\wedge (d-1)\sum\limits_{i=0}^{n-2} m_i.\Delta b_i^{(1)}.N^{(2)}_{i,d-2}\right\|}{\left\|\sum\limits_{i=0}^{n-1} b_i{}^{(1)} N^{(1)}_{i,d-1}(t)\right\|^3} \\ &= |d-1|\frac{\left\|\sum\limits_{i=0}^{n-1} b_i{}^{(1)} N^{(1)}_{i,d-1}(t)\wedge \sum\limits_{i=0}^{n-2} m_i.\Delta b_i^{(1)}.N^{(2)}_{i,d-2}\right\|}{\left\|\sum\limits_{i=0}^{n-1} b_i{}^{(1)} N^{(1)}_{i,d-1}(t)\right\|^3}. \end{aligned}$$

□

Theorem 3.8. *If $B(t)$ is a timelike uniform B-spline curve of degree d with the knot vector $t_0,...,t_m$ in Minkowski 3-space, the torsion of a timelike uniform B-spline curve $B(t)$ is computed by*

$$\tau=-(d-2)\frac{\det\left(\sum_{i=0}^{n-1}b_i{}^{(1)}N^{(1)}_{i,d-1}(t)\,,\ \sum_{i=0}^{n-2}m_i.\Delta b_i^{(1)}.N^{(2)}_{i,d-2},\ \sum_{i=0}^{n-3}p_i.\left(n_i.\Delta b_{i+1}^{(1)}-m_i\Delta b_i^{(1)}\right).N^{(3)}_{i,d-3}\right)}{\left\|\sum_{i=0}^{n-1}b_i{}^{(1)}N^{(1)}_{i,d-1}(t)\wedge\sum_{i=0}^{n-2}m_i.\Delta b_i^{(1)}.N^{(2)}_{i,d-2}\right\|^2}$$

Proof. Using the definition of torsion, we have the following equations:

$$\begin{aligned}
\tau &= \frac{\left(B^{(1)}(t)\ B^{(2)}(t)\ B^{(3)}(t)\right)}{\left\|B^{(1)}(t)\wedge B^{(2)}(t)\right\|^2}\\
&= \frac{\left(\sum_{i=0}^{n-1}b_i{}^{(1)}N^{(1)}_{i,d-1}(t)\quad (d-1)\sum_{i=0}^{n-2}m_i.\Delta b_i^{(1)}.N^{(2)}_{i,d-2}\quad (d-1)(d-2)\sum_{i=0}^{n-3}p_i.\left(n_i.\Delta b_{i+1}^{(1)}-m_i\Delta b_i^{(1)}\right).N^{(3)}_{i,d-3}\right)}{\left\|\sum_{i=0}^{n-1}b_i{}^{(1)}N^{(1)}_{i,d-1}(t)\wedge(d-1)\sum_{i=0}^{n-2}m_i.\Delta b_i^{(1)}.N^{(2)}_{i,d-2}\right\|^2}\\
&= -(d-2)\frac{\det\left(\sum_{i=0}^{n-1}b_i{}^{(1)}N^{(1)}_{i,d-1}(t)\,,\ \sum_{i=0}^{n-2}m_i.\Delta b_i^{(1)}.N^{(2)}_{i,d-2},\ \sum_{i=0}^{n-3}p_i.\left(n_i.\Delta b_{i+1}^{(1)}-m_i\Delta b_i^{(1)}\right).N^{(3)}_{i,d-3}\right)}{\left\|\sum_{i=0}^{n-1}b_i{}^{(1)}N^{(1)}_{i,d-1}(t)\wedge\sum_{i=0}^{n-2}m_i.\Delta b_i^{(1)}.N^{(2)}_{i,d-2}\right\|^2}
\end{aligned}$$

□

4. Conclusion

In this paper, we present a theoretical work about the timelike uniform B-spline curves in Minkowski-3 space. The timelike B-spline curve in Minkowski 3-space at first time is introduced. The derivatives of control points are calculated. Later Serret-Frenet frame of the timelike uniform B-spline curve is given. Moreover, the curvature and torsion of the B-spline curve are computed.

Acknowledgement

We would like to express our sincere thanks to the referee for the careful reading and very helpful comments on the earlier versions of this manuscript.

References

[1] I. J. Schoenbergc, *Contributions to the problem of approximation of equidistant data by analytic functions*, Quart. Appl. Math., **4**(1-2) (1946), 45-99, 112-141.
[2] C. D. Boor, *On calculating with B-splines*, J. Approx. Theory, **6**(1) (1972), 50–62.
[3] G. Farin, *Curves and Surfaces for Computer-Aided Geometric Design: A Practical Guide*, Elsevier, 2014.
[4] F. Yamaguchi, *Curves and Surfaces in Computer Aided Geometric Design*, Springer-Verlag, Berlin, 1988.
[5] W. J. Gordon, *B-spline curves and surfaces*, Comput. Aided Geom. Design, (1974), 95–126.
[6] M. Incesu, O. Gursoy *The similarity invariants of integral B-splines*, Int. Sci. Conf. Algebr. Geom. Methods Anal., (2017).
[7] R. Barnhill, R. F. Riesenfeld, *Computer aided geometric design*, Academic Press.
[8] P. D. Casteljau, *Shape Mathematics and CAD*, Kogan Page, London, 1986.
[9] D. Marsh, *Applied Geometry for Computer Graphics and CAD*, Springer-Verlag, Berlin, 2005.